EUMETSAT NWC SAF

SUPPORT TO NOWCASTING AND VERY SHORT RANGE FORECASTING

Scientific and Validation Report for the Precipitation Product Processors of the NWC/GEO

NWC/CDOP3/GEO/AEMET/SCI/VR/Precipitation, Issue 2, Rev. 0.1
28th February 2022

Applicable to

GEO-PC-v154 (NWC-019)
GEO-CRR-v402 (NWC-024)
GEO-PCPh-v2.0 (NWC-077)
GEO-CRRPh-v2.0 (NWC-081)

Prepared by AEMET

REPORT SIGNATURE TABLE

Function	Name	Signature	Date
Prepared by	José Alberto Lahuerta (AEMET)		*28th February 2022*
Reviewed by	Llorenç Lliso and Pilar Ripodas (GEO Managers)		*28th February 2022*
Authorised by	Pilar Rípodas NWC SAF Project Manager		*28th February 2022*

DOCUMENT CHANGE RECORD

Version	Date	Pages	CHANGE(S)
1.0	21 January 2019	61	First version of precipitation products validation for NWC SAF SW Package GEO v2018 DRR. Content derived from Scientific and Validation Report for the Precipitation Product Processors of the NWC/GEO v2016 NWC/CDOP2/GEO/AEMET/VR/Precipitation
1.1	18 December 2019	65	Updated with GOES-16 section
2.0	10 January 2022	68	CRRPh and PCPh are new algorithms, both based on a Principal Component Analysis. PC and CRR keep the same from the last version. Hence, sections 2 and 3 have not been altered from the last Validation Report for the Precipitation Product Processors of the NWC GEO "NWC/CDOP3/GEO/AEMET/SCI/VR/Precipitation" Issue 1, Rev. 1 ,18 December 2019
2.0.1	28 February 2022	71	Figures 28, 29 and 34 have been included. Text have been updated accordingly to DRR RID submissions and DRR v2021 revision

LIST OF TABLES AND FIGURES

1. INTRODUCTION

The EUMETSAT "Satellite Application Facilities" (SAF) are dedicated centres of excellence for processing satellite data, and form an integral part of the distributed EUMETSAT Application Ground Segment (http://www.eumetsat.int). This documentation is provided by the SAF on Support to Nowcasting and Very Short Range Forecasting, NWC SAF. The main objective of NWC SAF is to provide, further develop and maintain software packages to be used for Nowcasting applications of operational meteorological satellite data by National Meteorological Services. More information can be found at the NWC SAF webpage, http://www.nwcsaf.org. This document is applicable to the NWC SAF processing package for geostationary meteorological satellites, NWC/GEO.

1.1 SCOPE OF THE DOCUMENT

This document is the Validation Report (VR) for the precipitation GEO products Precipitating Clouds (PC), Convective Rainfall Rate (CRR) and Precipitation products from Cloud Physical Properties (PPh) of the NWC/GEO software package. PPh generates two different products: Precipitating Clouds from Cloud Physical Properties (PCPh) and Convective Rainfall rate from Cloud Physical Properties (CRRPh).

This document compares the accuracies of the GEO precipitation products to the threshold accuracies for CDOP3 listed in the " NCWSAF product requirements document" *[AD. 4]*.

1.2 SOFTWARE VERSION IDENTIFICATION

This document describes the algorithms implemented in the 2021 NWC-GEO software package release (GEO-PC v1.5.4, GEO-CRR v4.0.2, GEO-PCPh v3.0 and GEO-CRRPh v3.0).

1.3 IMPROVEMENT FROM PREVIOUS VERSIONS

- ✓ New CRRPh and PCPh algorithms based on a Principal Component Analysis. There is only one algorithm for each CRRPh and PCPh that includes both day and night conditions.
- ✓ Microphysical properties are simulated at night time and used in the algorithm.
- ✓ More information is extracted from the SEVIRI channels.
- ✓ CRRPh incorporates a Cloud Water Path enhancement correction factor, a stability correction factor and a lightning module.
- ✓ Adaptation to Himawari9 and GOES17. This adaptation is purely technical in order to use Himawari9 and GOES17 channels, but no objective validation has been performed for these satellites.

Note:
PC and CRR keep the same from previous 2018.1 version

1.4 DEFINITIONS, ACRONYMS AND ABBREVIATIONS

AEMET	Agencia Estatal de Meteorología
ATBD	Algorithm Theoretical Basis Document
BALTRAD	Baltic Radar Network
CAPPI	Constant Altitude Plan Position Indicator
COT	Cloud Optical Thickness
CRRPh	Convective Rainfall Rate from Cloud Physical Properties
CRR	Convective Rainfall Rate
CSI	Critical Success Index
CT	Cloud Type
CWP	Cloud Water Path
NCAR EOL	Earth Observing Laboratory
ET	Echotop
EUMETSAT	European Organisation for the Exploitation of Meteorological Satellites
FAR	False Alarm Ratio
HRIT	High Rate Information Transmission
ICD	Interface Control Document
ICP	Illumination Conditions Parameter
IQF	Illumination Quality Flag
IR	Infrared
MAE	Mean Absolute Error
CTMP	Cloud Top Microphysical Properties
ME	Mean Error
MRV	Maximum Reflectivity in the Vertical
MSG	Meteosat Second Generation
NIR	Near Infrared
NWCLIB	Nowcasting SAF Library
NWC SAF	Satellite Application Facility for Nowcasting
OPERA	Operational Programme for the Exchange of weather Radar information
PC	Precipitating Clouds
PC	Percentage of Corrects
PCPh	Precipitating Clouds from Cloud Physical Properties
PGE	Product Generation Element
POD	Probability of Detection
PoP	Probability of Precipitation
PPh	Precipitation from Cloud Physical Properties
PPI	Plan Position Indicator
PWRH	Moisture Correction Factor
R_{eff}	Effective Radius
RLR	Rainfall-Lightning Ratio
RMSE	Root Mean Square Error
RR	Rain Rate
SAF	Satellite Application Facility
SEVIRI	Spinning Enhanced Visible and Infrared Imager
SW	Software
USA	United States of America

VIS	Visible
VIS-N	Normalized Visible
WV	Water Vapour

1.5 REFERENCES

1.5.1 Applicable Documents

The following documents, of the exact issue shown, form part of this document to the extent specified herein. Applicable documents are those referenced in the Contract or approved by the Approval Authority. They are referenced in this document in the form [AD.X].
For dated references, subsequent amendments to, or revisions of, any of these publications do not apply. For undated references, the current edition of the document referred applies.
Current documentation can be found at the NWC SAF Helpdesk web: http://www.nwcsaf.org

Reference	Title	Code	Vers	Date
[AD. 1]	Proposal for the Third Continuous Development and Operations Phase (CDOP-3) March 2017 – February 2022	NWC SAF:CDOP-3 proposal	1.0	11/04/16
[AD. 2]	NWCSAF Project Plan	NWC/CDOP3/SAF/AEMET/MGT/PP	1.6	01/12/21
[AD. 3]	Configuration Management Plan for the NWC SAF	NWC/CDOP3/SAF/AEMET/MGT/CMP	1.1	15/04/20
[AD. 4]	NWCSAF Product Requirements Document	NWC/CDOP3/SAF/AEMET/MGT/PRD	1.5	01/12/21

Table 1. List of Applicable Documents

1.5.2 Reference Documents

The reference documents contain useful information related to the subject of the project. These reference documents complement the applicable ones, and can be looked up to enhance the information included in this document if it is desired. They are referenced in this document in the form [RD.X].
For dated references, subsequent amendments to, or revisions of, any of these publications do not apply. For undated references, the current edition of the document referred applies.
Current documentation can be found at the NWC SAF Helpdesk web: http://www.nwcsaf.org

Reference	Title	Code	Vers	Date
[RD 1]	Interface Control Document for Internal and External Interfaces of the NWC/GEO	NWC/CDOP3/GEO/AEMET/SW/ICD/1	2.0.1	28/02/22
[RD 2]	Data Output Format for the NWC/GEO	NWC/CDOP3/GEO/AEMET/SW/DOF	2.0.1	28/02/22
[RD 3]	Algorithm Theoretical Basis Document for SAFNWC/MSG "Precipitating Cloud" (PC-PGE04 v1.5)	SAF/NWC/CDOP2/SMHI/SCI/ATBD/4	1.5.4	15/07/13

Reference	Title	Code	Vers	Date
[RD 4]	Algorithm Theoretical Basis Document for the Precipitation Product Processors of the NWC/GEO	NWC/CDOP3/GEO/AEMET/SCI/ ATBD/Precipitation	1.0.1	29/10/21
[RD 5]	User Manual for the SAFNWC/MSG Parallax Correction Tool	GMV/SAFCDOP/VSAREP/02	1.0	02/06/08

Table 2. List of Referenced Documents

2. VALIDATION FOR PRECIPITATING CLOUDS PRODUCT

This section contains the results obtained from the validation of the PC product which is described in the Algorithm Theoretical Basis Document for SAFNWC/MSG “Precipitating Cloud” (PC-PGE04 v1.5) [RD 3].

2.1 SUBJECTIVE VALIDATION FOR PRECIPITATING CLOUDS (PC)

Many cases have been visually studied by comparing the probability of precipitation (PoP) obtained from the PC algorithm against the radar data. Since PC product estimates probability of precipitation occurrence, the most suitable product to compare with would be the one that assigns 100% PoP where it is raining and 0% otherwise. So PC product has been compared with modified PPI product radar images where pixels with rain rates higher than or equal to 0.2 mm/h are set as rainy pixels (red colour) and the others as no rainy pixels (black colour).

A selection of cases that show the general behaviour of this product can be seen below. Since satellite scanning over the Iberian Peninsula takes place about 10 minutes later than the satellite imagery nominal time, PC images have been compared to radar ones taken 10 minutes later for a better time matching.

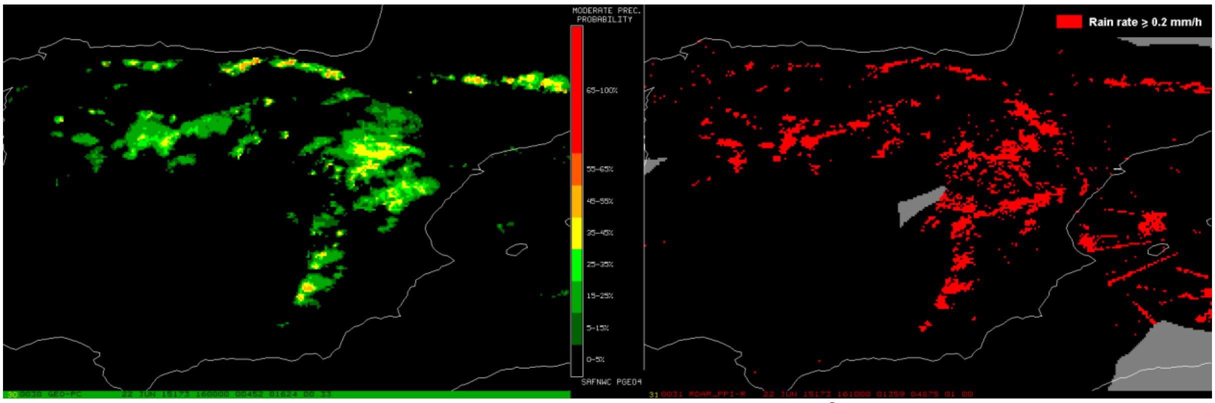

Figure 1. Comparison of PC product and radar (PPI) on 22nd June 2015 at 16:00UTC.

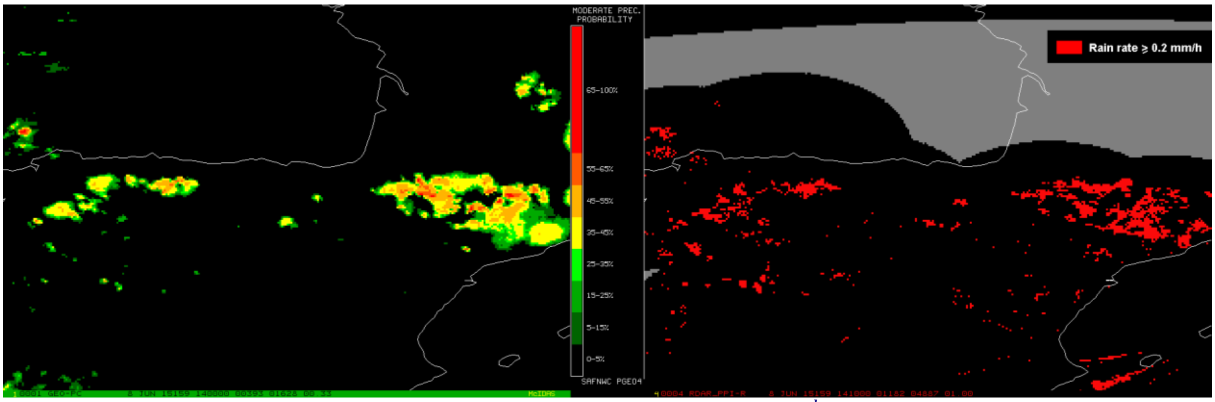

Figure 2. Comparison of PC product and radar (PPI) on 8th June 2015 at 14:00UTC.

Both Figure 1 and Figure 2 show day-time PC algorithm estimations where the overall precipitation areas are well depicted. However, PoP assigned are not so high, above all in the case of Figure 1, where few pixels take values of PoP higher than 50%. This fact could be explained by the time of the scanning of the satellite imagery used to compute the product. The set of satellite channels used by day-time PC algorithm includes some solar channels with valuable information for precipitation detection. The poorer are the illumination conditions, the lower is the confidence of the algorithm to assign higher PoPs.

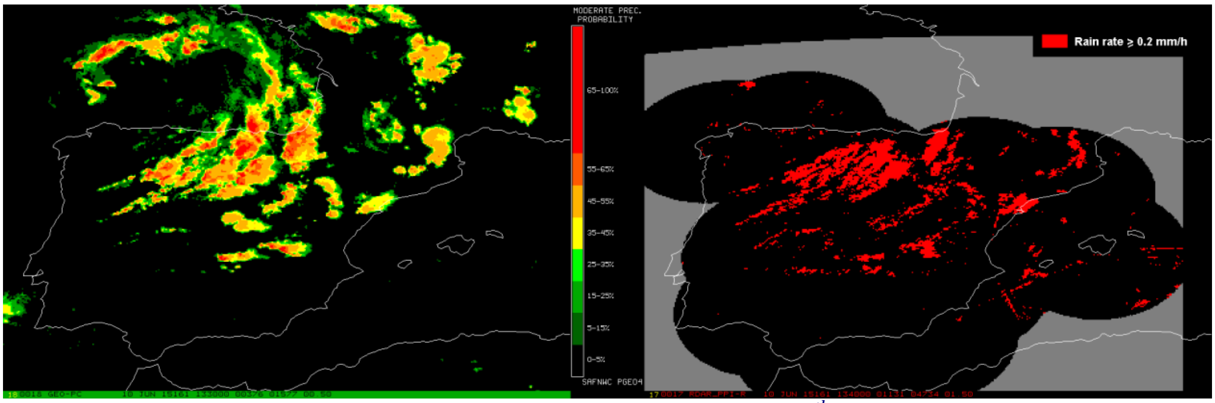

Figure 3. Comparison of PC product and radar (PPI) on 10th June 2015 at 13:30UTC.

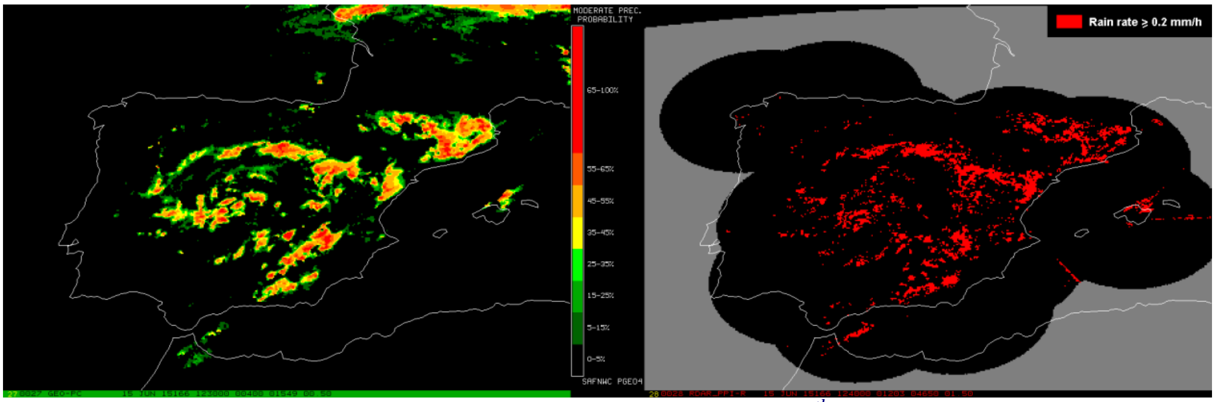

Figure 4. Comparison of PC product and radar (PPI) on 15th June 2015 at 12:30UTC.

Figure 3 and Figure 4 show day-time PC algorithm estimations with better illumination conditions than Figure 1 and Figure 2. In these cases it can be observed that the estimated precipitation areas are in good agreement with the radar ones and also that higher PoPs have been assigned.

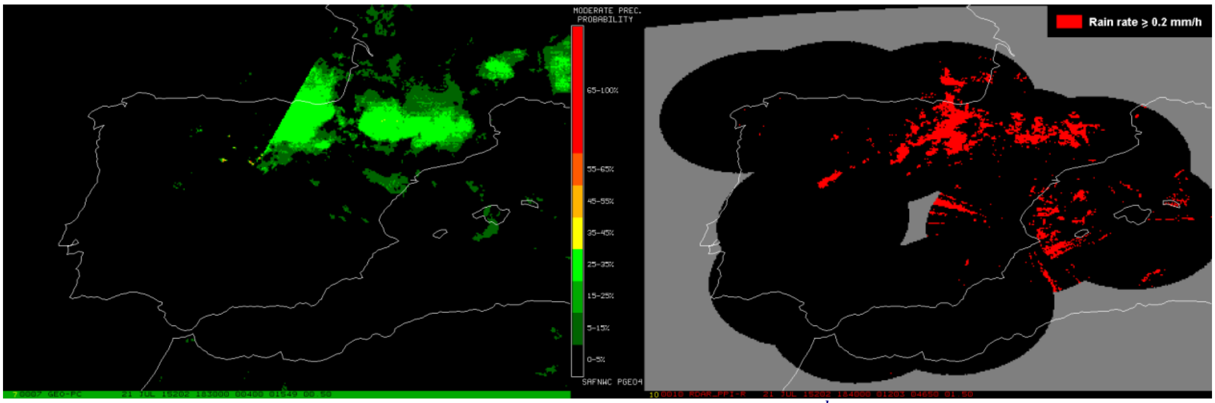

Figure 5. Comparison of PC product and radar (PPI) on 21th June 2015 at 18:30UTC

Figure 5 shows a scene with a day-night transition of PC algorithms. The day-time algorithm is displayed on the right side of the abrupt precipitation product transition. The night-time algorithm is displayed on the left side of this feature. At this time PC day-time algorithm is computed under poor illumination conditions, and so, there is a low confidence in the assignment of PoP. On the other hand night-time algorithm, which also shows a low confidence in the assignment of PoP, estimates bigger precipitation areas with more false alarms.

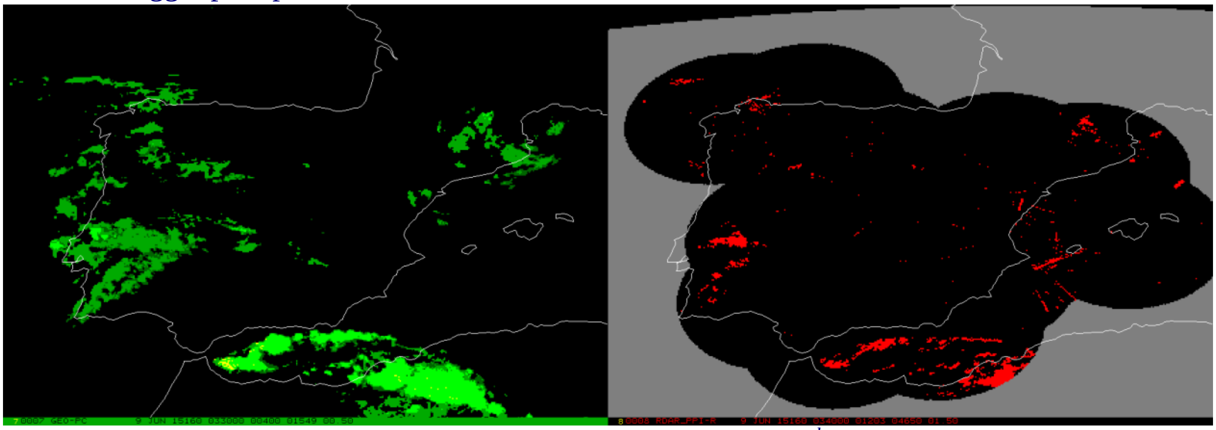

Figure 6. Comparison of PC product and radar (PPI) on 9th June 2015 at 03:30UTC

Figure 6 shows a night time scene where almost all precipitation areas depicted in the radar image are detected by PC product. However, since less information is contained in the night-time algorithm than in the day-time one, the confidence of PoP is lower. Also, the precipitation areas are overestimated providing a higher number of false alarms.

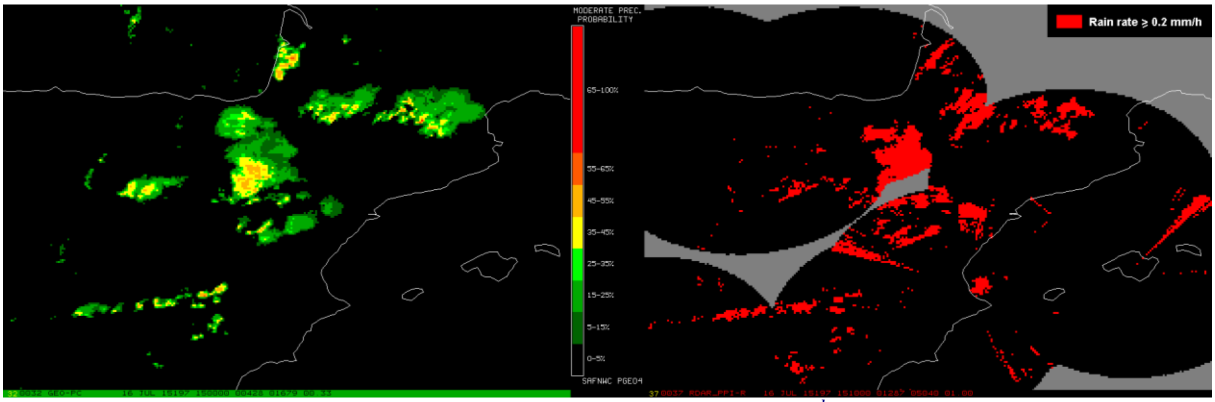

Figure 7. Comparison of PC product and radar (PPI) on 16th June 2015 at 15:00UTC.

Figure 7 shows a scene where there is a lack of several radars to compute a radar mosaic, and so there is no information over some areas. Here the usefulness of the PC product is shown. It is in agreement with the radar covered areas and complements its information over the rest of the image.

2.2 Objective Validation for Precipitating Clouds (PC)

2.2.1 Validation Procedure

An objective validation for the PC algorithm against Spanish composite radar data has been done. The dataset used for this validation contains 103 rainy days throughout 2008.

Both day-time and night-time algorithms have been validated. Day-time algorithm has been used for those cases with sun zenith angles lower than 80º and night-time algorithm has been used for the rest of the cases.

The original radar data is in Lambert projection, for a better matching, it has been customary reprojected to the MSG projection using a bi-linear interpolation scheme. The NWCSAF parallax tool *[RD 5]* has been applied to the PC product. A comparison against radar data in 3x3 MSG pixels boxes in a yes/no way has been done. The horizontal resolution of the pixels are 3kms at the sub-satellite point. It ranges from 6.88x3.51km at minimum resolution to 3.80x3.1km to the maximum resolution. As detection of very light rain rates using GEO satellite data is not possible, the threshold to consider a radar pixel as rainy has been fixed at 0.2 mm/h.

Ground echoes in PPI scenes have been removed. To do that, a filter image, available as a radar product, has been used in order to remove ground echoes (wind mills,…). Ground echoes, like anomalous propagation echoes, have been removed through the 10.8IR scene. To do that, a rain image has been obtained from the 10.8IR data using the basic AUTOESTIMATOR algorithm (Vicente et al., 1998). A pixel with significant radar echo is considered to be a ground echo and set to zero if no significant value is found in a 15x15 centred box in the AUTOESTIMATOR image.

Although satellite data have been used for decluttering the radar data, since this information has been used in a non-aggressive way, datasets are still independent enough for statistical comparison in the validation.

In order to avoid a high number of correct negative comparisons that can contaminate the computation of validation scores, the validation area has been restricted to 15x15 pixel boxes around radar pixels with at least 0.2 mm/h. As some PC rainy pixels can appear out of the previous validation area, those pixels have been added to the final validation area in order to include all the possible false alarms.

Due to the temporal resolution of the SEVIRI data in the normal mode, there are four PC outputs available every hour. The Spanish radar network generates a set of instantaneous products every 10 minutes. The MSG scanning over Spain is done over 10 minutes after the time of the slot. The only way to match temporally PC and radar scenes is choosing 0 and 30 minutes PC images corresponding to 10 and 40 minutes radar images respectively. As 15 and 45 minutes PC images don't match temporally with the radar ones, those images haven't been used in the validation process.

A smoothing in 3x3 MSG pixels boxes has been applied in order to reduce the radar and satellite estimations spatial mismatching. One every three ordered pixels of the smoothed fields have been taken into account.

The verification metric computed for this validation is described in ANNEX 1: .

Since this is a yes/no validation only categorical scores have been computed.

2.2.2 Probability of precipitation intervals validation:

Eight PoP intervals have been validated. These intervals have been chosen in line with the colour scale delivered with the product:

- 0-5%: $0\% < \text{PoP} \leq 5\%$
- 5-15%: $5\% < \text{PoP} \leq 15\%$
- 15-25%: $15\% < \text{PoP} \leq 25\%$
- 25-35%: $25\% < \text{PoP} \leq 35\%$
- 35-45%: $35\% < \text{PoP} \leq 45\%$
- 45-55%: $45\% < \text{PoP} \leq 55\%$
- 55-65%: $55\% < \text{PoP} \leq 65\%$
- 65-100%: $65\% < \text{PoP} \leq 100\%$

For each probability interval only the rainy area with the selected probability has been taken into account. According to this, POD will always be 100%. Attention should be focused on FAR. A region with the probability of precipitation interval (A-B] should have $100\text{-B} \leq \text{FAR} < 100\text{-A}$. For a better understanding of this, see Figure 8.Imagine a precipitation probability pattern estimated like the one in the left part of the image. And imagine that the 25-35% probability interval is going to be validated. In this case only the green area in the central part of the image would be taken into account for validation, for both observation and estimation. In this case, the entire green area would be a rainy area according to the estimation, and so, a probability of detection of 100% would be assigned to this area. This assumption is represented at the right part of the image. To check whether this area has in effect a 25-35% precipitation probability, attention should be focused on false alarms. So, if the precipitation probability is 25-35%, then, false alarm ratio should be 65-75%.

Figure 8. Drawing example of probability of precipitation intervals validation

The categorical scores obtained are showed in Table 3.

Probability interval (%)	N (Day algorithm)	FAR (%) (Day algorithm)	N (Night algorithm)	FAR (%) (Night algorithm)
0-5	580028	87,28	487349	88,17
5-15	874949	79,97	1238899	85,49
15-25	573867	67,38	1286422	73,09
25-35	331008	54,53	1100344	60,86
35-45	327523	47,64	191587	50,72
45-55	281118	37,56	1719	41,42
55-65	114062	27,21	527	9,11
65-100	24139	19,50	91	5,49

Table 3. Categorical scores for PC algorithm probability of precipitation intervals

It can be observed that PC algorithm provides FAR scores lower than expected, most of all for the highest probability intervals. It should be noted that the highest probability intervals include lower number of cases, most of all in the case of the night-time algorithm that assigns PoP with lower confidences, which is in agreement with the results observed during the subjective validation. The FAR for PoPs higher than 50% are even lower with respect to the FARs from the PoPs lower than 50%.

It can be also observed that the higher quality of the day-time algorithm obtained due to the valuable information provided by the solar channels, leads into lower FAR values for each probability interval.

2.2.3 Probability of precipitation thresholds validation:

Seven probability of precipitation thresholds have been validated. These thresholds are: 5%, 15%, 25% , 35% , 45% , 55% and 65% probability of precipitation.

For this kind of validation, the whole validation area has been taken into account and only pixels with a probability of precipitation higher than the specified threshold have been taken as satellite rainy pixels, all the other pixels are taken as non-rainy.

Probability of precipitation threshold (%)	N	FAR (%)	POD (%)	CSI (%)	PC (%)
5	5254532	61,91	87,09	36,06	67,52
15	5254532	52,34	71,23	39,97	77,50
25	5254532	44,34	54,29	37,90	81,29
35	5254532	39,82	40,67	32,05	81,86
45	5254532	33,71	25,15	22,30	81,57
55	5254532	25,86	9,27	8,98	80,24
65	5254532	19,50	1,76	0,02	0,79

Table 4. Categorical scores for PC day-time algorithm taking as rainy pixels those with probability of precipitation higher than the threshold

Probability of precipitation threshold (%)	N	FAR (%)	POD (%)	CSI (%)	PC (%)
5	6179225	72,44	89,55	26,70	53,23
15	6179225	66,18	74,26	30,27	67,47
25	6179225	59,31	44,81	27,11	77,08
35	6179225	50,50	8,17	7,54	80,95
45	6179225	32,73	0,13	0,13	80,99
55	6179225	8,58	0,05	0,05	80,99
65	6179225	5,49	0,01	0,01	80,98

Table 5. Categorical scores for PC night-time algorithm taking as rainy pixels those with probability of precipitation higher than the threshold

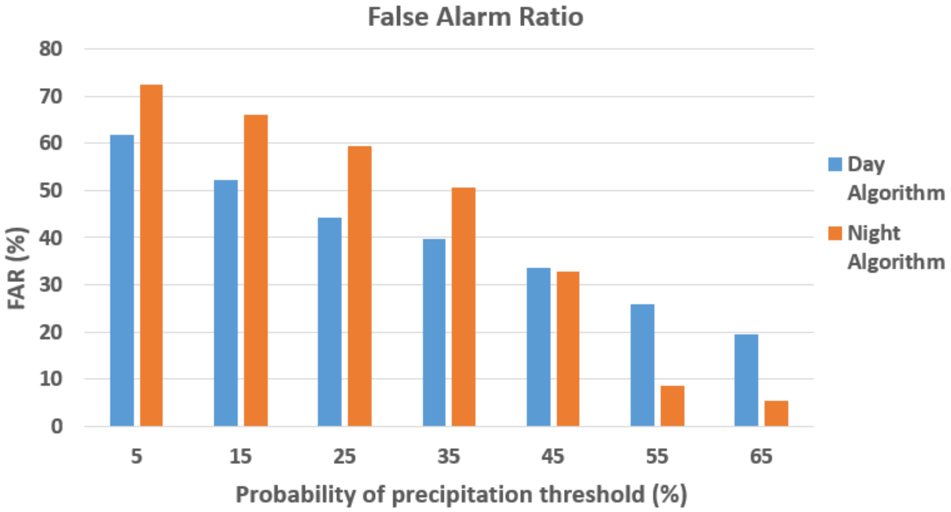

Figure 9. Comparison of day-time and night-time algorithms false alarm ratio

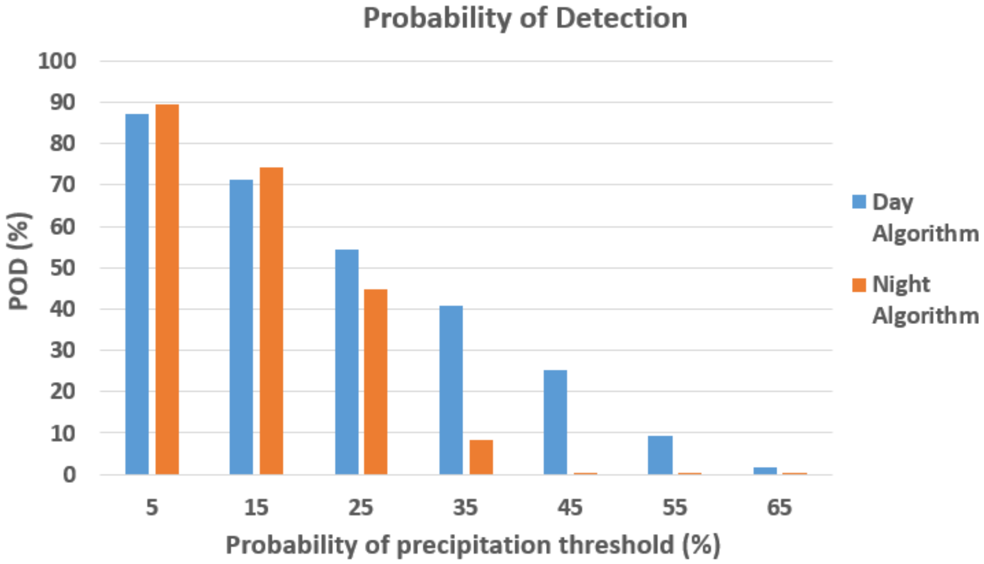

Figure 10. Comparison of day-time and night-time algorithms probability of detection

A clear better performance of the day-time algorithm over the night-time one can be observed in the graphs. Both lower FAR and higher POD have been obtained for the day-time algorithm for all the PoP thresholds. For 35% PoP and lower thresholds, POD is higher than FAR for the day-time algorithm. In the case of the night-time algorithm, this happens for 15% PoP threshold and the lower ones. For the higher PoP thresholds, scores get worse due to the low number of cases that reach these thresholds.

2.2.4 Conclusion

PC product catches most of the precipitation areas; however, probability of precipitation assigned, in a high number of cases, is underestimated. For this reason, although precipitation is detected, most of the time, is located in areas with PoPs lower than 55% for the day-time algorithm and lower than 45% in the case of the night-time one. PoPs higher than 65% are assigned few times in the case of the day-time algorithm and almost never in the case of the night-time one. So it is clear that the day-time algorithm provides better results than the night-time one due to the influence of the solar channels.

3. VALIDATION FOR CONVECTIVE RAINFALL RATE PRODUCT

This section contains the results obtained from the validation of the CRR product which is described in the "Algorithm Theoretical Basis Document for the Precipitation Product Processors of the NWC/GEO" *[RD 4]*.

3.1 SUBJECTIVE VALIDATION FOR CONVECTIVE RAINFALL RATE (CRR)

The monitoring of the precipitation pattern as well as its evolution is valuable information for the forecaster. In order to show the valuable information that CRR product can provide, a set of examples of CRR have been selected and compared to the radar estimations.

Next colour rain rate palate (mm/h) applies to figures 11-17 :

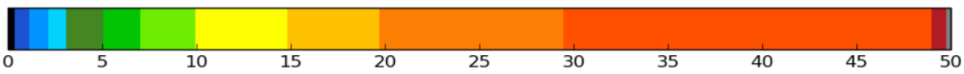

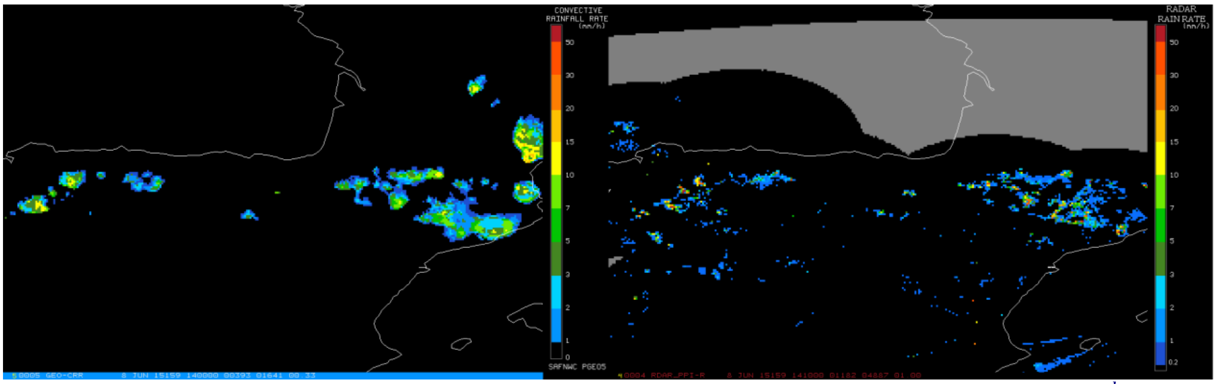

Figure 11. Comparison of CRR instantaneous rates product and radar rainfall rate on 8th June 2015 at 10:00UTC

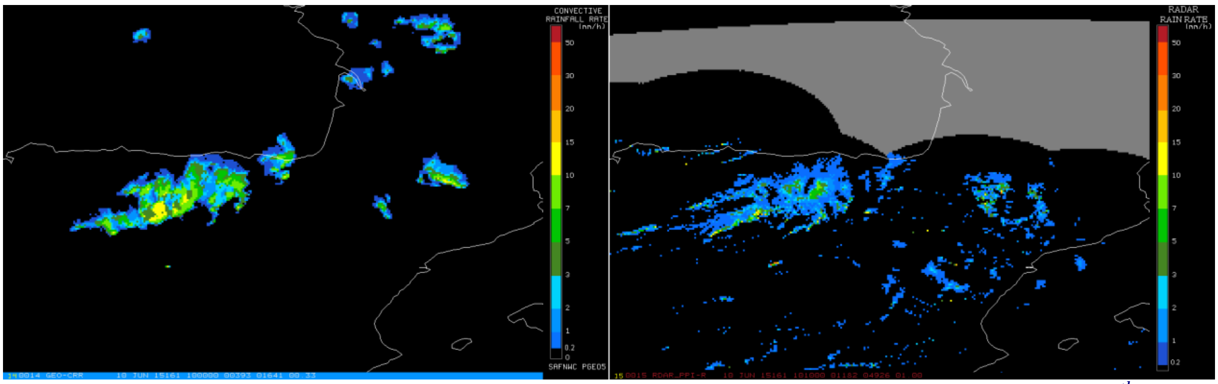

Figure 12. Comparison of CRR instantaneous rates product and radar rainfall rate on 10th June 2015 at 10:00UTC

Figure 11 and Figure 12 show a couple of comparisons of CRR instantaneous rain rates with radar PPI product where most of the precipitation areas have been detected by CRR. Although the CRR precipitation pattern is quite similar to the radar one and the maxima of precipitation match well in location, maximum CRR rain rates are in general lower than the radar ones.

It is well known that for this kind of product directly based on cloud top radiances it is very difficult to detect the smallest precipitation nuclei. And it is also difficult to detect the lowest rain rates. It can be observed in the images that the rainy area is well depicted but sometimes is overestimated, being very similar to the cloud top structure. And it can also be observed a general underestimation of the highest rain rates.

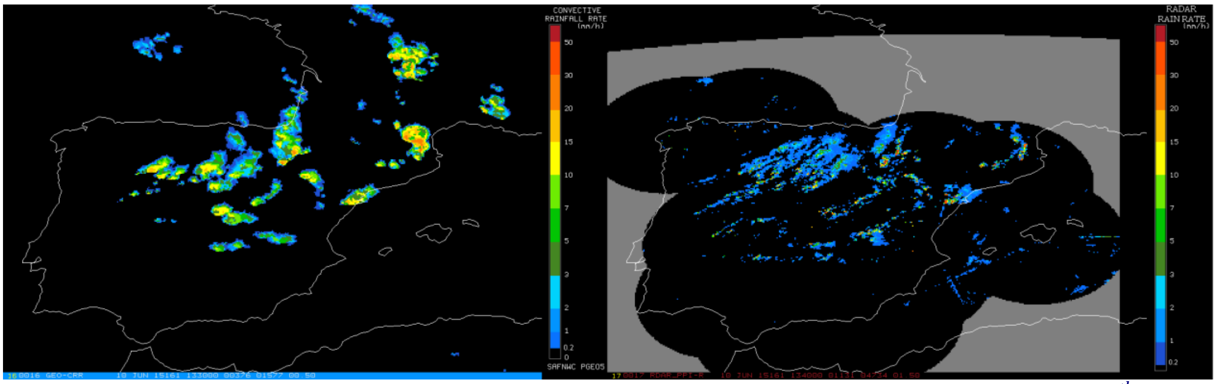

Figure 13. Comparison of CRR instantaneous rates product and radar rainfall rate on 10th June 2015 at 13:30UTC

Figure 13 shows an example of a good performance of CRR product day-time algorithm. Although the smallest rain nuclei are missed by CRR, the precipitation pattern is very similar to the radar one and the maximum rain rates are also very similar.

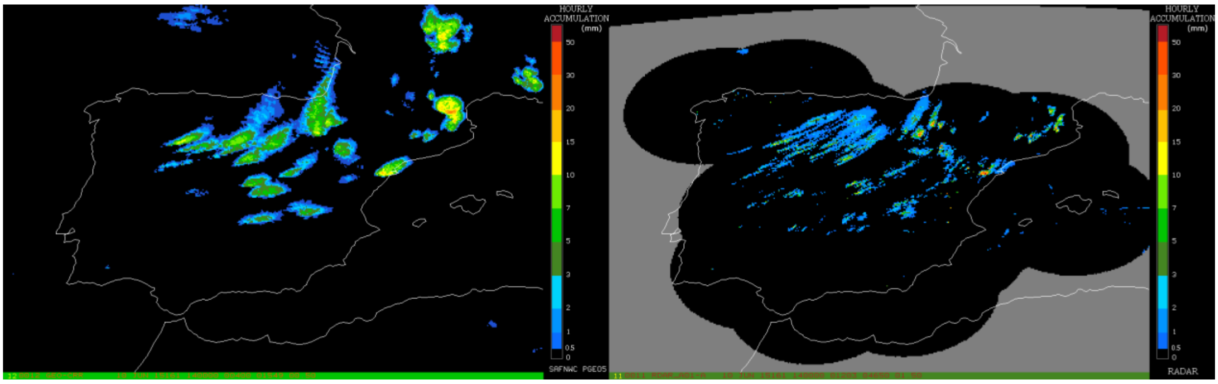

Figure 14. Comparison of CRR hourly accumulation product and radar hourly accumulation on 10th June 2015 at 14:00UTC

Figure 14 shows a comparison of hourly accumulation estimated by CRR and radar. Similar conclusions as in the case of instantaneous rain rates can be reached for hourly accumulations since hourly accumulations are obtained by using the instantaneous rain rates.

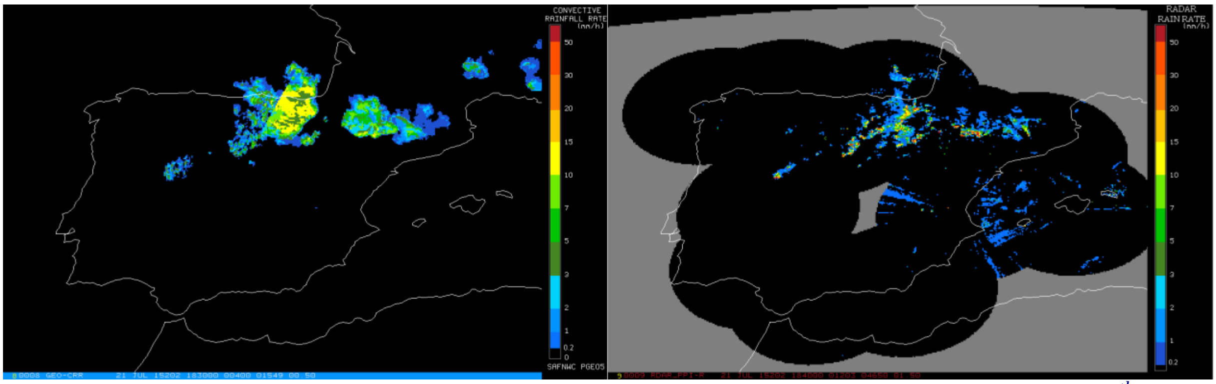

Figure 15. Comparison of CRR instantaneous rates product and radar rainfall rate on 21th June 2015 at 18:30UTC

Figure 15 shows a CRR day-night algorithm transition. The day-time algorithm is displayed on the left side of the abrupt precipitation product transition. The night-time algorithm is displayed on the right side of this feature. It is quite clear through this example the main differences between both algorithms. Day-time algorithm provides a rain pattern more adjusted to the radar one while night-time one is more similar to the cloud top, overestimating rainy areas. Day-time algorithm provides better results due to the important information included in the visible channel related to the cloud optical thickness.

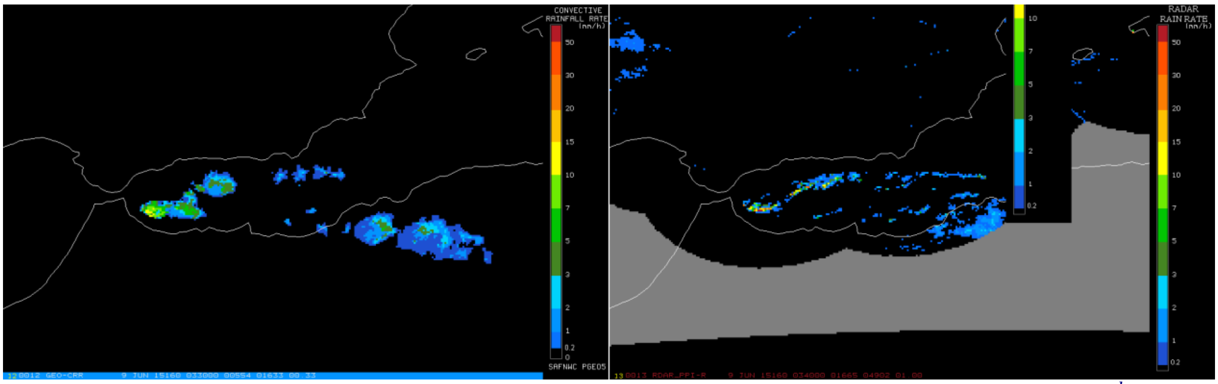

Figure 16. Comparison of CRR instantaneous rates product and radar rainfall rate on 9th June 2015 at 03:30UTC

Figure 16 shows an example of the night-time algorithm. Although quality is not as good as in the case of the day-time one, precipitation areas are very similar to the radar one, and maximum rain rates are well located.

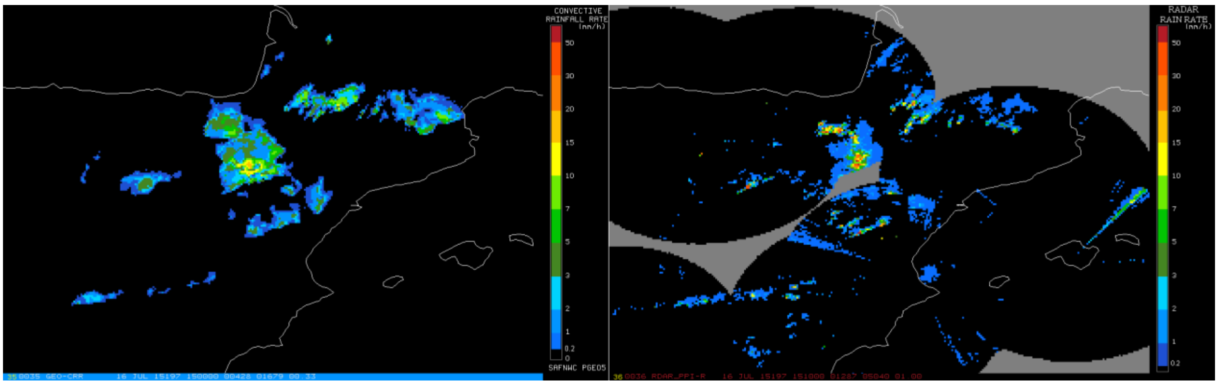

Figure 17. Comparison of CRR instantaneous rates product and radar rainfall rate on 16th June 2015 at 15:00UTC

Figure 17 shows an example of the usefulness of CRR information when radar does not totally cover the studied area. Precipitation areas in those places covered by radar are similar and complementary information can be obtained through CRR out of those areas.

3.2 OBJECTIVE VALIDATION FOR CONVECTIVE RAINFALL RATE (CRR)

3.2.1 Validation Procedure

The objective instantaneous rain rates validation has been done against instantaneous rates taken from Spanish radar PPI data and the hourly accumulations have been done against radar hourly accumulations obtained from the 500m Pseudo-CAPPI. The original data in Lambert projection has been customary reprojected on the MSG projection using a bi-linear interpolation scheme.

Ground echoes in PPI scenes have been removed. To do that, a filter image, available as a radar product, has been used in order to remove ground echoes (windmills, …). For instantaneous products there exists the possibility to remove ground echoes, like anomalous propagation echoes, through the 10.8IR scene. A rain image has been obtained from the 10.8IR data using the basic AUTOESTIMATOR algorithm (Vicente et al., 1998). A pixel with significant radar echo is considered to be a ground echo and set to zero if no significant value is found in a 15x15 centred box in the AUTOESTIMATOR image.

Although satellite data have been used for decluttering the radar data, since this information has been used in a non-aggressive way, datasets are still independent enough for statistical comparison.

In the instantaneous cases, since CRR product addresses convective situations, only images with convective echoes should be validated. In order to select those images, when in the ECHOTOP image the ratio between the number of pixels with ECHOTOP higher than 6 Km and the number of pixels with ECHOTOP higher than 0 Km is lower than 15%, the radar images have been rejected. This procedure tends to discard non-convective precipitation.

Images with convective situations can also include non-convective echoes. In order to validate only the convective ones, a validation area has been selected taking into account the convective area that has been calculated in each image. To do that, PPI and ECHOTOP images have been used. The convective area in the instantaneous images has been made up of 15x15 pixels boxes centred on pixels that reach a top of 6 km and a rainfall rate of 3 mm/h simultaneously. In the hourly accumulations, the validation area has been chosen adding the validation areas in the corresponding instantaneous images. As some CRR rainy pixels can appear out of the convective area, these pixels have been added to the validation area in order to include all the possible false alarms.

The perfect matching between images will never be reached so a smoothing process in a 3x3 pixels base has been done. The horizontal resolution of the pixels are 3kms at the sub-satellite point. Pixel resolution ranges from 6.88x3.51km at the north of the Spanish Península to 3.8x3.1km at the south. Then a pixel by pixel (every three pixels) comparison has been carried out. The definition of the statistics computed can be checked at ANNEX 1: .

The CRR values have been obtained applying all the corrections with the default values *[RD 4]*. The fields for the moisture, parallax and orographic corrections have been extracted from ECMWF at 0.5 x 0.5 degree spatial resolution, every 3h.

The dataset used for the validation of both algorithms contains 78 days with convective events along 2008. Accuracy and categorical statistics described in ANNEX 1: have been computed for instantaneous rain rates and for hourly accumulations.

3.2.2 Instantaneous Rain Rates

According to the procedure described above, the statistical accuracy measurements are shown in the following table:

Algorithm	N	Mean (mm/h)	ME (mm/h)	MAE (mm/h)	RMSE (mm/h)
Day time	832614	0,58	0,54	1,19	2,97
Night time	877299	0,62	0,82	1,55	3,18

Table 6. Accuracy measurements for instantaneous rates

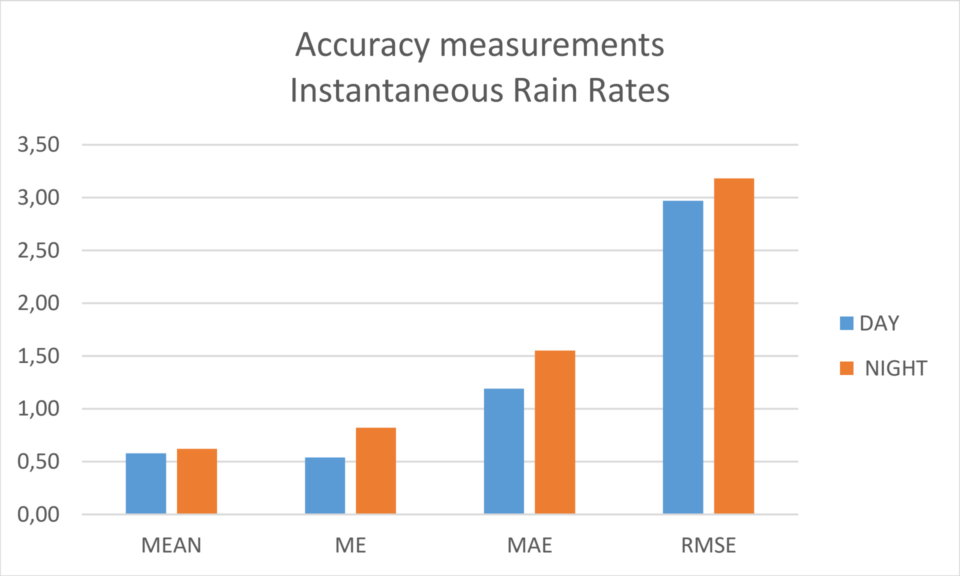

Figure 18. Accuracy measurements for CRR instantaneous rates

Although both day-time and night-time algorithms provide similar results, it can be observed a slight better performance in the day-time algorithm according to the results showed in Figure 18. This can be explained, as seen during the subjective validation, because day-time algorithm adjust better precipitation areas reducing error with respect to the night-time ones.

Categorical scores for CRR can be obtained assuming that values higher than or equal to 0.2 mm/h for instantaneous rates are considered rainy. Results are shown in Table 7.

Algorithm	FAR (%)	POD (%)	CSI (%)	PC (%)
Day time	34,13	63,26	47,64	64,55
Night time	45,53	53,74	37,08	54,57

Table 7. Categorical scores for CRR instantaneous rates

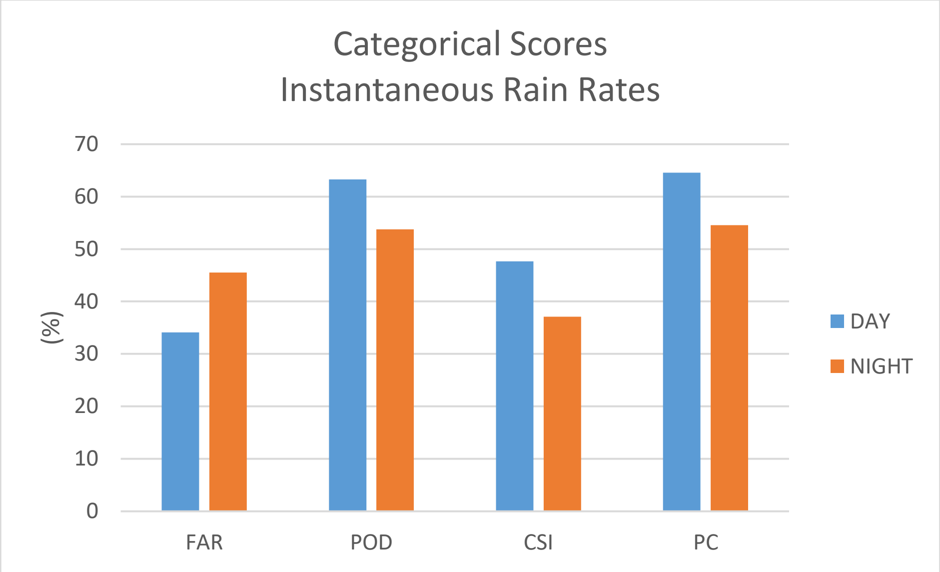

Figure 19. Categorical scores for CRR instantaneous rates

Figure 19 also brings to light the better estimations of the day-time algorithm that provides lower FAR and higher POD than the night-time one. These results, showed also in Table 7, fulfil the FAR and POD target values defined in the "NWCSAF Product Requirements document "*[AD. 4]*.

3.2.3 Hourly accumulations

Accuracy measurements, obtained statistically as explained above, for hourly precipitation accumulations are shown in Table 8.

Algorithm	N	Mean (mm/h)	ME (mm/h)	MAE (mm/h)	RMSE (mm/h)
Day time	465555	0,37	0,43	0,80	1,96
Night time	598562	0,40	0,57	0,99	2,19

Table 8. Accuracy measurements for CRR hourly accumulations

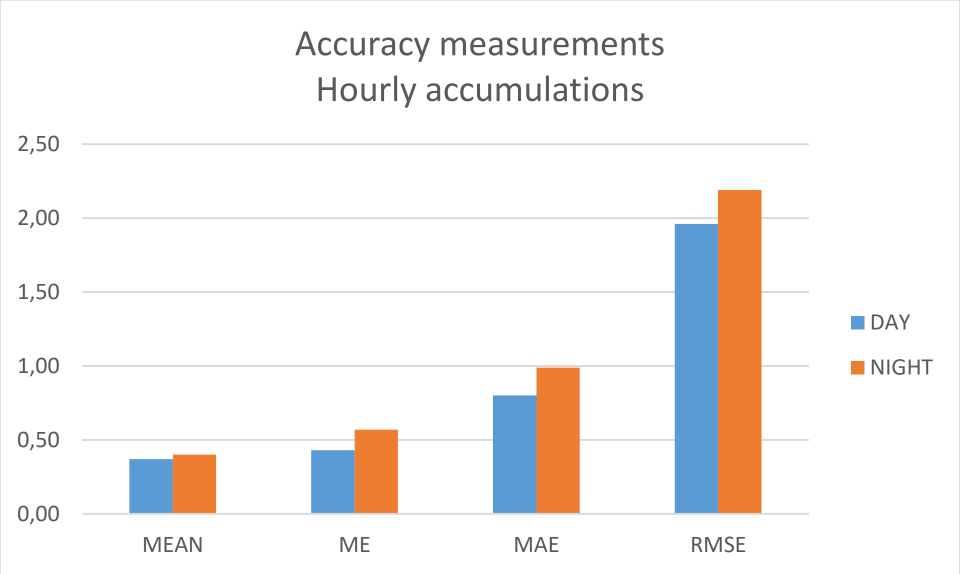

Figure 20. Accuracy measurements for CRR hourly accumulations

Since hourly accumulations have as a base the instantaneous rain rates, similar results are expected. Figure 20 show that accuracy measurements take lower values for hourly accumulations than for instantaneous rain rates. This happens because hourly accumulations fields are smoother than instantaneous rain rates ones. Better performance of the day-time algorithm with respect to the night-time one can be seen.

Categorical scores can be obtained assuming that values higher than or equal to 0.2 mm/h for hourly precipitation accumulations are considered rainy. Results are shown in Table 9.

Algorithm	FAR (%)	POD (%)	CSI (%)	PC (%)
Day time	51,07	65,33	38,84	63,17
Night time	58,19	56,43	31,61	56,29

Table 9. Categorical scores for CRR hourly accumulations

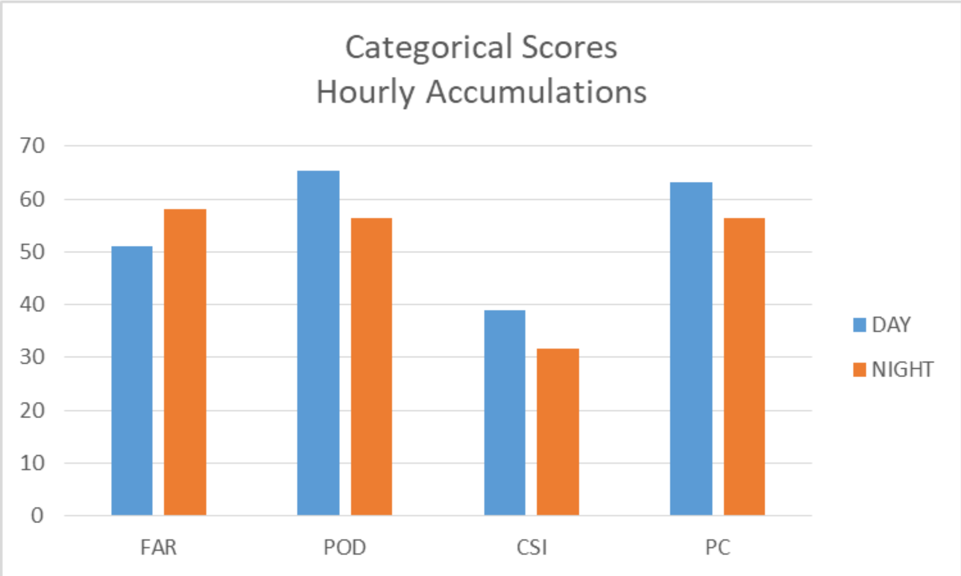

Figure 21. Categorical scores for CRR hourly accumulations

As for categorical scores, Figure 21 shows also the better estimations provided by the day-time algorithm and results from Table 9 fulfil the FAR and POD target values defined in the "NWCSAF Product Requirements document "*[AD. 4]*.

3.2.4 Conclusion

Algorithm	Threshold Accuracy FAR (%)	Target Accuracy FAR (%)	Optimal Accuracy FAR (%)	FAR (%)
3 - Variables	<60	<40	<38	34.13
2 - Variables	<65	<50	<44	45.53

Table 10. Comparison of CRR instantaneous rates FAR scores and FAR accuracy values defined in the NWCSAF Product Requirement table

Algorithm	Threshold Accuracy POD (%)	Target Accuracy POD (%)	Optimal Accuracy POD (%)	POD (%)
3 - Variables	>40	>53	>87	63.26
2 - Variables	>35	>47	>85	53.74

Table 11. Comparison of CRR instantaneous rates POD scores and POD accuracy values defined in the NWCSAF Product Requirement table

Algorithm	Threshold Accuracy FAR (%)	Target Accuracy FAR (%)	Optimal Accuracy FAR (%)	FAR (%)
3 - Variables	<65	<55	<45	51.07
2 - Variables	<70	<60	<50	58.19

Table 12. Comparison of CRR hourly accumulations FAR scores and FAR accuracy values defined in the NWCSAF Product Requirement table

Algorithm	Threshold Accuracy POD (%)	Target Accuracy POD (%)	Optimal Accuracy POD (%)	POD (%)
3 - Variables	>45	>58	>95	65.33
2 - Variables	>37	>50	>90	56.43

Table 13. Comparison of CRR hourly accumulations POD scores and POD accuracy values defined in the NWCSAF Product Requirement table

4. VALIDATION FOR PRECIPITATING CLOUDS FROM CLOUD PHYSICAL PROPERTIES PRODUCT

This section contains the results obtained from the validation of the PCPh product which is described in the "Algorithm Theoretical Basis Document for the Precipitation Product Processors of the NWC/GEO "*[RD 4]*.

The validation procedure consists of two parts:

- ✓ A subjective validation
- ✓ An objective validation

The first method of validation consist of visually checking the PCPh output against a radar composite for different time slots.

The objective validation is based on a categorical pixel by pixel comparison between the Spanish composite radar data and the PCPh product.

POD and FAR scores will be the metrics used to evaluate the product.

4.1 SUBJECTIVE VALIDATION FOR PRECIPITATING CLOUDS FROM CLOUD PHYSICAL PROPERTIES (PCPH)

In this section a visual check is possible by comparing the probability of precipitation (PoP) obtained from the PCPh algorithm against the radar data.

This subjective study has focused on rainy episodes throughout 2016. Different day and night time slots have been chosen to depict the PCPh general behaviour.

A pair of images are shown to subjectively validate the PCPh product: Rainy pixels extracted from the Spanish radar reflectivity composition and the probability of precipitation.

The image on the right side corresponds with the radar rainfall rate (RFR) and the image on the left side corresponds with the PCPh output (see Figures 22-29 for day time and Figures 30-34 for night time).

4.1.1 DAY

As far as the visualization of PCPh output is concerned pixels with NO DATA have been plotted in grey, due to an undefined phase or No data or corrupted data input. Black colour stands for no probability of rain.

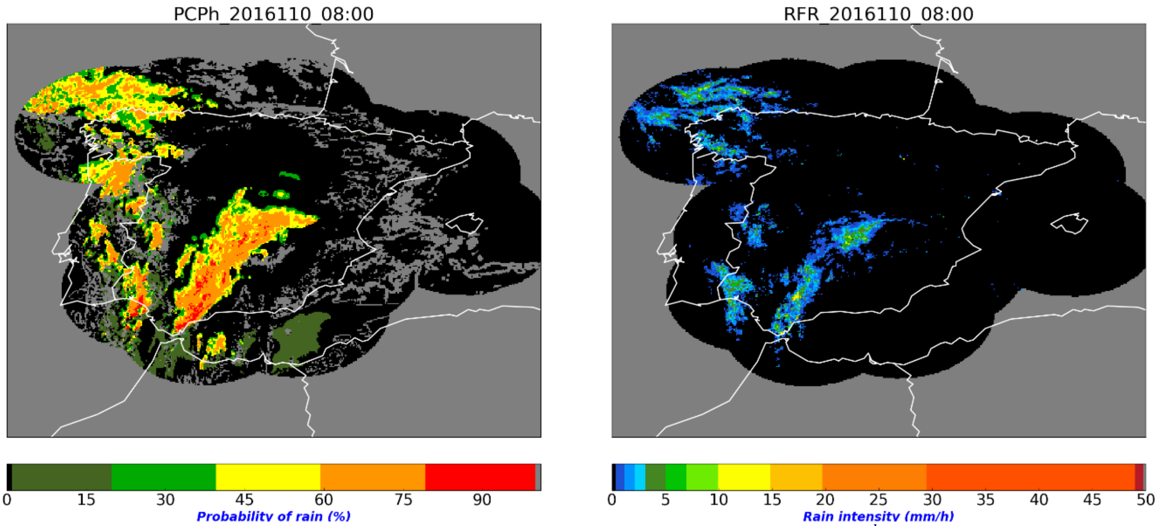

Figure 22. Comparison of PCPh day product and radar rainfall rate on 19th April 2016 at 08:00UTC

Figure 22 is an example of PCPh day algorithm. There is a general good agreement between the precipitating area provided by the Spanish radar and the probability of rain.

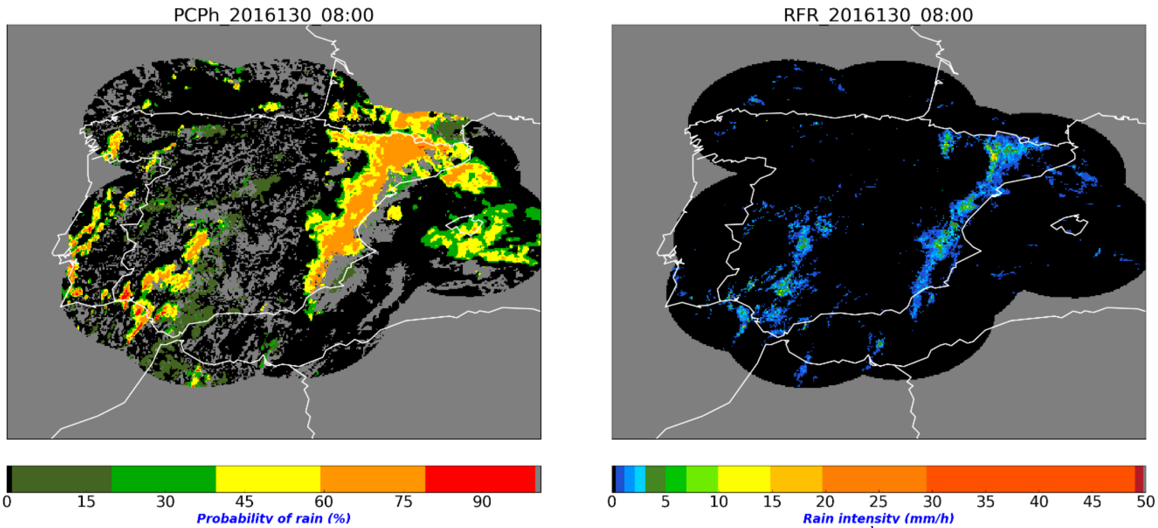

Figure 23. Comparison of PCPh day product and radar rainfall rate on 9th May 2016 at 08:00UTC

In Figure 23, it can also be checked that the rainy areas depicted by the Spanish radar match with the higher values of the PCPh day output. In this occasion, it appear an area near the Balearic Islands where the probability of rain is higher to 30% and there are only little pixels classified as rainy in the Spanish composite radar.

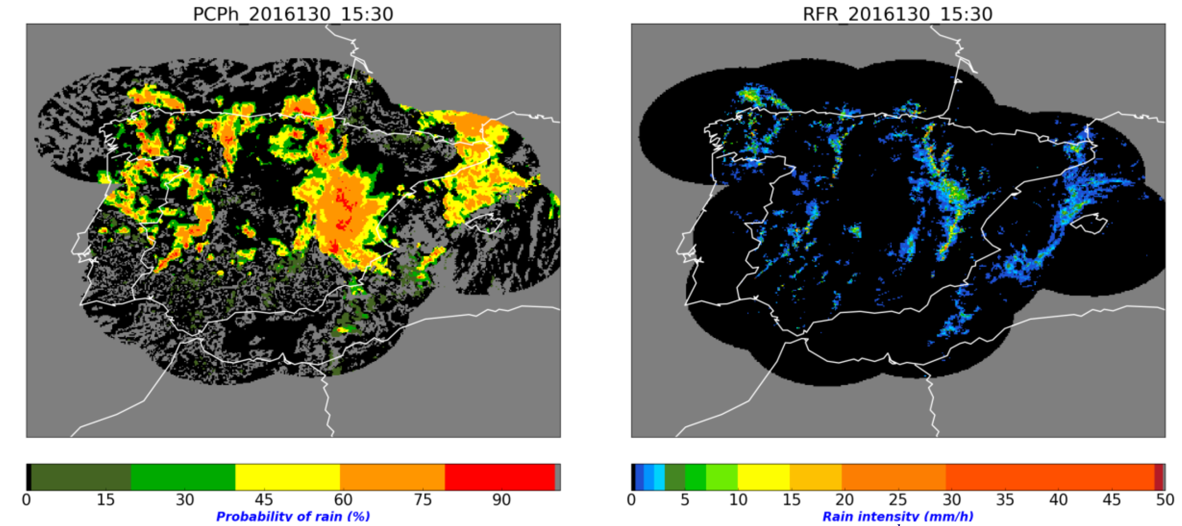

Figure 24. Comparison of PCPh day product and radar rainfall rate on 09th May 2016 at 15:30UTC

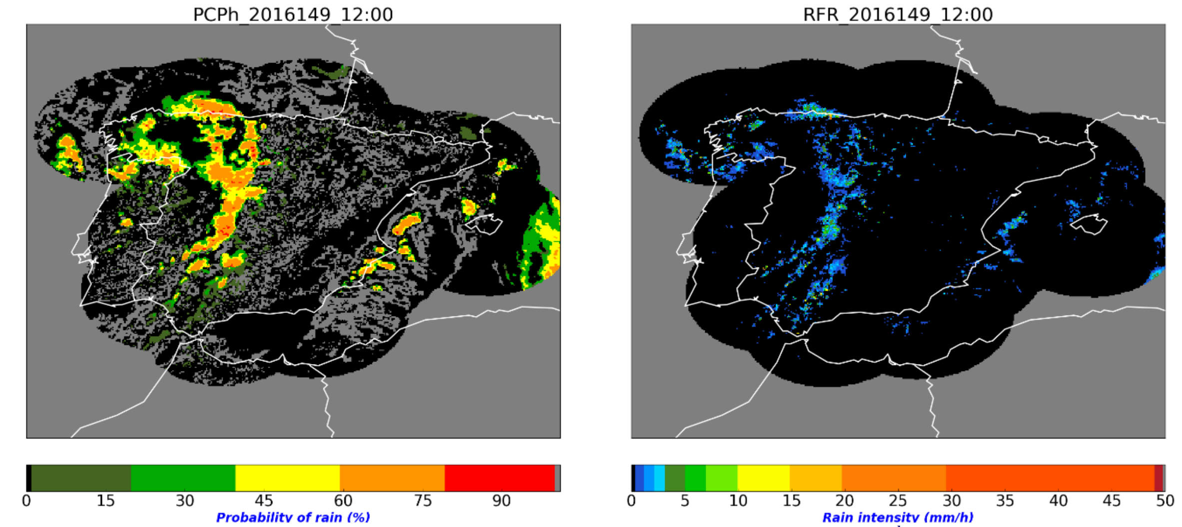

Figure 25. Comparison of PCPh day product and radar rainfall rate on 28th May 2016 at 12:00UTC

Figures 24 and 25 are good examples of a good performance of PCPh day product. Almost every area with rain represented in the Spanish composite radar has a correspondence in the probability of rain. It can also be noticed that the higher rain rates values provided by the Spanish radar correspond with the higher values in the probability of rain.

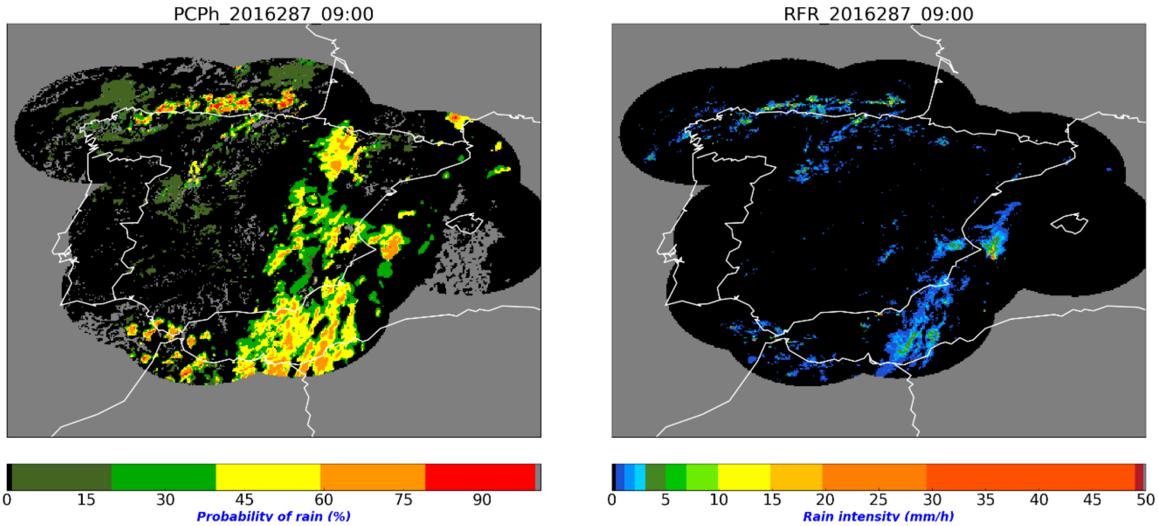

Figure 26. Comparison of PCPh day product and radar rainfall rate on 13th October 2016 at 09:00UTC

In Figure 26, it can be noticed that, in the Iberian mountain range there is black hole with the shape of a ring, just inside an area with probability of rain. It is due to the stability correction factor. This correction factor is set by default but it can be turned off. What this correction factor do is to remove areas with no probability of rain based on NWP stability indexes (Showalter, Lifted and K). That is the reason why in some occasions it appears a black whole inside a probability of rain precipitating area. More information about this correction factor can be found in the "Algorithm Theoretical Basis Document for the Precipitation Product Processors of the NWC/GEO "*[RD 4]*.

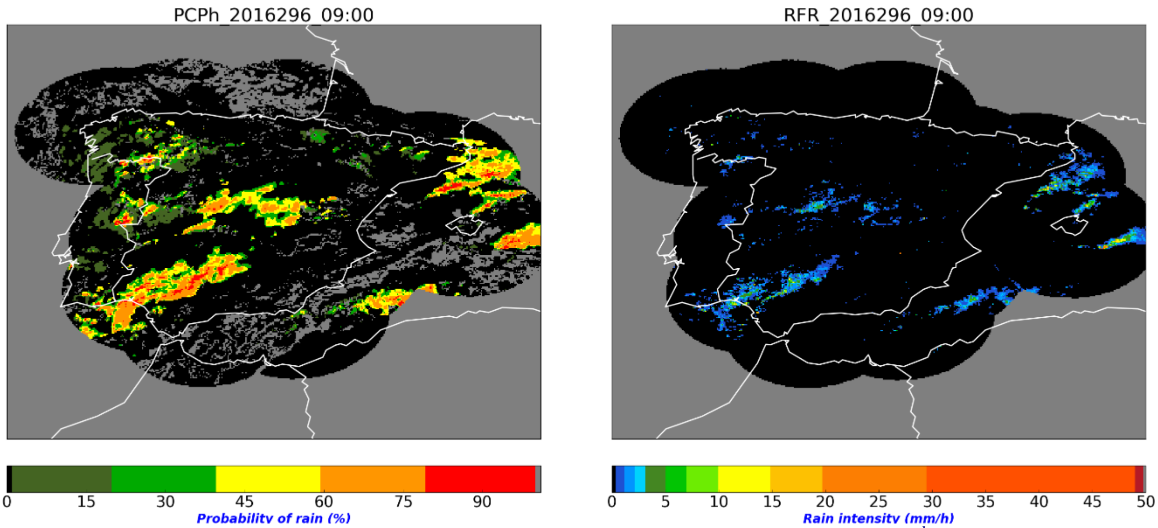

Figure 27. Comparison of PCPh day product and radar rainfall rate on 22th October 2016 at 09:00UTC

This last example of PCPh day algorithm shows the product is able to detect little precipitation areas located in several regions of the Iberian Peninsula: in the mountains of León, south of the Pyrenees, the central part of the Iberian Peninsula and in between the Cape of Gata and the Cape of Palos, for example.

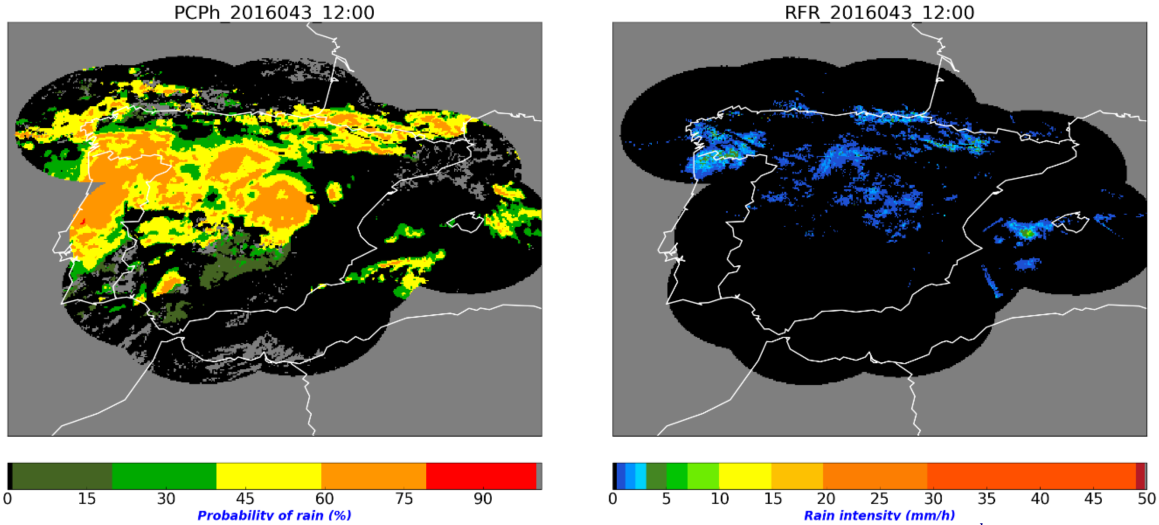

Figure 28. Comparison of PCPh day product and the Spanish radar composite on 12th February 2016 at 12:00UTC

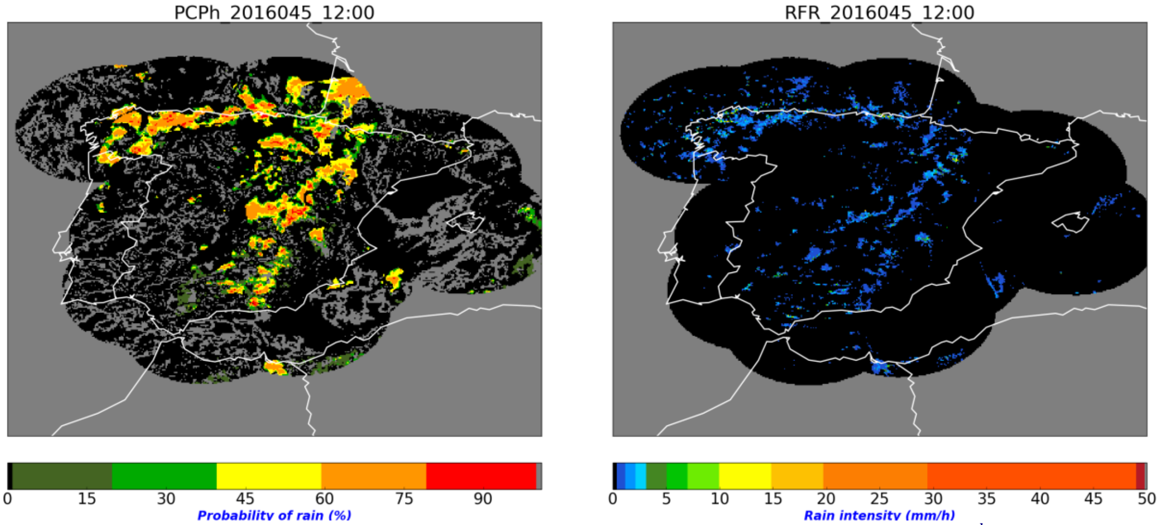

Figure 29. Comparison of PCPh day product and the Spanish radar composite on 14th February 2016 at 12:00UTC

To finish with the subjective validation of PCPh day algorithm, to more examples are displayed, corresponding with winter time (Figures 28 and 29). In Figure 28, PCPh tends to extend the PoP to a wider area, whilst in Figure 29 the visual match seems to be more accurate.

4.1.2 NIGHT

PCPh night standards visualization are the same as day time. Hence, grey colours apply to NO DATA pixels, due to an undefined phase or No data or corrupted data input. Black colour stands for no probability of rain.

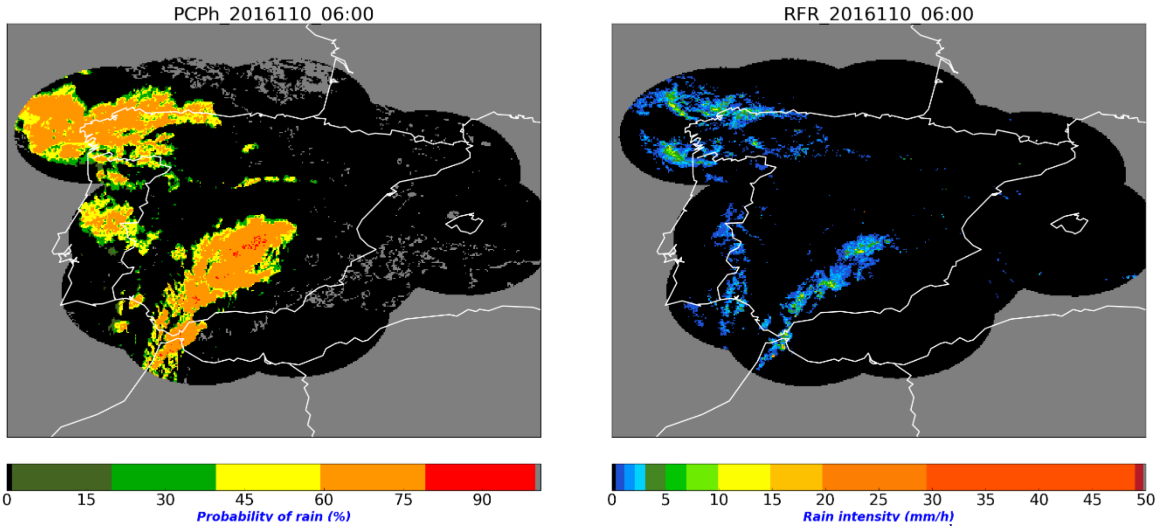

Figure 30. Comparison of PCPh night product and radar rainfall rate on 19th April 2016 at 06:00UTC

In this example of PCPh night algorithm there also exits a good agreement between the rainy areas depicted in the Spanish radar and the probability of rain. However, it seems the precipitating areas are overestimated. That will be traduced in a higher proportion of False Alarm rates.

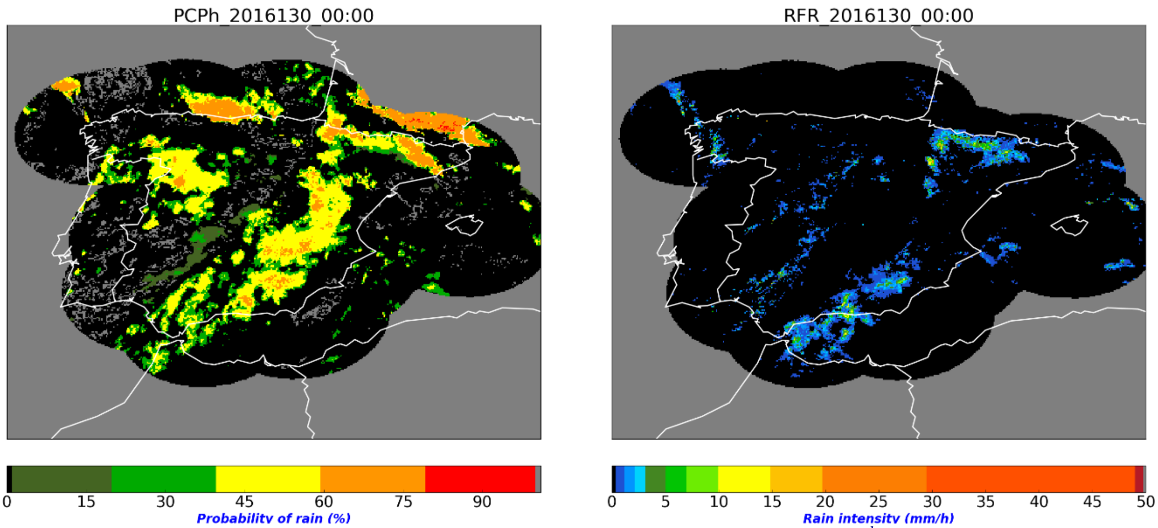

Figure 31. Comparison of PCPh night product and radar rainfall rate on 9th May 2016 at 00:00UTC.

As happened in the previous example, there is a general good performance of the PCPh night algorithm, except for the region in the North of the Iberian Peninsula covering Asturias and Cantabria where it seems it is not raining according to the Spanish radar.

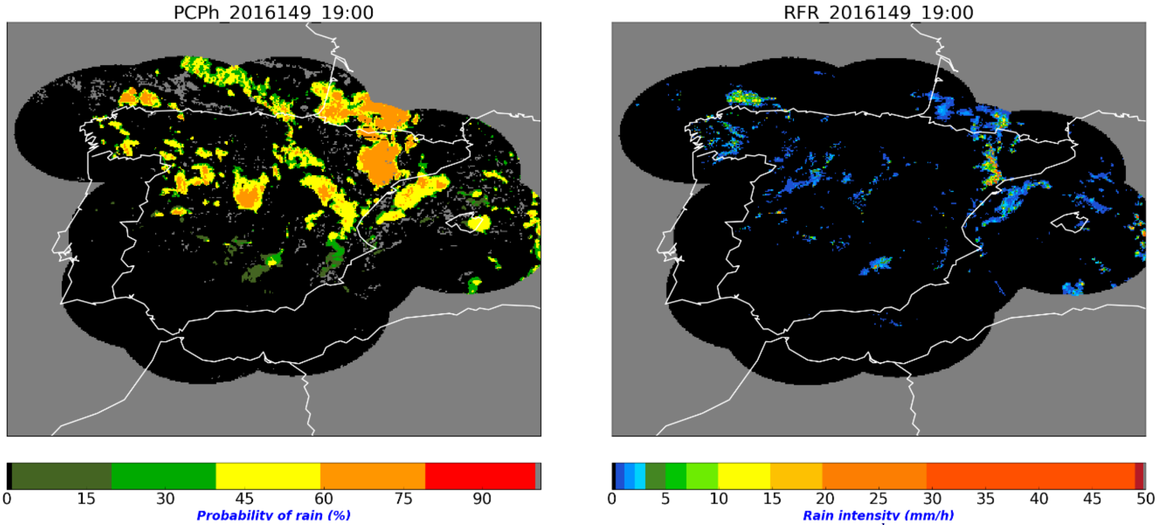

Figure 32. *Comparison of PCPh night product and radar rainfall rate on 28th May 2016 at 19:00UT*

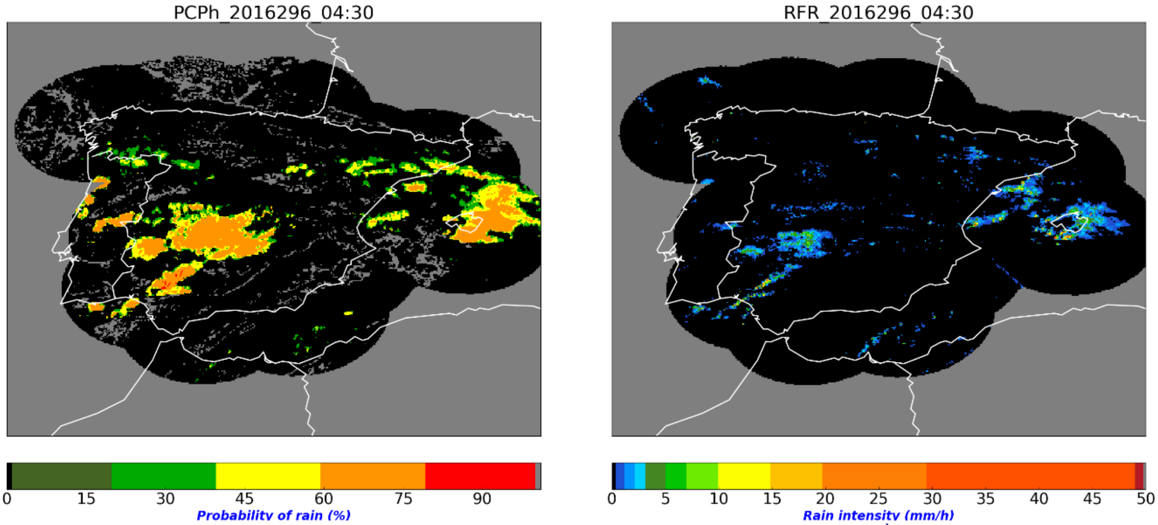

Figure 33. Comparison of PCPh night product and radar rainfall rate on 22th October 2016 at 04:30UT

Figures 32 and 33 show a night scene where, overall, almost all precipitation areas depicted in the radar image are detected by PCPh. It can be noticed that PCPh night version tends to show larger precipitation areas than the radar (False alarms increases). At night time, it can also be observed that PCPh do not reach some high values of probability of precipitation compared with day time PCPh algorithm. This can be attributed to the lack of the visible channels and the cloud microphysics. Although a simulation of the VIS0.6 and the Cloud Water Path is done at night time, this simulations are not perfect. That is possibly the reason why PCPh night algorithm tends to provide lower values. More information about PCPh day and night algorithm can be found in the "Algorithm Theoretical Basis Document for the Precipitation Product Processors of the NWC/GEO "*[RD 4]*.

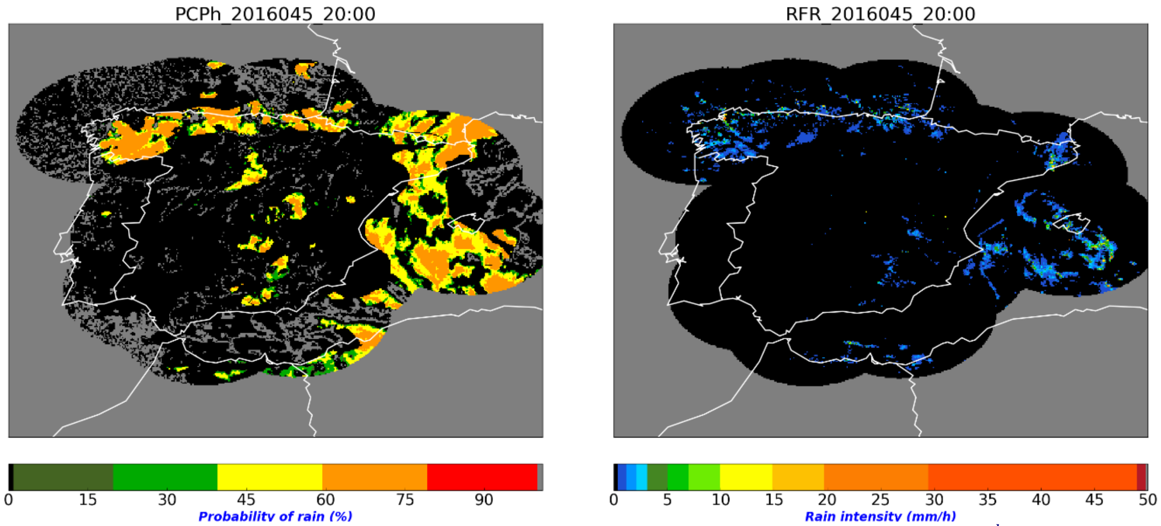

Figure 34. Comparison of PCPh night product and the Spanish radar composite on 14th Febrary 2016 at 20:00UTC.

Figure 34 corresponds with an example of PCPh night performance in winter season. At first sight it seems that most of the precipitation areas seems to be well reproduced. At the north of Spain the effects of the stability correction are noticed, reducing the number of PoP cells. Additionally, according to the national radar composite (on the right side) there are some little precipitating areas in the Alboran sea that the PCPh product does not detect.

4.2 Objective validation for Precipitating Clouds from Cloud Physical Properties (PCPh)

4.2.1 Validation Procedure: Common to PCPh and CRRPh

PCPh and CRRPh algorithms have been compared against the Spanish composite radar. An objective validation based on POD and FAR metrics has been conducted. It will be checked if the Requirements included in the "NWCSAF Product Requirements Document" [AD 4] are met.
A day-night distinction has been included.

Every slot has been classified as day slot, night slot or mixed, depending on the number of day or night pixels of each image. In order to evaluate the day algorithm separately from the night algorithm, mixed slots have been discarded. This way a day or night slot only contains pixels of the same category.

PCPh and CRRPh products have been calibrated with a list of days throughout 2015 that accomplished at least one of two criteria. They are based on echotop (ET) and rainfall rate (RFR). Another list of days has been created throughout 2016, with the same criteria as 2015, to validate the product.

RFR in mm/h is obtained from the lowest Plan Position Indicator (PPI) of the radar using the Marshal-Palmer relation, $Z=200R^{1.6}$, where Z ($mm^6\ mm^{-3}$) is the reflectivity factor and R($mm\ h^{-1}$)

is the rainfall rate. Echotop values in km. correspond with the maximum height that echoes bigger than 12dBz are able to reach.

First criterion: A particular day is included in the calibration and validation list if the percentage of pixels with ET>6km. with respects to pixels with ET>0 km exceeds the threshold of 65% at least for one slot of this day.

Second criterion: It is calculated the proportion of radar pixels with RFR>=0.2mm/h with respect to the whole image. Whenever at least one slot of a day reaches the percentage limit of 8% the day was also included in the calibration and validation list.

Since Microphysical Cloud Top parameters used by PCPh and CRRph have been computed only for sun zenith angles lower than 70º, this validation has been undertaken under the same condition.

Both PCPh and CRRPh products assign NO DATA value to those pixels with undefined phase according to the phase output of the CMIC product, which means that no information on whether the cloud consists of water or ice is available. Those pixels have been excluded in the algorithm validation.

Radar data, which are in Lambert Projection with a 1km*1km pixel resolution, have been converted into the MSG projection, using a bi-linear interpolation. The horizontal resolution of the MSG pixels are 3kms at the sub-satellite point, that in case of our area of interest, ranges from 6.9x3.5km at the north of the Spanish Península to 3.8x3.1km at the south. Parallax correction has been applied to PCPh and CRRPh. As a perfect matching between Radar and MSG images is not possible, a smoothing process in 3x3 boxes pixels has been done. The threshold to consider a pixel to rainy has been fixed at 0.2 mm/h because detection of very light rain rates using GEO satellite data is not possible.

A radar quality image has been used as a filter image to get rid of spurious echoes, such as windmill echoes. Anomalous propagation echoes have been removed through the 10.8IR scene. A rain image has been obtained from the 10.8IR data using the basic AUTOESTIMATOR algorithm (Vicente et al., 1998). A pixel with significant radar echo is considered to be a ground echo and set to zero if no significant value is found in a 15x15 box centred in the AUTOESTIMATOR image.

Due to the temporal resolution of the SEVIRI data in the normal mode, there are four satellite derived outputs available every hour. The Spanish radar network generates a set of instantaneous products every 10 minutes. The MSG scanning over Spain is done over 10 minutes after the slot hour. The only way to temporally match precipitating products (PCPh and CRRPh) with radar images is choosing 0 and 30 minutes PCPh/CRRPh images corresponding to 10 and 40 minutes radar images respectively. This way 15 and 45 minutes PCPh/CRRPh images, which do not temporally match with the radar images, have not been used in the validation process.

PCPh and CRRPh values have been obtained applying all the corrections with the default values *[RD 4]*. The fields for the stability correction have been extracted from ECMWF at 0.5 x 0.5 degree spatial resolution, every 6h.

Categorical statistic have been used to validate de product. They are explained in ANNEX 1: VERIFICATION METRIC.

ONLY TO PCPh:

PCPh has been validated in the same conditions it have been calibrated. Hence, Boxes size of 25*25 pixels centred in those radar pixels with rain rates > 0.2 mmh^{-1} have been selected. No restriction to echotops have been set.

4.2.2 Probability of precipitation categorical thresholds validation

Six different probability of precipitation thresholds have been stablished to check the dependence of the categorical validation process with those thresholds. The chosen thresholds go from 10% to 60% in increasing steps of 10% probability of precipitation for the PCPh product.
Within all of the following PCPh categorical thresholds validation, rainy pixels from the radar are fixed to at least 0.2 mm/h in every of them.

DAY:

PoP threshold (%)	N	POD (%)	FAR (%)	CSI (%)	PC (%)
10%	28839291	**75.38**	**51.35**	41.98	86.62
20%	28839291	**68.12**	**47.41**	42.2	88.03
30%	28839291	60.86	**43.63**	41.37	88.93
40%	28839291	51.02	**37.99**	38.87	89.7
50%	28839291	37.25	**30.46**	32.02	89.85
60%	28839291	20.55	**21.2**	19.47	89.09

Table 14. Categorical scores for PCPh day algorithm taking as rainy pixels those with probability of precipitation higher than the threshold.

NIGHT:

PoP threshold (%)	N	POD (%)	FAR (%)	CSI (%)	PC (%)
10%	135968389	**62.63**	66.64	27.82	83.88
20%	135968389	**57.82**	65.12	27.80	85.10
30%	135968389	**53.63**	63.87	27.43	86.02
40%	135968389	46.37	62.55	26.13	86.99
50%	135968389	36.37	60.95	23.20	88.05
60%	135968389	25.08	**59.53**	18.32	88.90

Table 15. Categorical scores for PCPh night algorithm taking as rainy pixels those with probability of precipitation higher than the threshold.

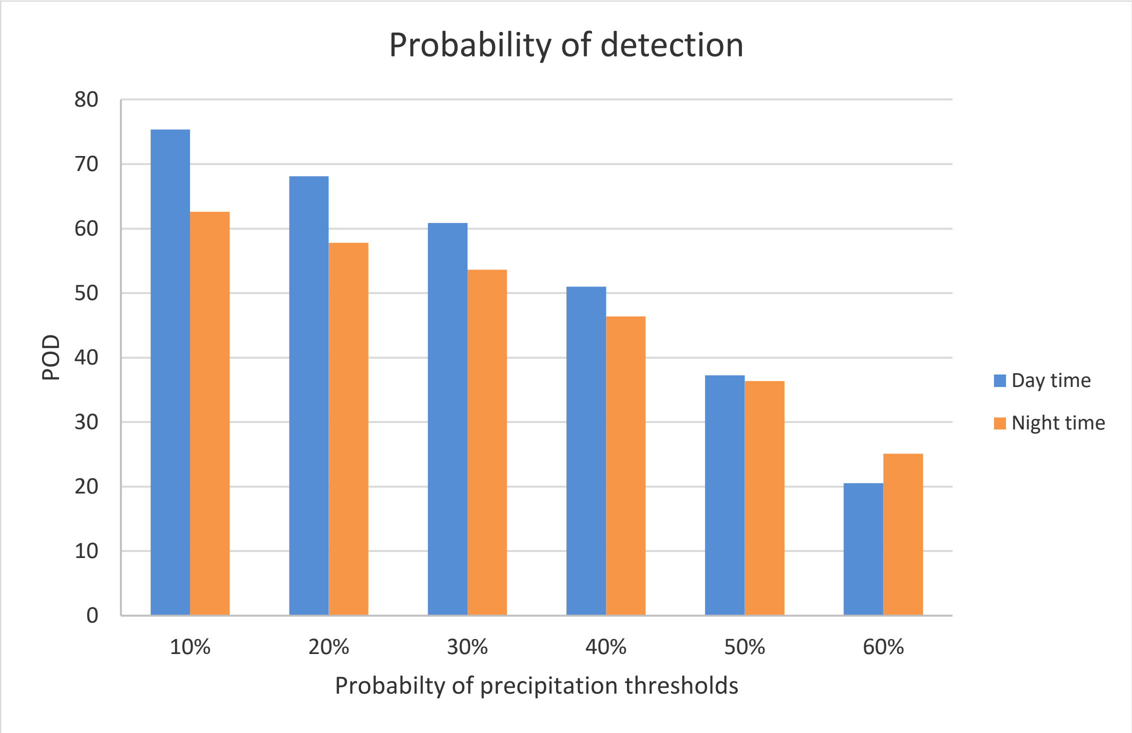

Figure 35. Probability of detection comparison between day time and night time algorithms.

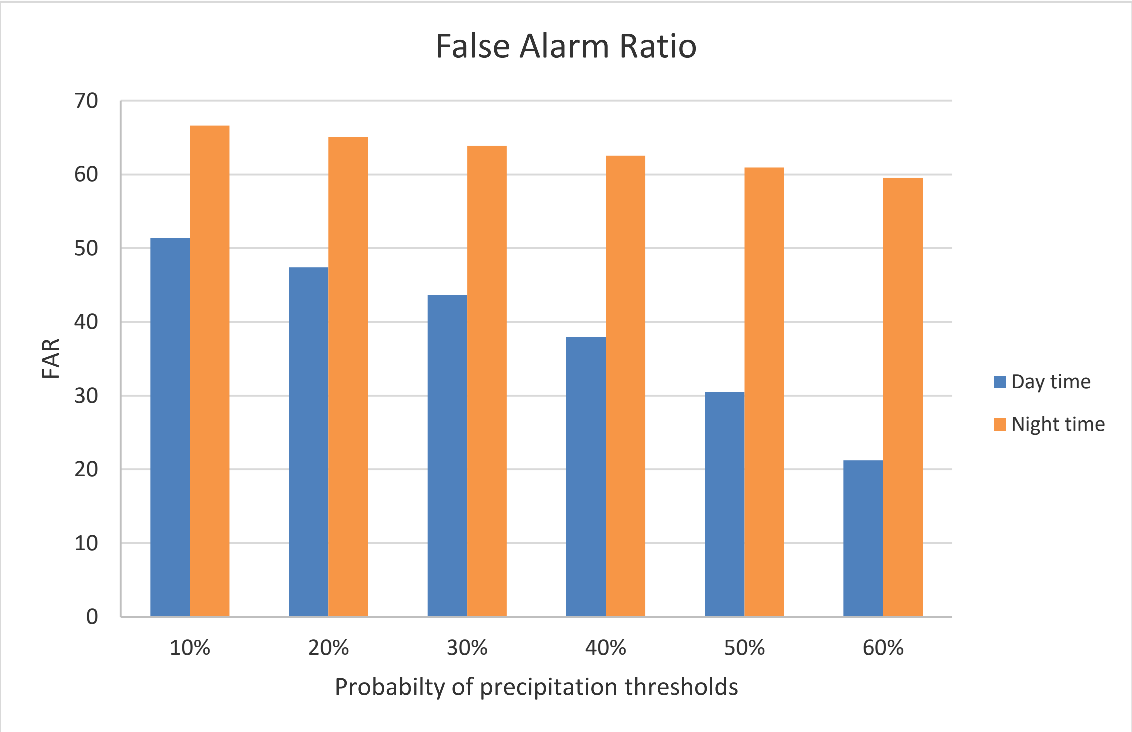

Figure 36. False alarm ratio comparison between day time and night time algorithms.

As it can be appreciated in Figure 35, the probability of detection decrease with the increase of the established thresholds. POD is always higher in day time algorithm compared with the night version, except for the last threshold (60%). POD values get worse with increasing values of the

probability of precipitation thresholds. This POD reduction is expected since there are fewer PCPh points insid the higher thresholds intervals.
As regards Figure 36, FAR in day time algorithm are lower than night time cases.Like POD, there is a reduction in FAR with incresing probability of detection theresholds. This reduction is more noticeable in day time than in night time. As in previous case, FAR reduction is also logical due to the fewer PCPh points inside the higher thresholds intervals.

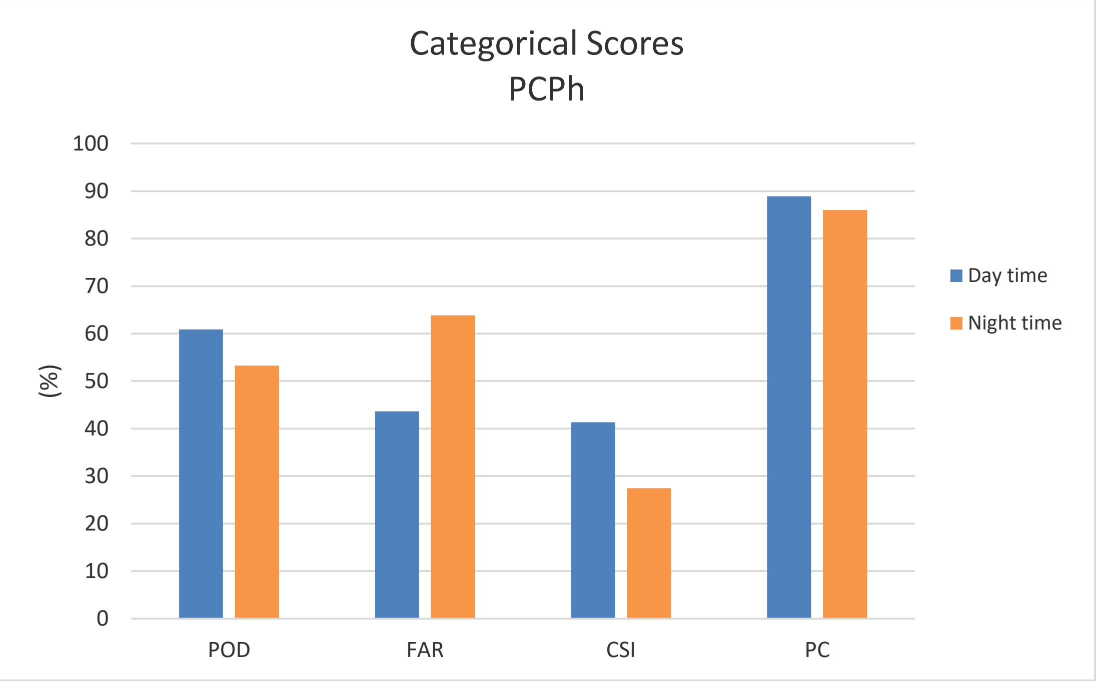

Figure 37. Categorical scores for PCPh day and night time algorithms taking as rainy pixels those with probability of precipitation higher than 30% and higher than 0.2mm/h in case of radar pixels.

A clear better performance of PCPh day time algorithm compared with PCPh night algorithm can be deduced from Figure 37. Higher values of POD, PC and CSI in day algorithm against the night version and also a lower value of False Alarm allow us infer PCPh day algorithm outplay the night version.

4.2.3 Conclusions

Validation results for the PCPh are going to be compared with those requirements included in the "NWCSAF Product Requirements Document" [AD.4]. According to this document, PCPh pixels with probability of precipitation higher than 30% are considered rainy and are compared with radar pixels with rain intensity equal or higher than 0.2 mm/h.

PCPh Algorithm	Threshold Accuracy POD(%)	Target Accuracy POD (%)	POD (%)	Threshold Accuracy FAR(%)	Target Accuracy FAR (%)	FAR (%)
Day time	>55	>65	60.86	<70	<65	43.63
Night time	>45	>50	53.63	<70	<60	63.87

Table 16. Comparison of PCPh values against POD and FAR scores defined in the NWCSAF Product Requirement table.

With the intention of showing the evolution of the product and the progress in its performance, results for the former PCPh product (version 2018) are shown below.

PCPh Algorithm	Threshold Accuracy POD(%)	Target Accuracy POD (%)	POD (%)	Threshold Accuracy FAR(%)	Target Accuracy FAR (%)	FAR (%)
Day time	>55	>65	34.84	<70	<65	35.95
Night time	>45	>50	30.15	<70	<60	66.49

Table 17. Comparison of PCPh v2018 version against POD and FAR scores defined in the NWCSAF Product Requirement table.

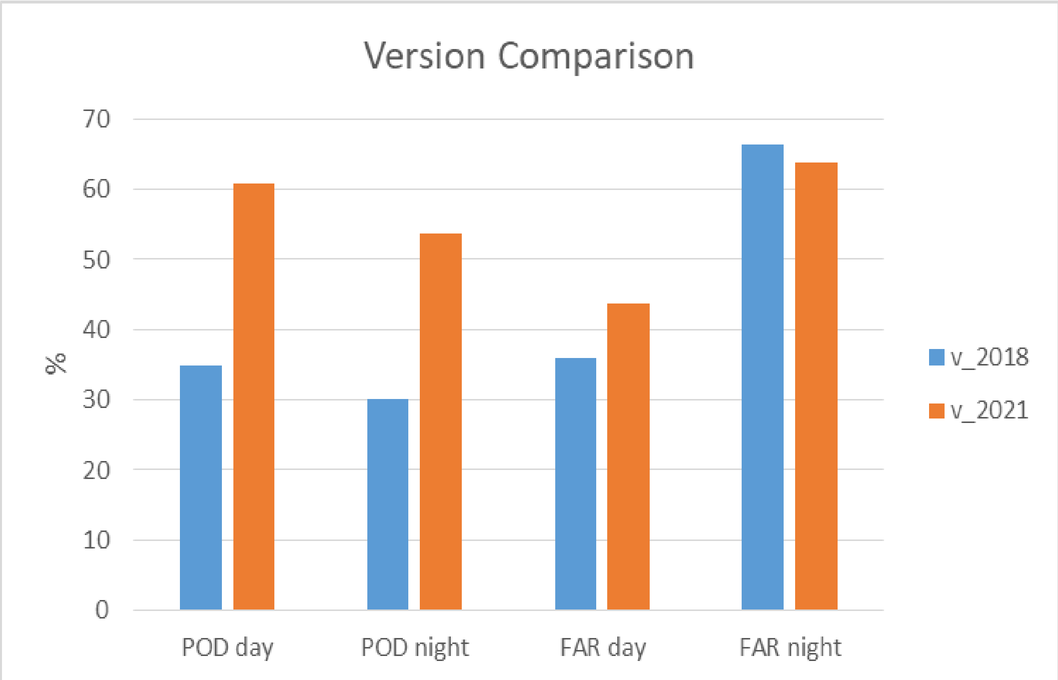

Figure 38. Comparison between 2018 and 2021 PCPh versions. Categorical scores for PCPh day and night time algorithms taking as rainy pixels those with probability of precipitation higher than 30% and higher than 0.2mm/h in case of radar pixels.

In spite of the fact 2021 PCPh version does not reach the commitments for the product only for a little it means a substantial improvement respect the previous version that had a preoperational status.

PCPh product provide us with a general good depiction of the precipitation areas. The higher values of the PCPh products are obtained at day time in correspondence with the higher radar rain rates. Night time tends to slightly overestimate the precipitation area along with no so high values.

According to the categorical validation, POD and FAR requirements are met for the "Threshold Accuracy limits" for day and night time. If we move to the "Target Accuracy", then at day time neither POD score is reached by a little (61 vs 65 %) nor FAR score at night time (64 vs 60%).

Taking into account day and night requirements and the threshold and target limits, PCPh achieved quality is in between both of them in the Iberian Península.

Green bold colour is chosen when stablished limits are fulfilled for the "Target accuracy".

As far as the visual validation is concerned, it has been visually checked that the orography may produce some unrealistic shapes. These artefacts produced by mountains are steady and it appears in the same places so it can be easily detected. Apart from that, the stability correction factor finally depends on the NWP model. If a specific meteorological pattern is wrongly reproduced, it will have an impact on the precipitation product. If the NWP model fails at detecting stable areas some holes inside precipitating areas may appear.

5. VALIDATION FOR CONVECTIVE RAINFALL RATE FROM CLOUD PHYSICAL PROPERTIES PRODUCT

This section contains the results obtained from the validation of the CRRPh product which is described in the "Algorithm Theoretical Basis Document for the Precipitation Product Processors of the NWC/GEO" *[RD 4]*.

The validation procedure consists of two parts:

- ✓ Subjective validation
- ✓ Objective validation

The subjective validation compares 2 images: The radar rainfall rate (RFR) for the Spanish composition with the CRRPh product.
The objective validation is based on a pixel to pixel comparison between the radar data and the CRRPh product. As far as the objective validation is concerned, different categorical scores have been calculated (see Annex I at the end).

5.1 SUBJECTIVE VALIDATION FOR CONVECTIVE RAINFALL RATE FROM CLOUD PHYSICAL PROPERTIES (CRRPH)

The monitoring of the precipitation pattern as well as its evolution is a valuable information for the forecaster. In order to check this information, visual comparisons between CRRPh and radar images have been done. A summary of these comparisons containing different study cases that represent the general behaviour of these algorithms have been selected for this purpose.

CRRPh product includes a set of corrections that can be applied. In the default configuration, the Cloud Water Path Correction Factor and the Stability Correction are turned on. All the images and results inside this document include those corrections factors. More information about this correction factor can be found in the "Algorithm Theoretical Basis Document for the Precipitation Product Processors of the NWC/GEO "*[RD 4]*.

Regarding CRRPh visualization, pixels with NO DATA have been plotted in grey, due to an undefined phase or No data or corrupted data input. Black colour stands for no rain. This apply to day and night time algorithms.

5.1.1 DAY

A pair of images are shown to subjectively validate the CRRPh day product: The image on the right side corresponds with the radar rainfall rate (RFR) and the image on the left side corresponds with the rain rates of the CRRPh product (see Figures 39-47).

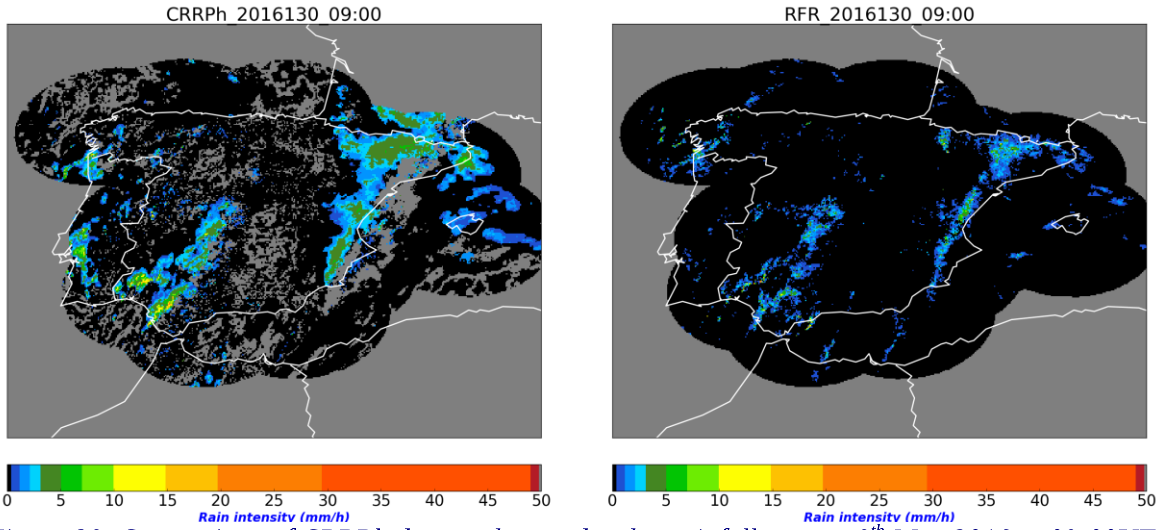

Figure 39. Comparison of CRRPh day product and radar rainfall rate on 9th May 2016 at 09:00UTC

This is a good example of the general CRRPh day time algorithm. According to the radar image that is on the right side, there is a line of precipitation coming from the northeast to the southeast of the Iberian Peninsula, close to the Mediterranean coast well detected by the product. There is another precipitation area in the centre of Spain with higher rain rates at the south.Finally, there are more little cells spread at the northwest that the product is able to detect. In this occasion is the Balearic Island the region where the product performs worse.

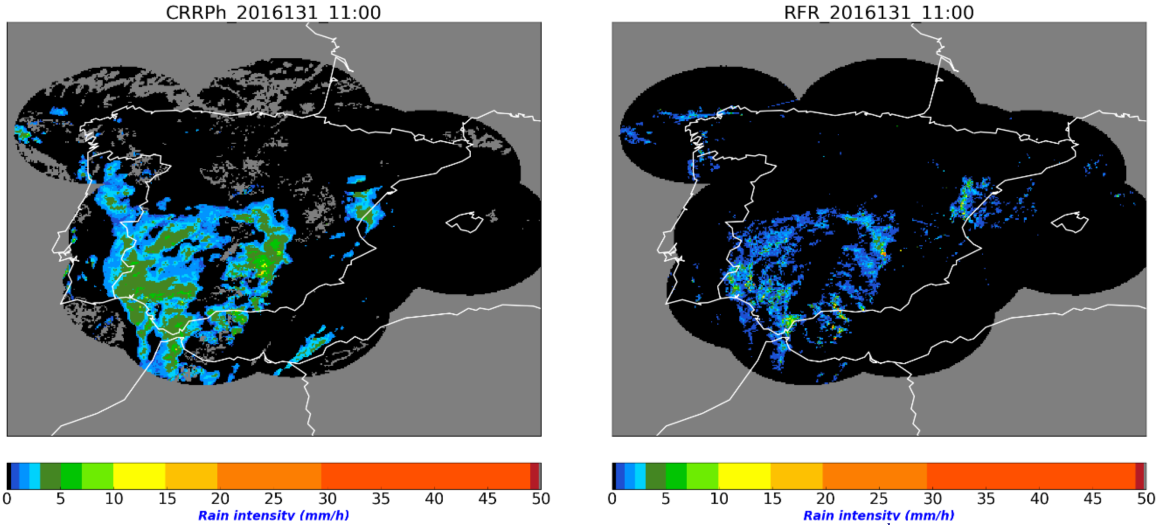

Figure 40. Comparison of CRRPh day product and radar rainfall rate on 10th May 2016 at 11:00UTC

In this second example a wide precipitation area extends all over the Centre and South of the Iberian Peninsula. The precipitation area is well represented by the product with a slight overestimation of it. At the north of Valencia and the west part of Galicia rainy areas are represented.

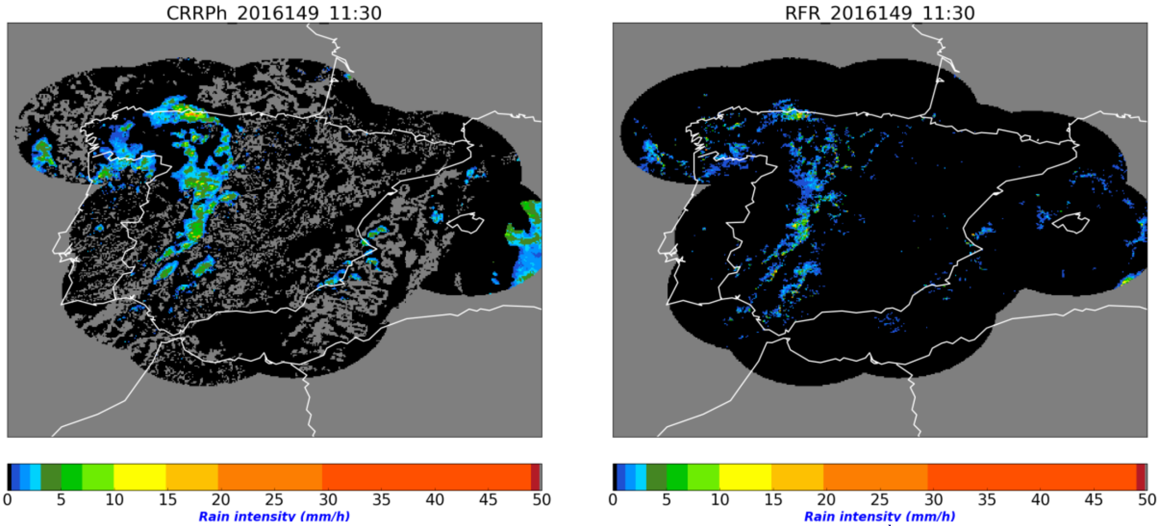

Figure 41. Comparison of CRRPh day product and radar rainfall rate on 28th May 2016 at 11:30UTC

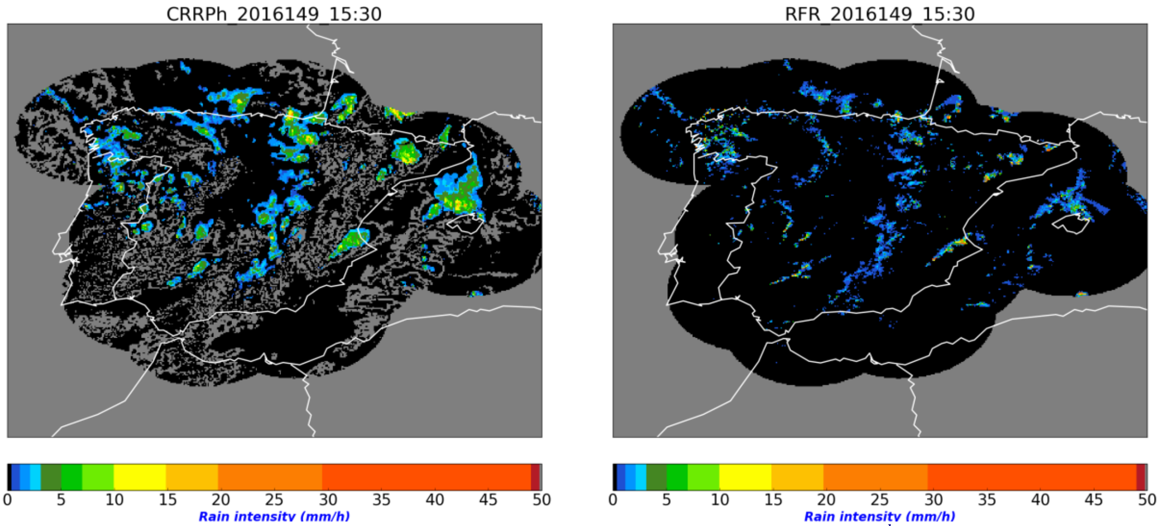

Figure 42. Comparison of CRRPh day product and radar rainfall rate on 28th May 2016 at 15:30UTC

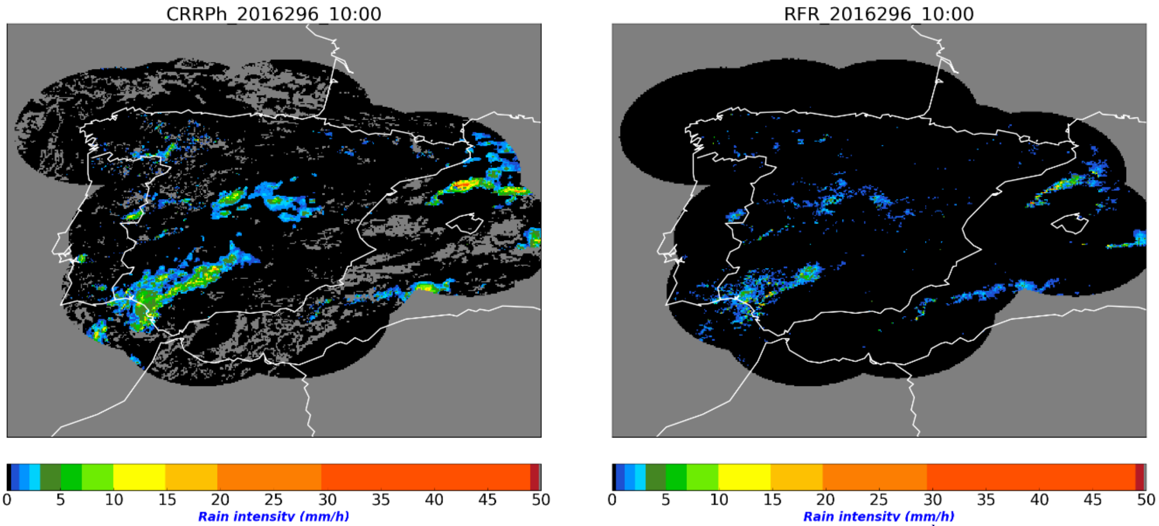

Figure 43. Comparison of CRRPh day product and radar rainfall rate on 22th October 2016 at 10:00UTC

Figures 41, 42 and 43 are good examples of the CRRPh ability to detect early stages of convective nuclei. From the point of view of a forecaster the early detection of growing cumulus that may end in active thunderstorms add valuable information.

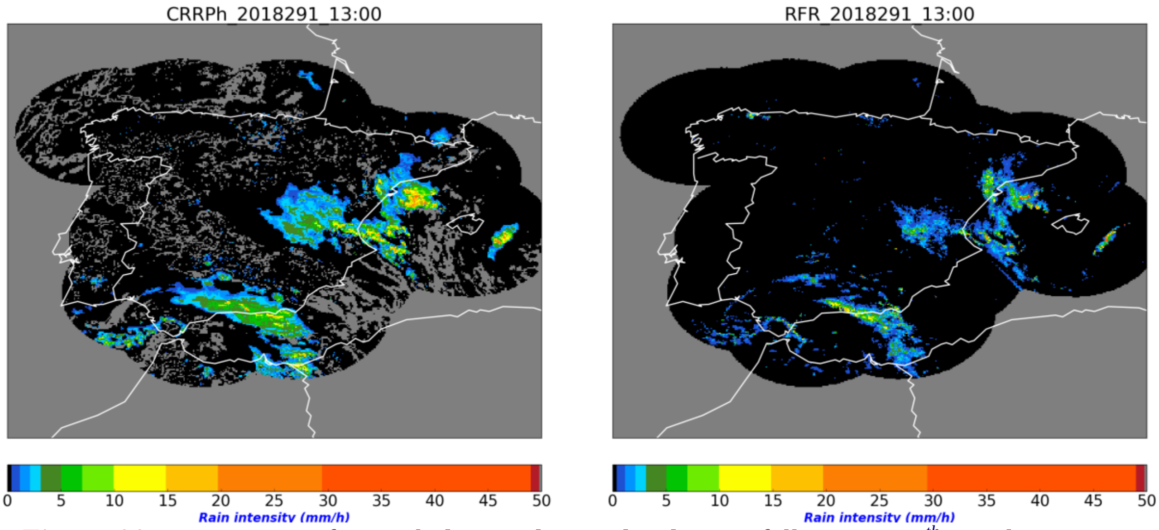

Figure 44. Comparison of CRRPh day product and radar rainfall rate on 18th October 2018 at 13:00UTC

Figure 44 is an example of active convective nuclei with high rain rates associated to them. CRRPh detect the precipitating areas and assign high rates in the same areas the Spanish radar does.

An example of the CRRPh performance out of the area the product has been calibrated is shown below. In this case, black colour stands for no precipitating areas and NO DATA input values due to an undefined phase or No data or corrupted data input.

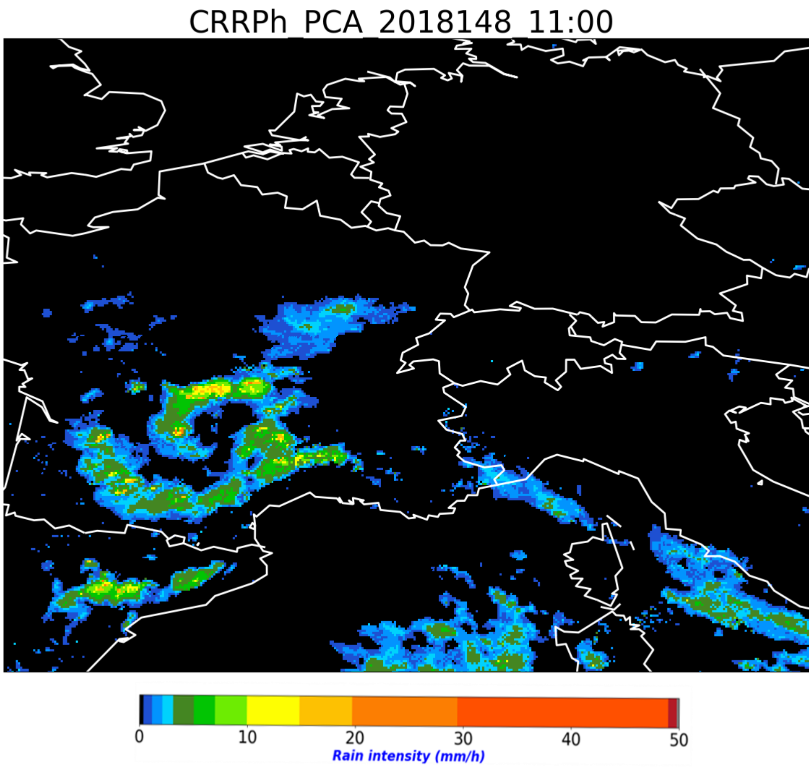

Figure 45. CRRPh day product on 28th May 2018 at 11:00UTC

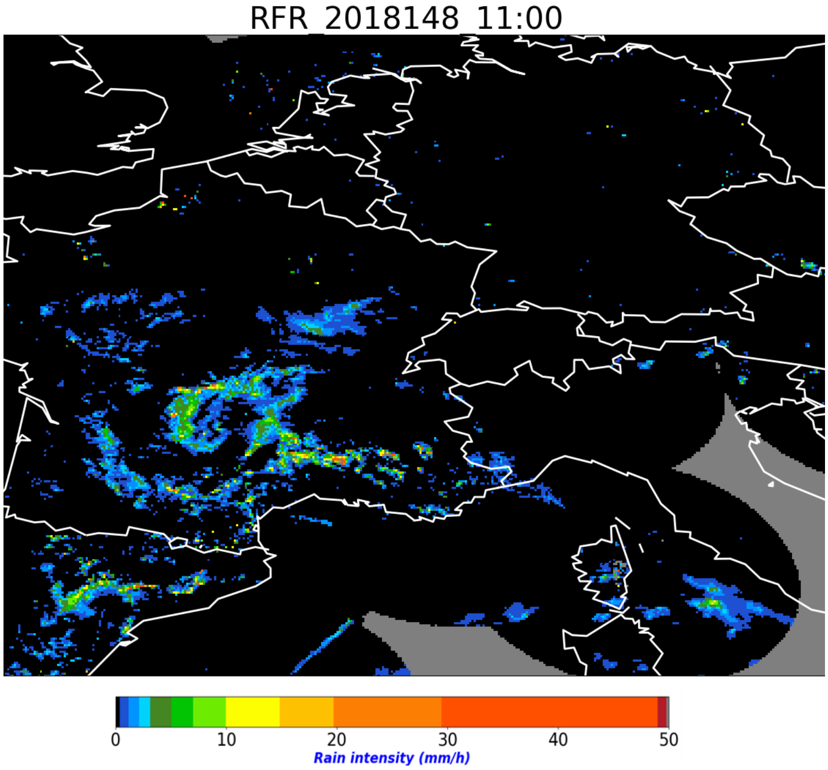

Figure 46. OPERA radar composite the 28th May 2018 at 11:00

In this event there was significant convection activity throughout all the day in France, middle Europe and also in Spain. At first sight it can be noticed a big extension of precipitation at the south of France that CRRPh detected with good detail. There were many convective nuclei that CRRPh was able to depict. This is another example of the CRRPh ability to detect not only the more developed convective nuclei but also the first stages of growing thunderstorms.

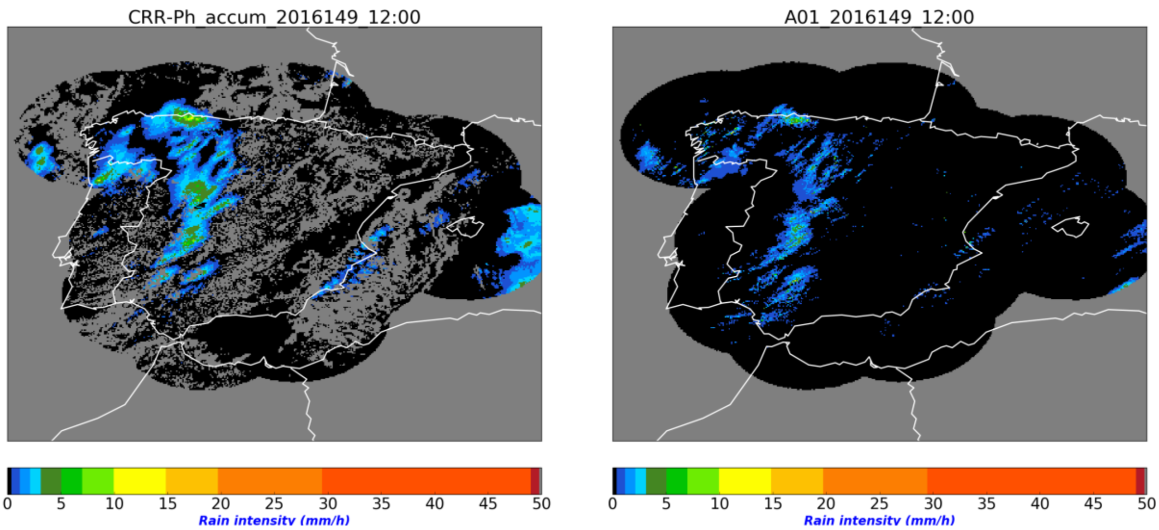

Figure 47. Comparison of CRRPh hourly accumulation day product and radar hourly accumulation on 28th May 2016 at 12:00UTC

Since the hourly accumulation is based on the CRRPh output for 4 consecutive slots, it has a similar performance compared with the instantaneous rain rates. This is an example of an hourly accumulation at day time. There is a general visual agreement in both images. Near the Balearic Islands the precipitating area is overestimated.

5.1.2 NIGHT

With the aim of visually validate the CRRPh night product two images are plotted. The one on the right side corresponds with the reflectivity of the radar (PPI image) and the image on the left side corresponds with the rain rates of the CRRPh product.

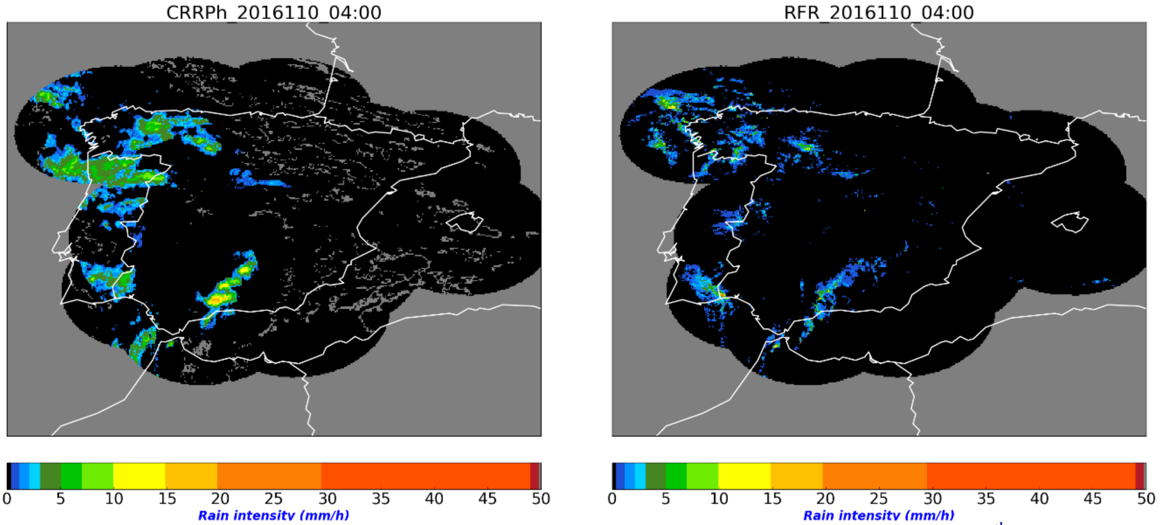

Figure 48. Comparison of CRRPh day product and the Spanish radar composite on 19th April 2016 at 04:00UTC

In this first night example it can be noticed a reasonable good correspondence between both images. Rain intensities assignation is not so good compared with day time.

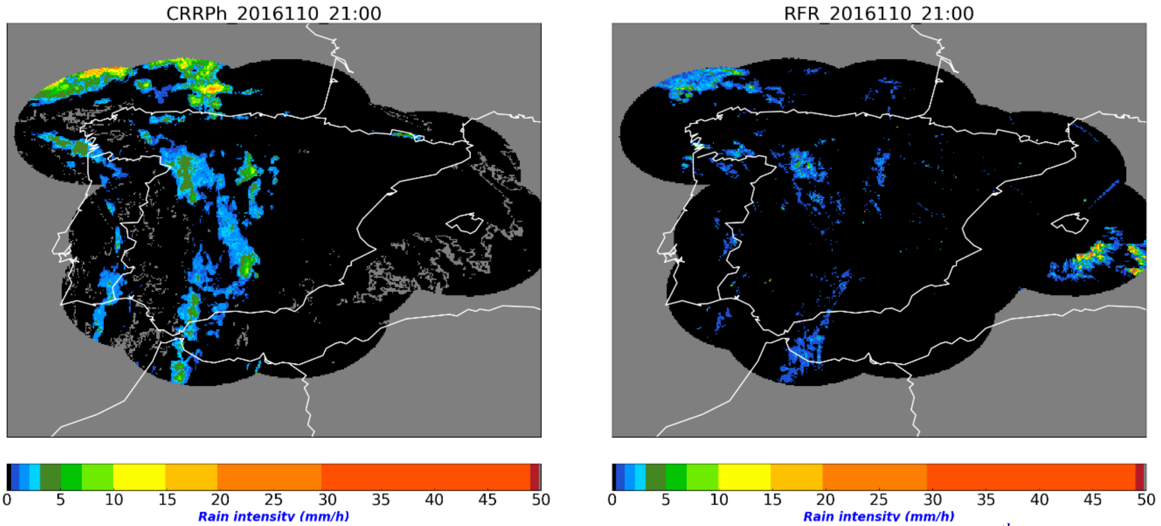

Figure 49. Comparison of CRRPh day product and the Spanish radar composite on 19th April 2016 at 21:00UTC

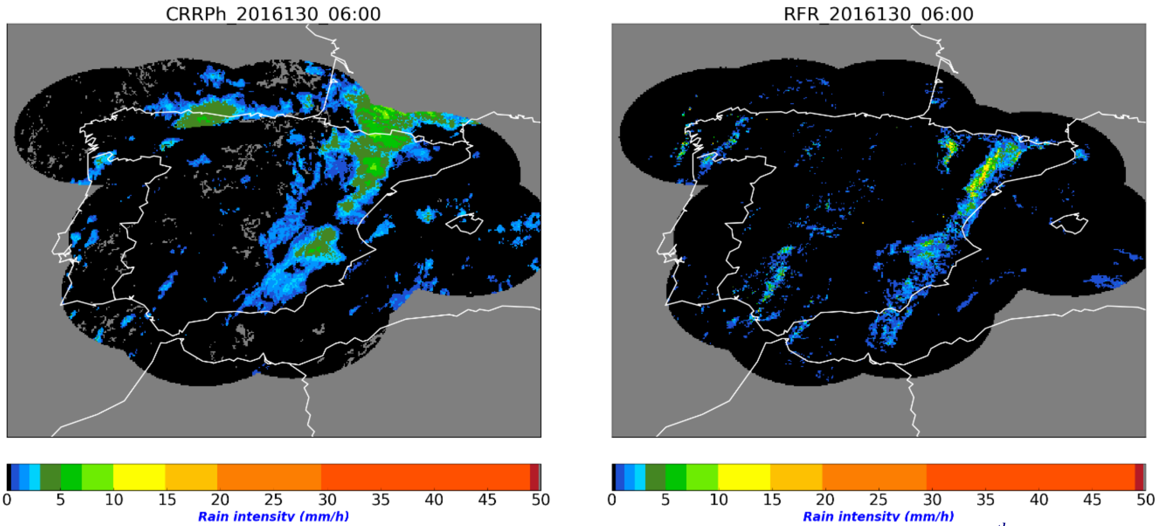

Figure 50. Comparison of CRRPh day product and the Spanish radar composite on 9th May 2016 at 06:00UTC

Figures 49 and 50 show how the product detect rainy areas at night. The extension of those areas are in general wider than at day time. The product tends to extent the night precipitation areas and introduces more False Alarm proportion. In Figure 49 there is an active precipitation area near the Balearic Islands not detected by the product. Like PCPh, the detail and accuracy of CRRPh night version reduces compared with the day algorithm because visible channels and cloud microphysics are not available. Although a simulation of these channels is done and used in the algorithm, this simulations are not perfect.

More information about CRRPh day and night algorithm can be found in the "Algorithm Theoretical Basis Document for the Precipitation Product Processors of the NWC/GEO "*[RD 4]*.

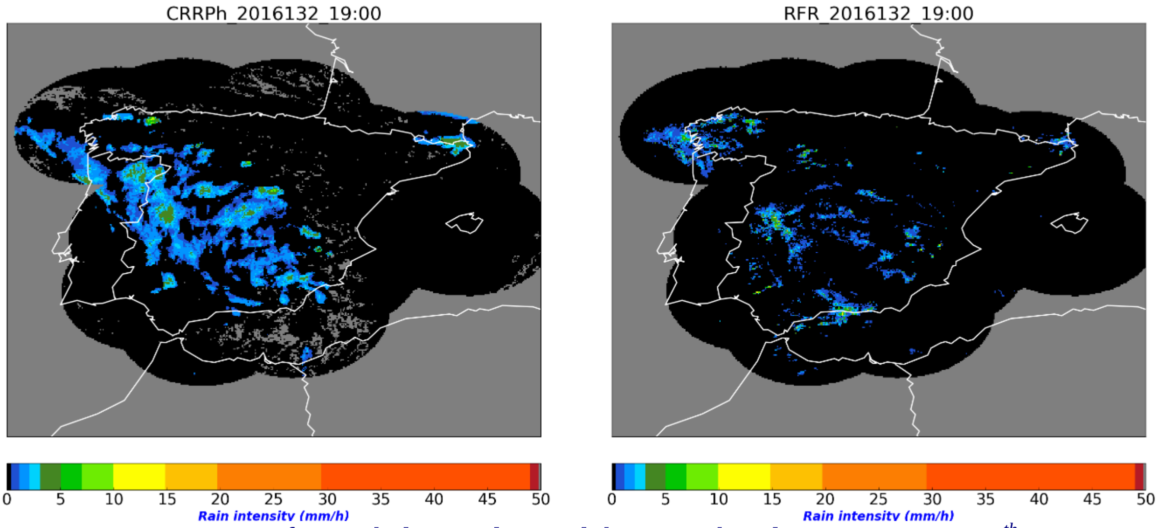

Figure 51. Comparison of CRRPh day product and the Spanish radar composite on 11th May 2016 at 19:00UTC

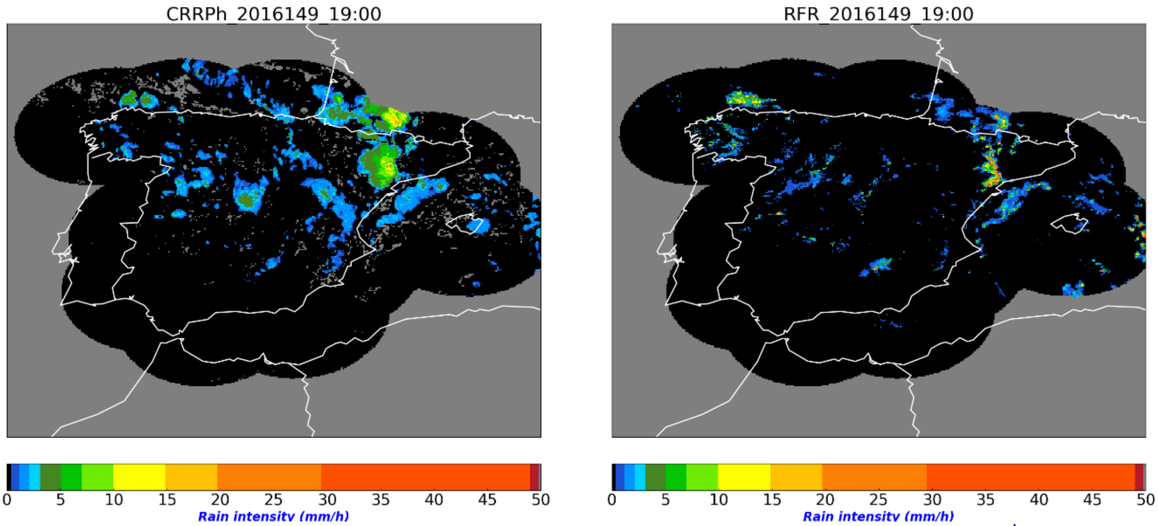

Figure 52. Comparison of CRRPh day product and the Spanish radar composite on 28th May 2016 at 19:00UTC

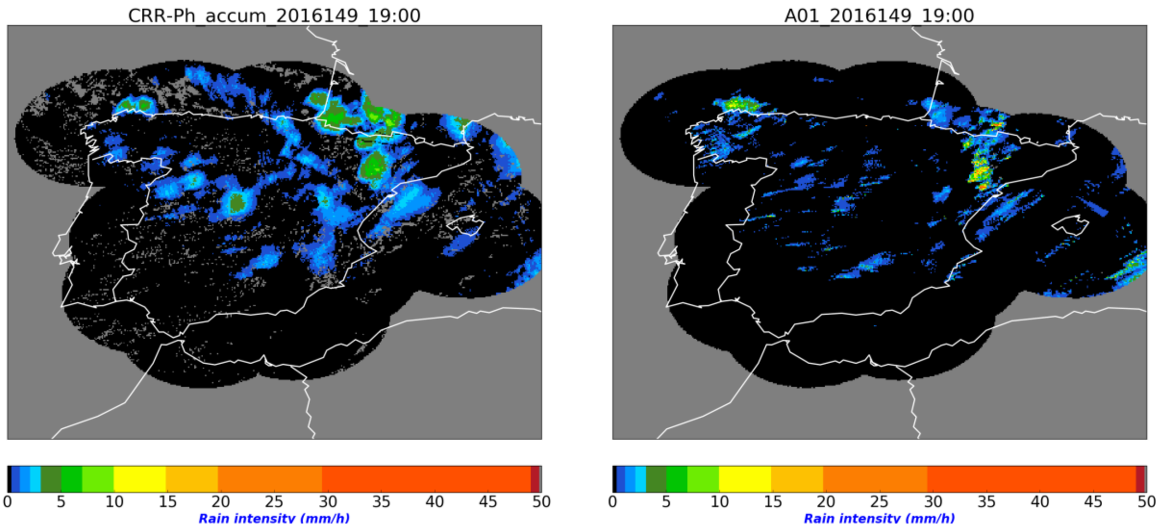

Figure 53 . Comparison of CRRPh hourly accumulation night product and radar hourly accumulation on 28th May 2016 at 19:00UTC

Figures 51 and 52 show a good performance of the night product. Not only is the product able to detect the bigger and with higher rain rates convective nuclei but also a big quantity of the smaller ones.
Figure 53 is an example of the CRRPh hourly accumulations.

5.2 Objective validation for Convective Rainfall rate from Cloud Physical Properties (CRRPh)

5.2.1 Validation Procedure

Section 4.2.1 also applies to this section.

As far as the hourly accumulations is concerned, the validation has been done against the radar hourly accumulations, obtained from the 500m Pseudo-CAPPI. In this case a day-night distinction has also be taken into account, validating only pixels of the same category.

Despite the fact the product has been calibrated in the Iberian Península only in convective events, it has been also been generated in non-convective situations. CRRPh requirements included in the "NWCSAF Product Requirements Document" [AD.4] refers exclusively to convective areas. CRRPh main goal is to detect convective zones. However it has also been validated (Iberian Península) in all areas for the final user to have more detailed information and give a sense of completeness. For this reason it has been done a double validation: one in convective pixels, and the second one in all pixels. While the convective validation has been put into practise in the Iberian Península, a criterion to select convective areas is also necessary. The criteria consist of selecting those areas with ET>=6km, RFR>=10mm/h and a box size=25*25 pixels. This is the same criteria followed in the calibration process. Undoubtedly, there may be a little bit of arbitrariness behind this election, because other options can also be possible.

5.2.2 Instantaneous Rain Rates

5.2.2.1 CATEGORICAL VALIDATION

In order to compute the categorical scores, two thresholds have been stablished, one for the CRRPh intensity and another one for the rainy pixels of the radar.
The CRRPh intensity threshold for an instantaneous rain rate is fixed to 0.2 mm/h or higher.
The rainy pixels from the radar are fixed to at least 0.2 mm/h.

Operational Programme for the exchange of weather radar information (OPERA) provides RFR in the lowest radar level and maximum column dBZ parameters. (It does not include Echotop).
As for validating in OPERA region, in this validation report a threshold of dBz = 40 in the vertical column was chosen. Additionally, a threshold of RFR = 3 mm/h was used to ensure that moderate rainfall was present on surface level in order to compare with the satellite derived surface precipitation. When a pixel was classified as convective, a box of 25x25 pixels centred in that pixel was chosen.

5.2.2.1.1 DAY

5.2.2.1.1.1 Convective areas over the Iberian Península

N	POD (%)	FAR (%)	CSI (%)	PC (%)
1386323	**77.92**	**27.40**	60.21	76.65

Table 18. Categorical scores for CRRPh intensity day algorithm in convective areas

5.2.2.1.1.2 All Areas over the Iberian Península

N	POD (%)	FAR (%)	CSI (%)	PC (%)
4208125	70.99	47.48	43.24	88.07

Table 19. Categorical scores for CRRPh intensity day algorithm in all areas

5.2.2.1.1.3 Convective areas over OPERA_region (Europe)

N	POD (%)	FAR (%)	CSI (%)	PC (%)
3600322	64.71	25.00	53.23	76.31

Table 20. Categorical scores for CRRPh day algorithm in convective areas over OPERA region

5.2.2.1.2 NIGHT

5.2.2.1.2.1 Convective areas over the Iberian Península

N	POD (%)	FAR (%)	CSI (%)	PC (%)
4051369	70.54	34.26	51.58	67.41

Table 21. Categorical scores for CRRPh intensity night algorithm in convective areas

5.2.2.1.2.2 All Areas over the Iberian Península

N	POD (%)	FAR (%)	CSI (%)	PC (%)
15403702	55.85	65.88	26.87	84.92

Table 22. Categorical scores for CRRPh intensity night algorithm in all areas

5.2.2.1.2.3 Convective areas over OPERA region (Europe)

N	POD (%)	FAR (%)	CSI (%)	PC (%)
7264709	49.52%	34.47%	39.29%	65.84%

Table 23. Categorical scores for CRRPh night algorithm in convective areas over OPERA region.

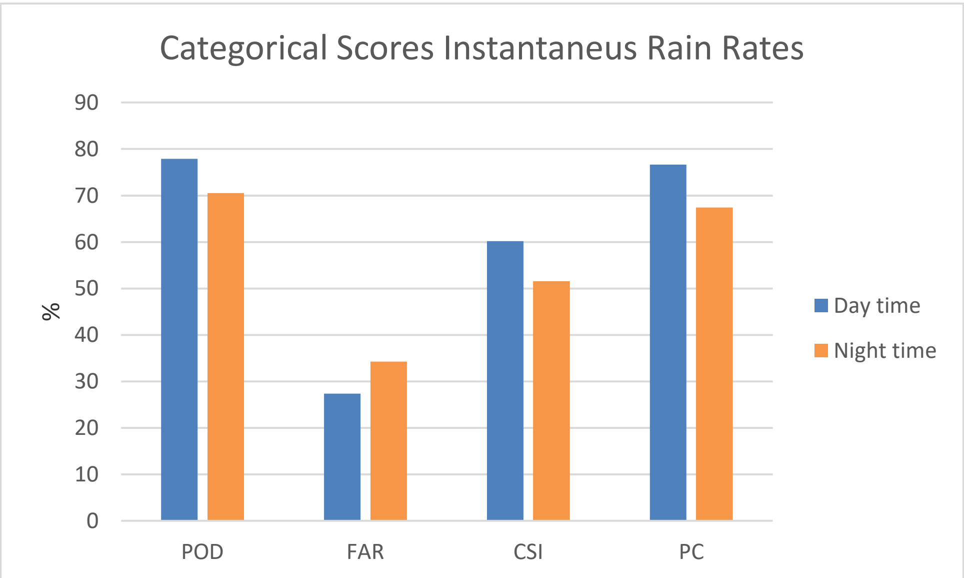

Figure 54. Categorical scores for CRRPh instantaneous rain rates in convective areas over the Iberian Península.

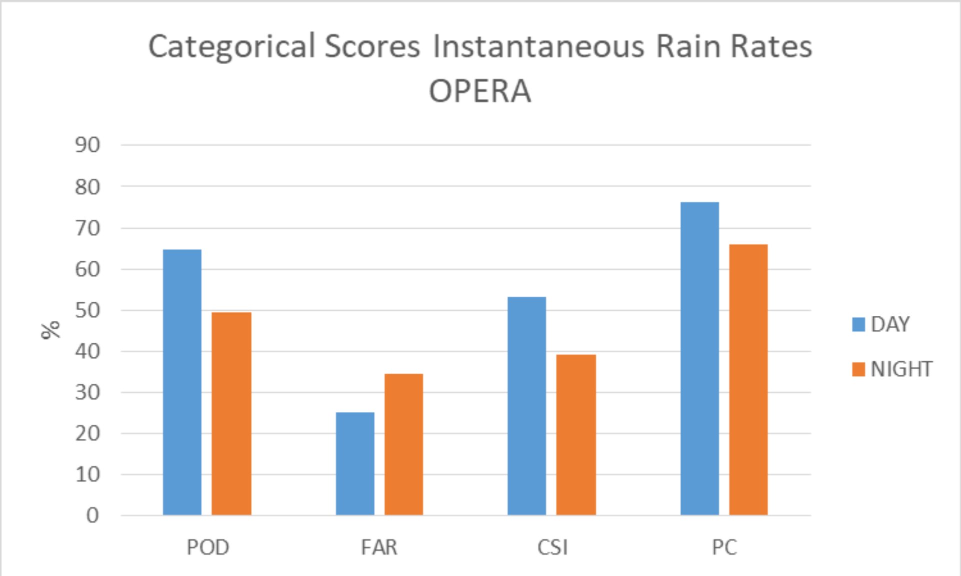

Figure 55. Categorical scores for CRRPh instantaneous rain rates in convective areas over OPERA region

Hourly Accumulations

With the aim of computing the categorical scores for the hourly accumulations, two thresholds have been stablished, one for the CRRPh and another one for the rainy pixels of the radar.
The CRRPh threshold is fixed to 0.2 mm/h or higher.
The rainy pixels from the radar are fixed to at least 0.2 mm/h.

As it can be noticed, it has been established a discrimination between convective and non-convective areas. Since the hourly accumulation involves four different slots, the current one and the three preceding, convective areas have been selected for the four time slots. It may have happened that a 25*25 convective box that have been selected for a time slot, will not remain convective for the next time slot (within the same hour). In that case, the box has not been excluded for the analysis. In other words, Once a pixel is considered convective (ET>6km, RFR>10km) for a time slot, a box size of 25*25 pixels is taken, centred in that pixel, and that box is again used in the next time slot (within the same hour) for computing the hourly accumulation.

Having stablished the difference between convective and non-convective areas, the improvement in the categorical scores in convective areas becomes evident in comparison with all areas. This way, POD and FAR scores are fulfilled for both, day and night, in convective areas.

5.2.2.2 DAY

N	POD (%)	FAR (%)	CSI (%)	PC (%)
265782	**83.12**	**30.24**	61.10	75.90

Table 24. Categorical scores for CRRPh hourly accumulation day algorithm in convective areas

N	POD (%)	FAR (%)	CSI (%)	PC (%)
2198129	77.08	52.48	41.64	84.78

Table 25. Categorical scores for CRRPh hourly accumulation day algorithm in all areas

5.2.2.3 NIGHT

N	POD (%)	FAR (%)	CSI (%)	PC (%)
885197	**74.60**	**36.37**	52.29	66.36

Table 26. Categorical scores for CRRPh hourly accumulation night algorithm in convective areas

N	POD (%)	FAR (%)	CSI (%)	PC (%)
8815013	60.70	68.94	25.86	81.88

Table 27. Categorical scores for CRRPh hourly accumulation night algorithm in all areas

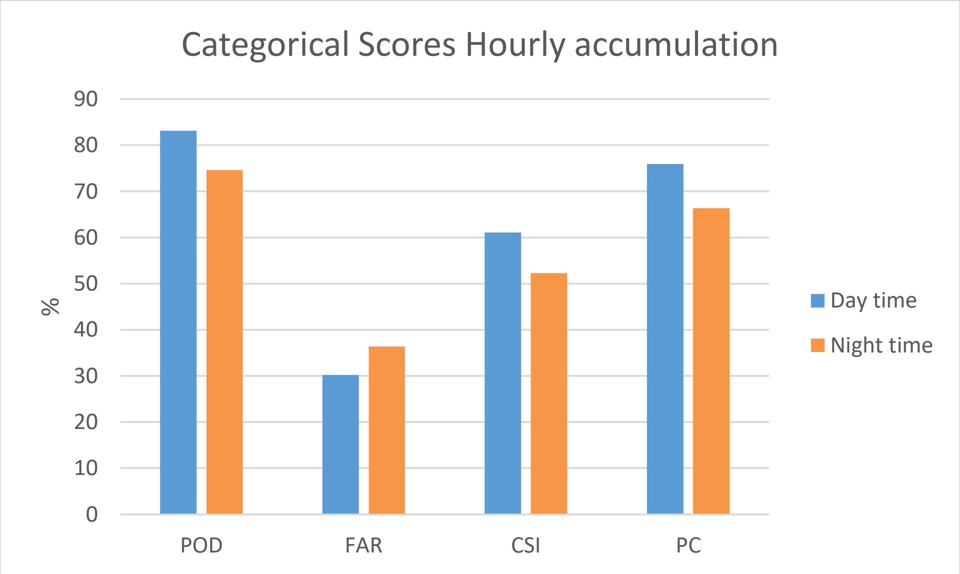

Figure 56. Categorical scores for CRRPh hourly accumulations in convective areas

5.2.3 Conclusions

Validation results for the CRRPh are going to be compared with those requirements included in the "NWCSAF Product Requirements Document" [AD.4] for both the CRRPh intensity and the CRRPh hourly accumulation. The commitment for the product is to reach the requirement in the convective areas. An additional table with the performance in OPERA (Europe) region is included.

CRRPh Algorithm	Threshold Accuracy POD (%)	**Target Accuracy POD (%)**	Optimal Accuracy POD (%)	POD (%)
Day time	>50	>75	>90	**77.92**
Night time	>35	>47	>80	**70.54**

Table 28. Comparison of CRRPh values against POD scores defined in the NWCSAF Product Requirement table

CRRPh Algorithm	Threshold Accuracy FAR (%)	**Target Accuracy FAR (%)**	Optimal Accuracy FAR (%)	FAR (%)

Day time	<65	<50	<45	**27.40**
Night time	<70	<60	<50	**34.26**

Table 29. Comparison of CRRPh values against FAR scores defined in the NWCSAF Product Requirement table

CRRPh Hourly accumulations	Threshold Accuracy POD (%)	**Target Accuracy POD (%)**	Optimal Accuracy POD (%)	**POD (%)**
Day time	>60	>80	>95	**83.12**
Night time	>37	>50	>85	**74.60**

Table 30. Comparison of CRRPh hourly accumulations FAR scores defined in the NWCSAF Product Requirement table

CRRPh Hourly accumulations	Threshold Accuracy FAR (%)	**Target Accuracy FAR (%)**	Optimal Accuracy FAR (%)	**FAR (%)**
Day time	<60	<55	<45	**30.24**
Night time	<70	<60	<50	**36.37**

Table 31. Comparison of CRRPh hourly accumulations FAR scores defined in the NWCSAF Product Requirement table

CRRPh Algorithm	Threshold Accuracy POD (%)	**Target Accuracy POD (%)**	Optimal Accuracy POD (%)	**POD (%)**
Day time	>50	>75	>90	64.71
Night time	>35	>47	>80	**49.52**

Table 32. Comparison of CRRPh values against POD scores defined in the NWCSAF Product Requirement table over OPERA region

CRRPh Algorithm	Threshold Accuracy FAR (%)	**Target Accuracy FAR (%)**	Optimal Accuracy FAR (%)	**FAR (%)**
Day time	<65	<50	<45	**25.00**
Night time	<70	<60	<50	**34.47**

Table 33. Comparison of CRRPh values against FAR scores defined in the NWCSAF Product Requirement table over OPERA region

With respects to the instantaneous rain rates, POD and FAR scores are better in convective areas than in all areas and results are also better during day time than during night time.

Despite a general good behaviour of the CRRPh day product in convective areas there isn't a perfect spatial matching between radar pixels and the CRRPh product. A spatial displacement between radar pixels and CRRPh pixels penalizes the product. It is known that in an objective validation made pixel by pixel, collocation problems between radar and satellite makes the double penalty problem visible.

According to the "NWCSAF Product Requirements Document" [AD 4], POD and FAR scores corresponding to the CRRPh instantaneous rate during day time and also at night time on convective areas are achieved (Green bold colour is chosen when stablished limits are fulfilled).

Regarding the CRRPh hourly accumulation, it inherits the same strong and weak points from its precursor CRRPh instantaneous rain rate. Better results are obtained at day time than at night time and also are better in convective areas compared with all areas.

POD and FAR requirements are both fulfilled in convective areas for day and night time cases in the Iberian Peninsula. Good results are also obtained if the validation is extended to Europe (OPERA region).

Regarding the visual validation, it has visually checked that the orography may produce unrealistic shapes. These artefacts produced by mountains are steady and it appears in the same places so it can be easily detected. The stability correction finally depends on the NWP model. Hence, if the NWP model fails at detecting stable regions, black holes with unrealistic shapes inside precipitating areas may appear. The stability correction seems to be beneficial on average for the whole year and Europe extension.

According to the objective and subjective validations this product can be stated as operational.

6. HIMAWARI DATA

Precipitation products have been computed in ASIA region for Himawari-8 satellite. In order to have a visual validation, some radar images have been depicted. The Japanese radar reflectivity composite imagery have been downloaded from the following website: "http://agora.ex.nii.ac.jp/digital-typhoon/archive/radar/intensity/". This website was accessed for the last time the 22th December 2021.
Two days have been represented: the 28th and 30th of August 2021 at 0Z UTC (09 Japan Standard Time). Despite the fact the whole image have been created with the intention of having day and night time algorithm at the same time in the same frame. It has been zoomed in Japan region where the radar images were available.

The following colour palette applies to the Japan Radar Echo images:
Radar Echo Intensity (Unit: Milimeters)

-0	0-1	1-2	2-4	4-8	8-12	12-16	16-24	24-32	32-40	40-48	48-56	56-64	64-80	80-

6.1 30TH AUGUST 2018

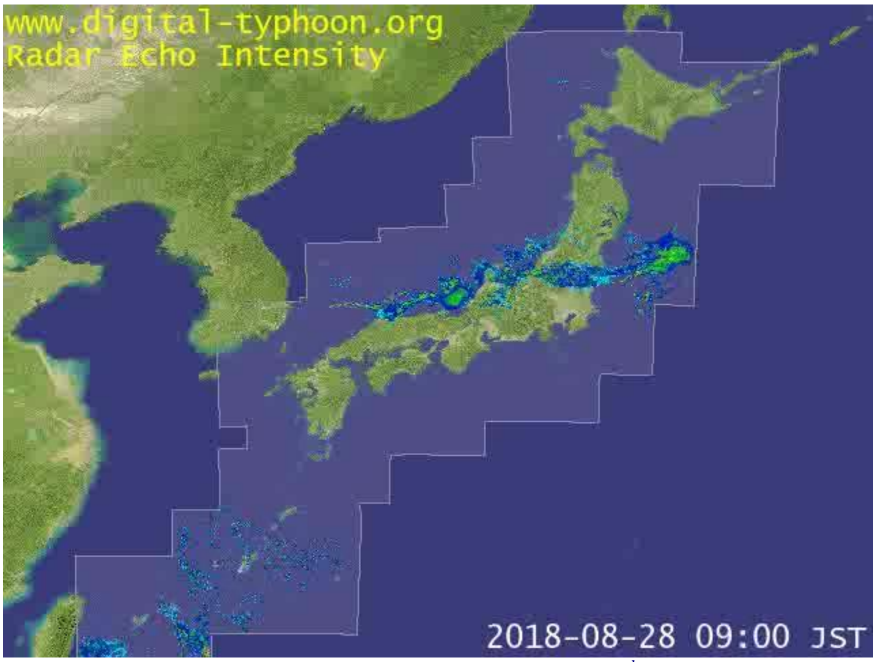

Figure 57. Composite weather radar echoes (mm/h) on 28th August 2018 at 00:00 UTC

According to Figure 57, the wider precipitating area was located in the centre of Japan. In that area there was convective nuclei which were detected by the CRRPh (see Figure 58). At the southwest Japan islands there was another precipitating area that was also depicted. Regarding PCPh (see Figure 59), all those areas were painted with very high probability of rain.

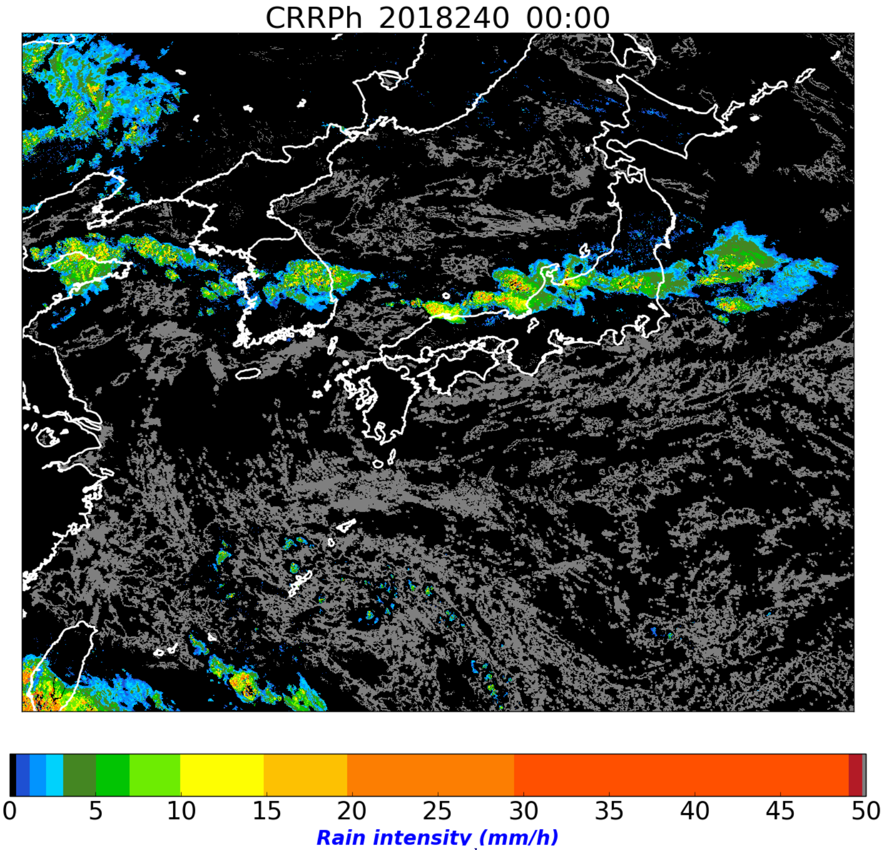

Figure 58.CRRPh product on 28th August 2018 at 00:00 UTC

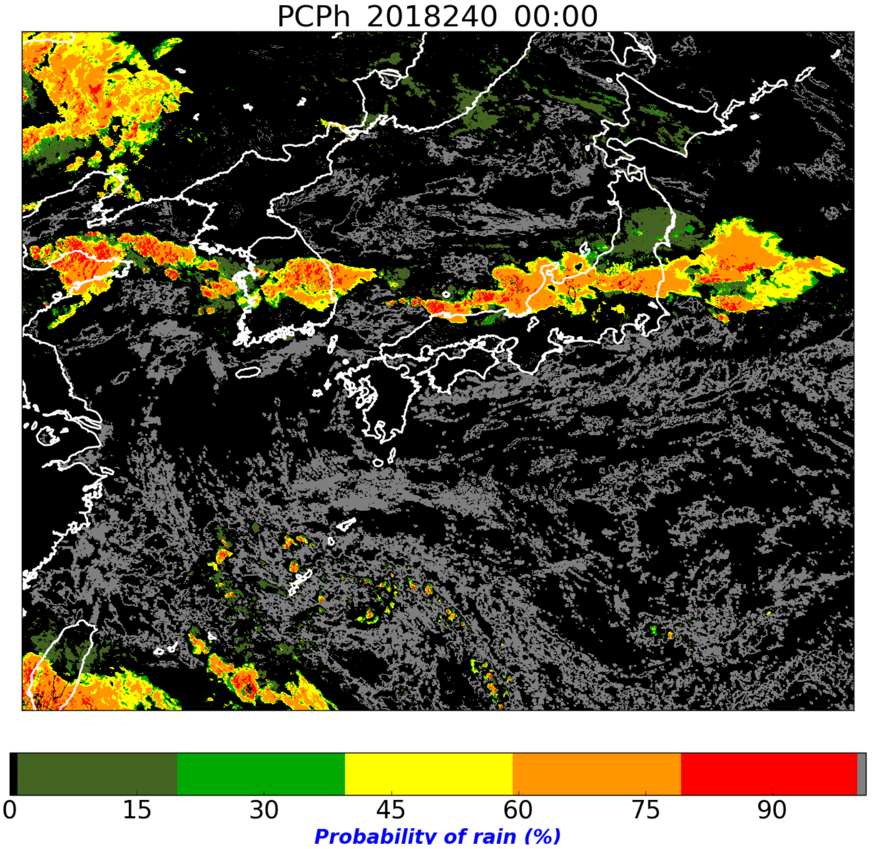

Figure 59. PCPh product on 28th August 2018 at 00:00 UTC

6.2 30TH AUGUST 2018

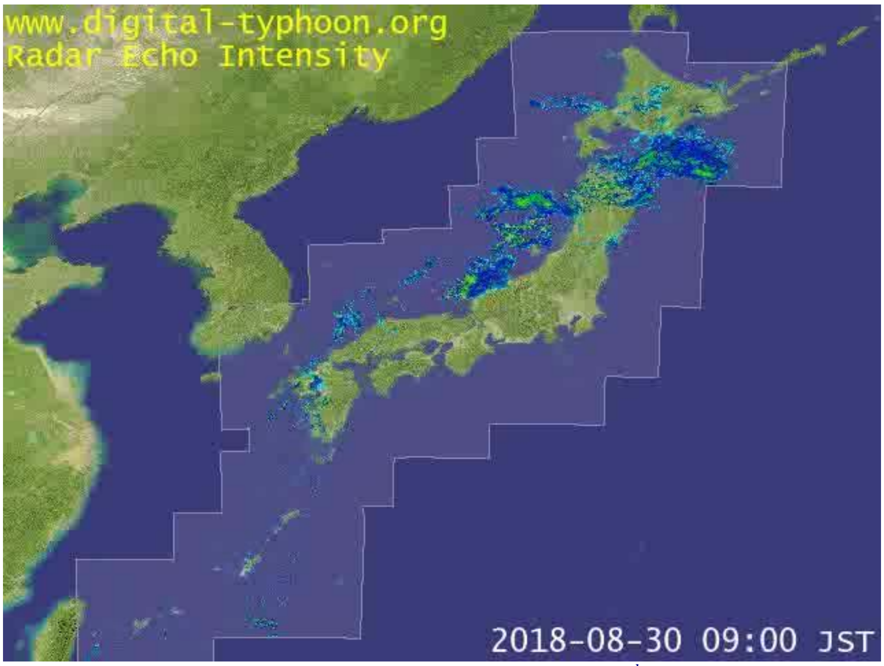

Figure 60. Composite weather radar echoes (mm/h) on 30th August 2018 at 00:00 UTC

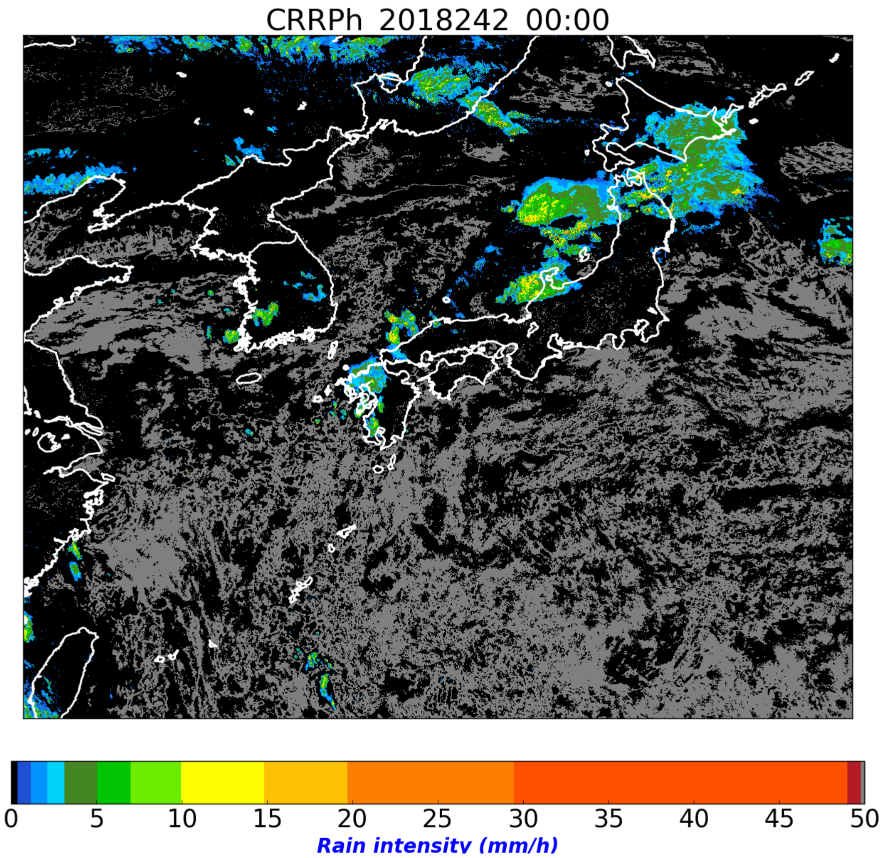

Figure 61.CRRPh product on 30th August 2018 at 00:00 UTC

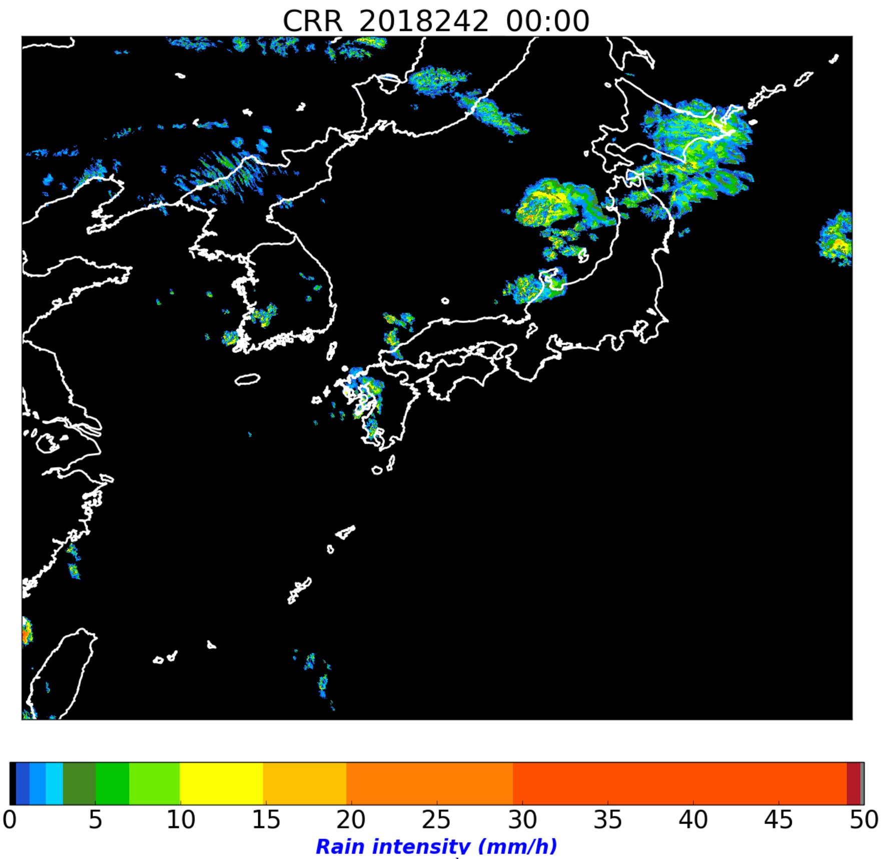

Figure 62.CRR product on 30th August 2018 at 00:00 UTC

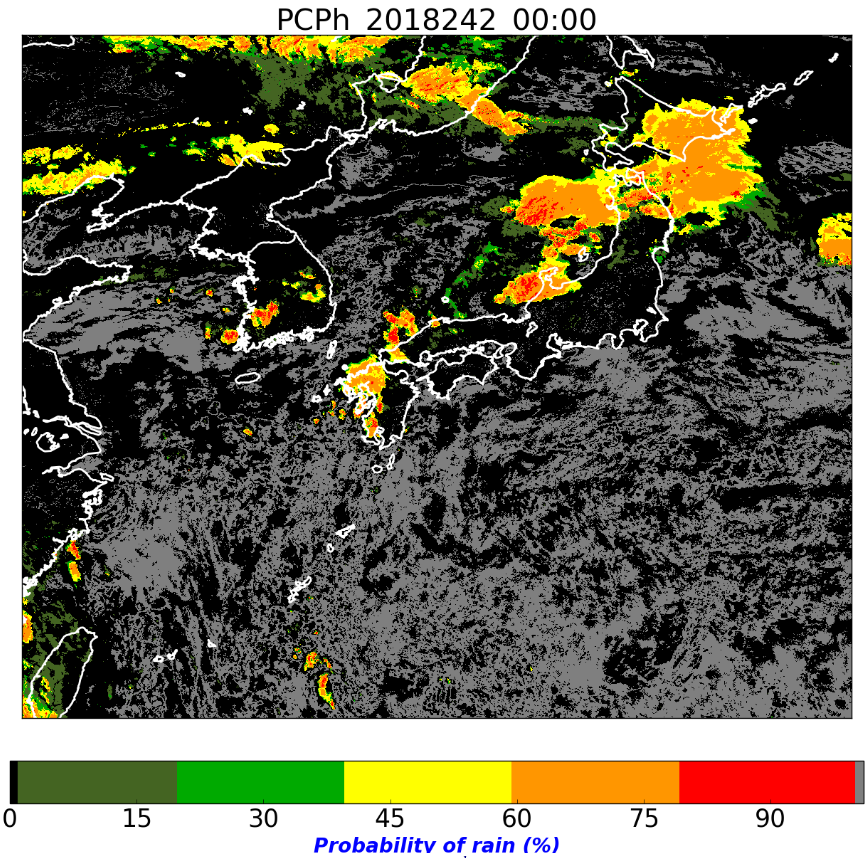

Figure 63.PCPh product on 30th August 2018 at 00:00 UTC

In this another event, there are several convective nuclei coming to southwest to the northeast of Japan island. This time an example of CRR is been introduced. Both CRRPh and CRR detect the same precipitating areas. However, it seems to have more detail the CRRPh version. PCPh reproduces the precipitating areas with high values of probability of rain.

7. GOES-16 DATA

CRR , PCPh and CRRPh have been computed over North America. A composite imagery of radar data have been downloaded from the following website https://www.ncei.noaa.gov/maps/radar/.
A visual validation between the precipitating products and the radar data (in dBz) have been done. GOES-16 satellite data, NWP models, CMIC and Cloud products have been necessary to generate the precipitating products.

Three days have been selected to validate the precipitating products: 7th July 2019 for checking day time algorithm and the 7th and 8th of May 2019 to test the night time performance.

The following colour palette applies to the United States of America Radar mosaic (dBz)

7.1 7TH JULY 2019

Figure 64. USA Radar mosaic (dBz) on 7th July 2019 at 20:40 UTC

According to Figure 64, on this first date, there were many convective cells all over the country. The more developed ones were located on the east and little growing thunderstorms can be found on the west. PCPh on Figure 65 represented well these precipitating areas, giving higher probability of rain to the ones on the east where were placed the higher rain rates.
Both CRR (Figure 67) and CRRPh (Figure 66) detected many of the convective nuclei on the west with similar rain intensity. However, when it comes to the little cells on the east part of the country, it seems the CRRPh detect a little bit more and with higher intensity.

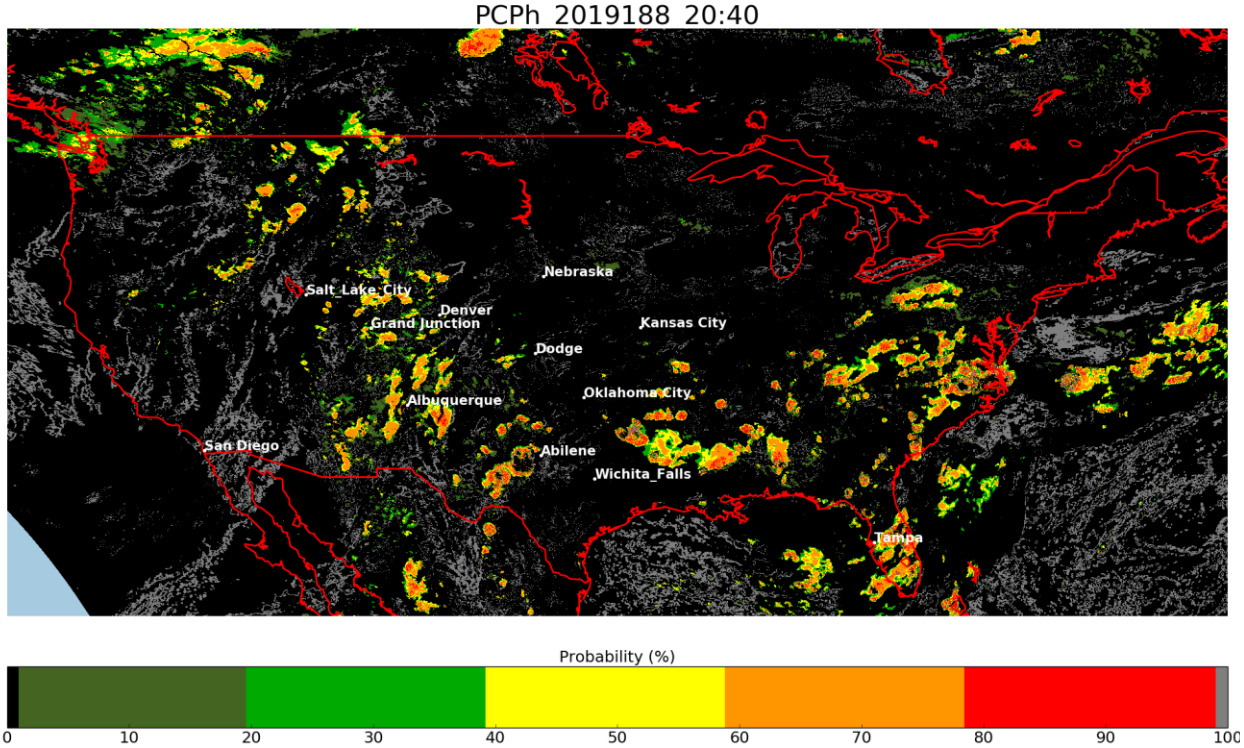

Figure 65. PCPh product on 7th July 2019 at 20:40 UTC over USA.

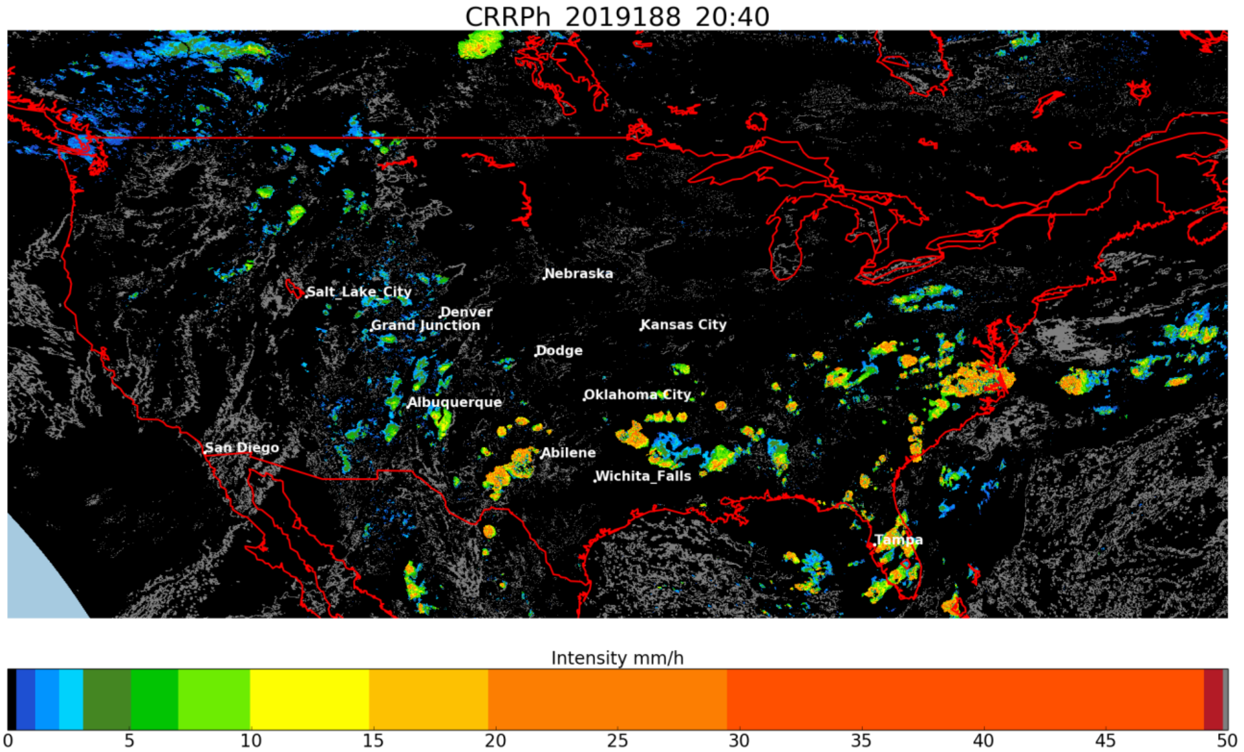

Figure 66. CRRPh product on 7th July 2019 at 20:40 UTC over USA.

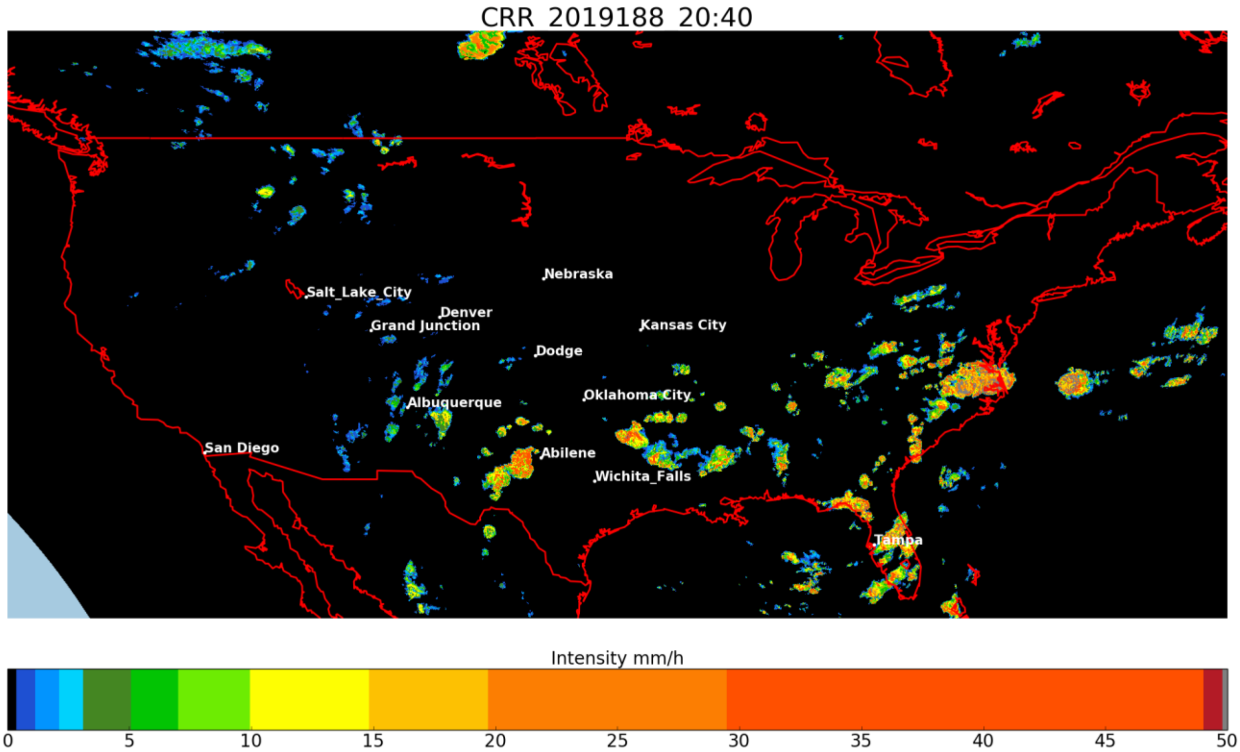

Figure 67. CRR product on 7th July 2019 at 20:40 UTC over USA.

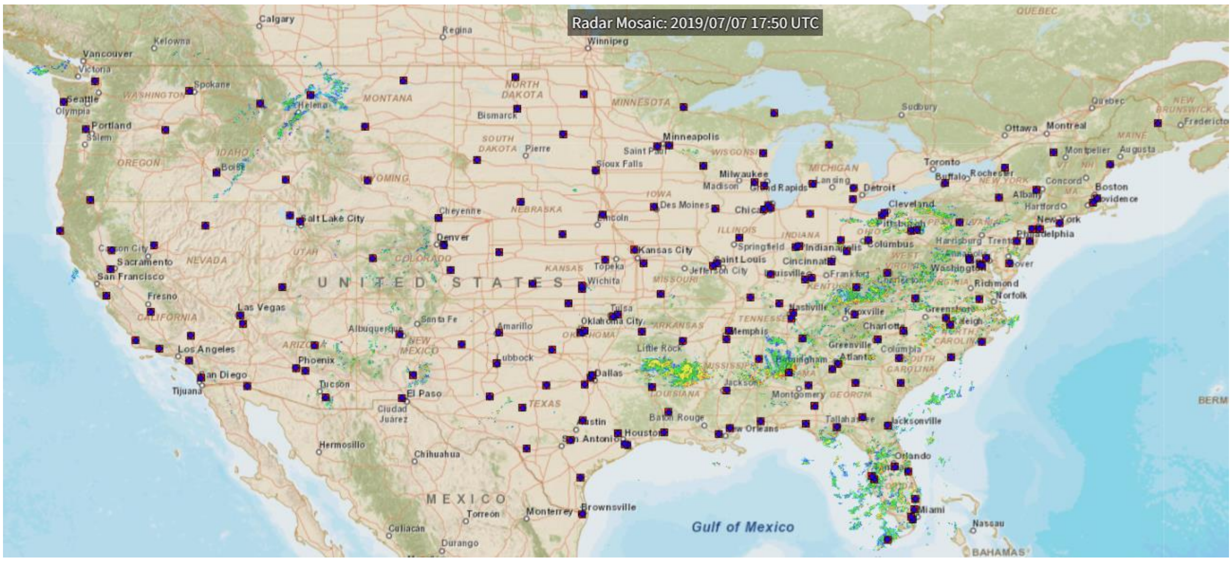

Figure 68. USA Radar mosaic (dBz) on 7th July 2019 at 17:50 UTC

Three hours before, there is still convective activity on the east. If we zoom in on this east area, many convective nuclei were active from Miami to Cleveland. CRR (Figure 72) and CRRPh (Figure 71) again reproduced with detail the situation, with a little bit more accuracy from the CRRPh. PCPh (Figure 69) had again a good performance .

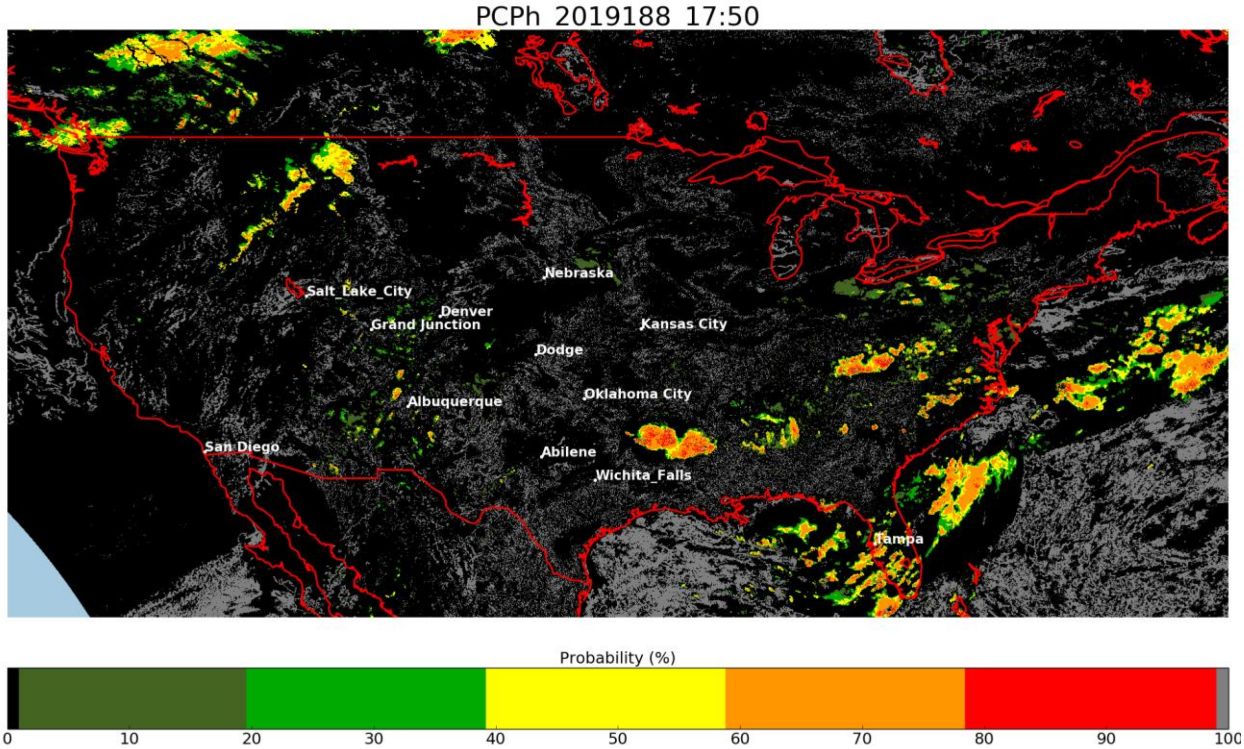

Figure 69. PCPh product on 7th July 2019 at 17:50 UTC over USA.

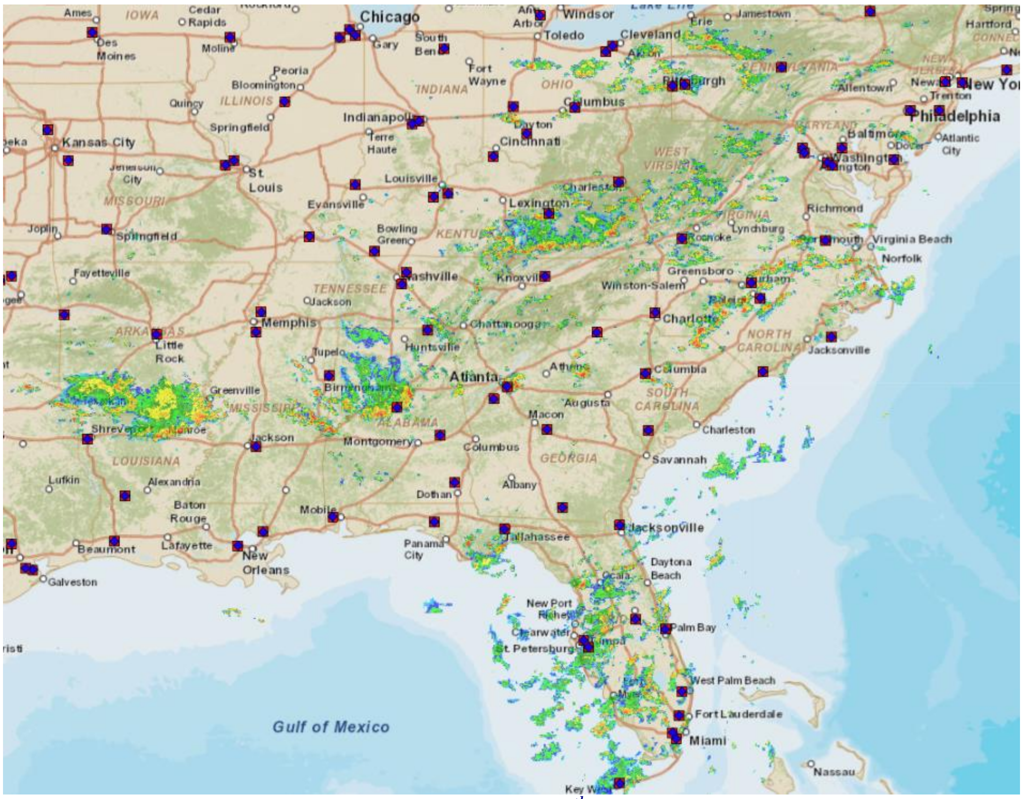

Figure 70. Radar mosaic (dBz) on 6th July 2018 at 00:00 UTC.

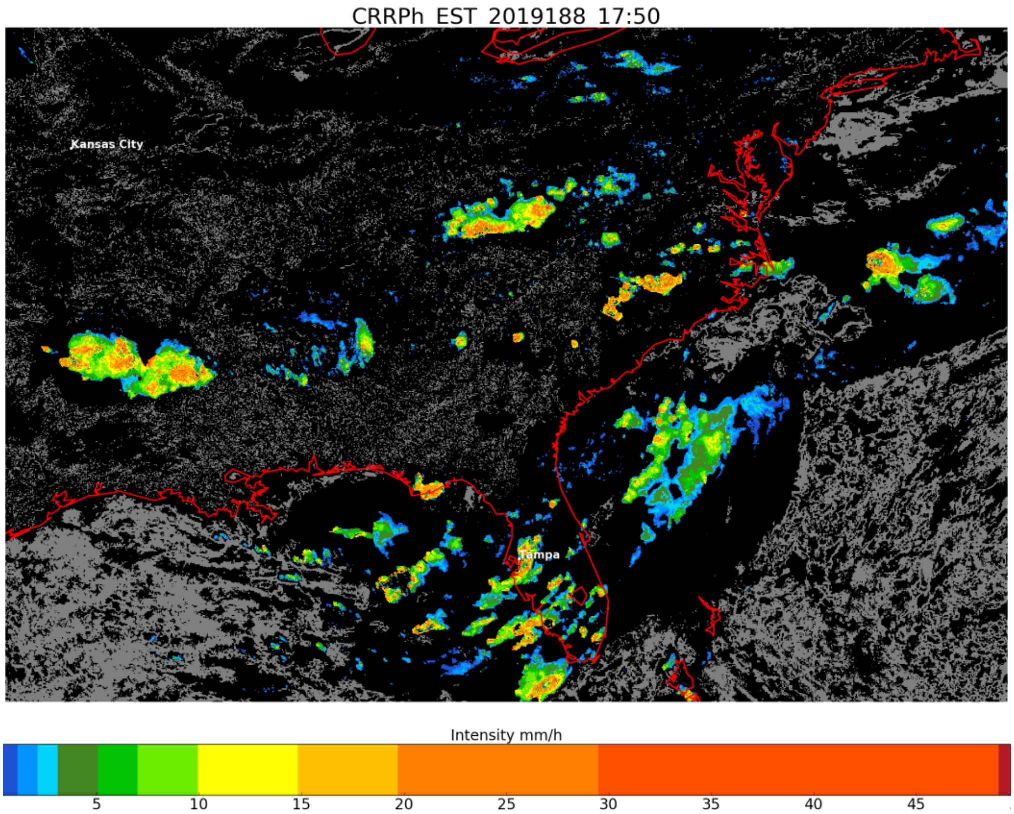

Figure 71. CRRPh product on 7th July 2019 at 17:50 UTC over USA.

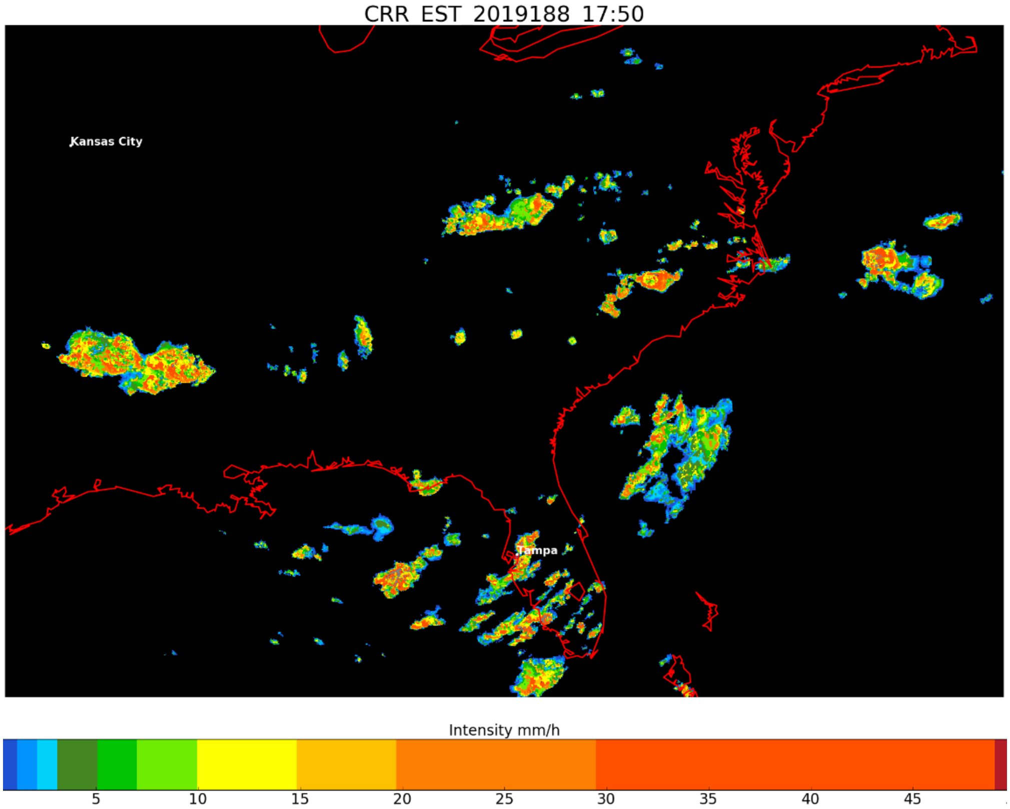

Figure 72. CRR product on 7th July 2019 at 17:50 UTC over USA.

7.2 7TH JULY 2019

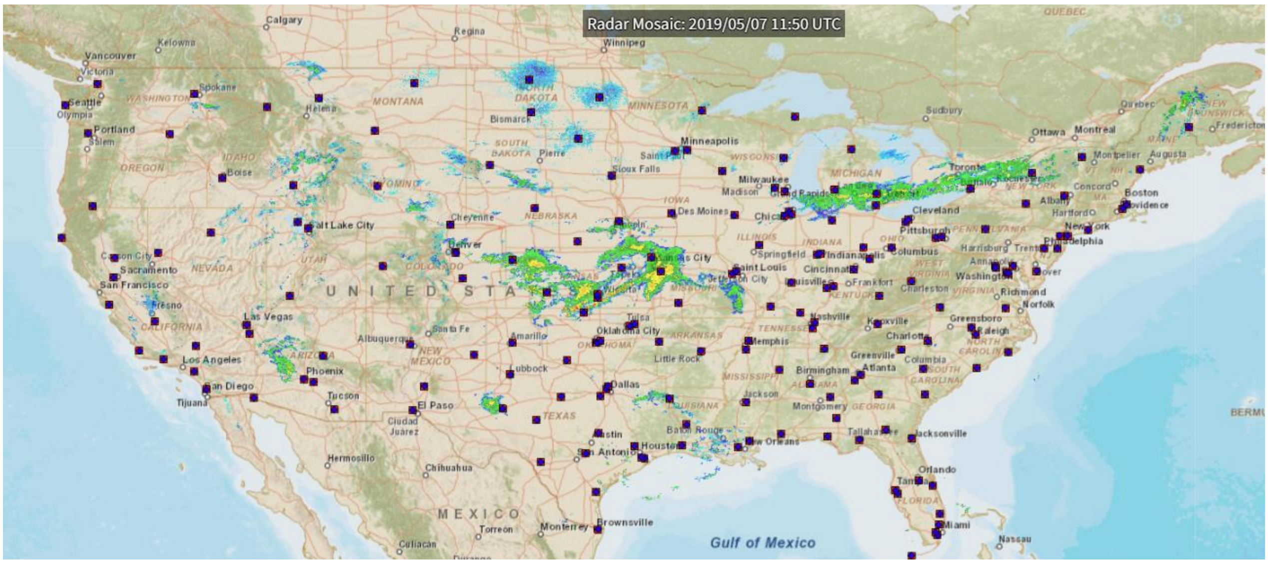

Figure 73. USA Radar mosaic (dBz) on 7th May 2019 at 11:50 UTC

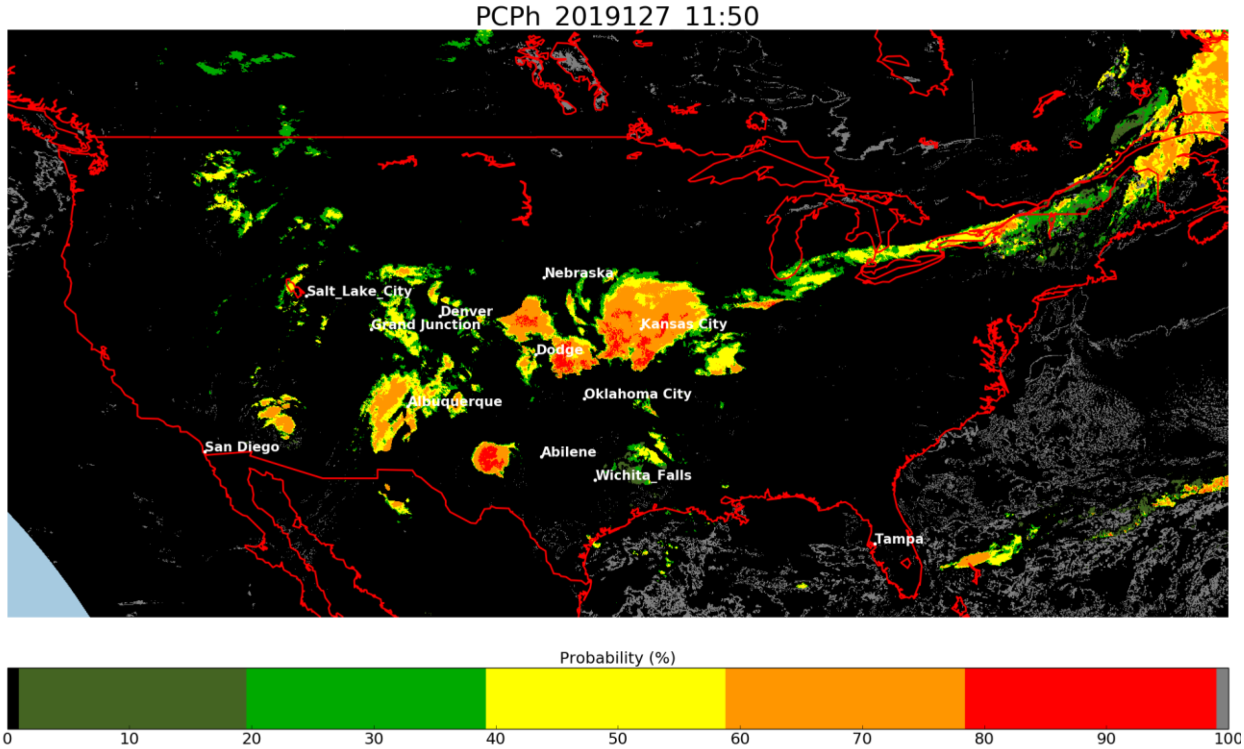

Figure 74. PCPh product on 7th May 2019 at 11:50 UTC

This is an example of a severe weather event. During this day took place strong storms with hail and some tornados associated to them. In the centre of the image there is large area with several thunderstorms taking place. PCPh detected quite well all the precipitating areas. CRR was able to depict the biggest ones. CRRPh represented more rainy areas at the east and a line of precipitation in the Great Lakes Region.

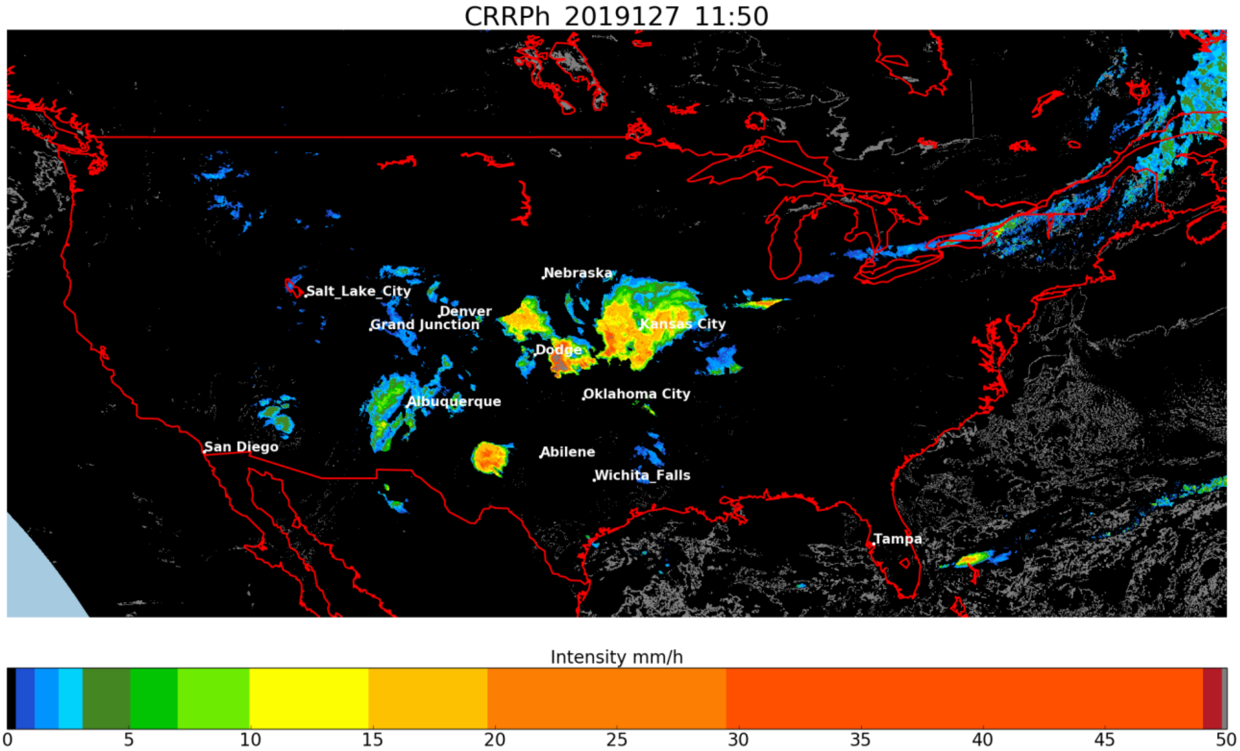

Figure 75. CRRPh product on 7th May 2019 at 11:50 UTC

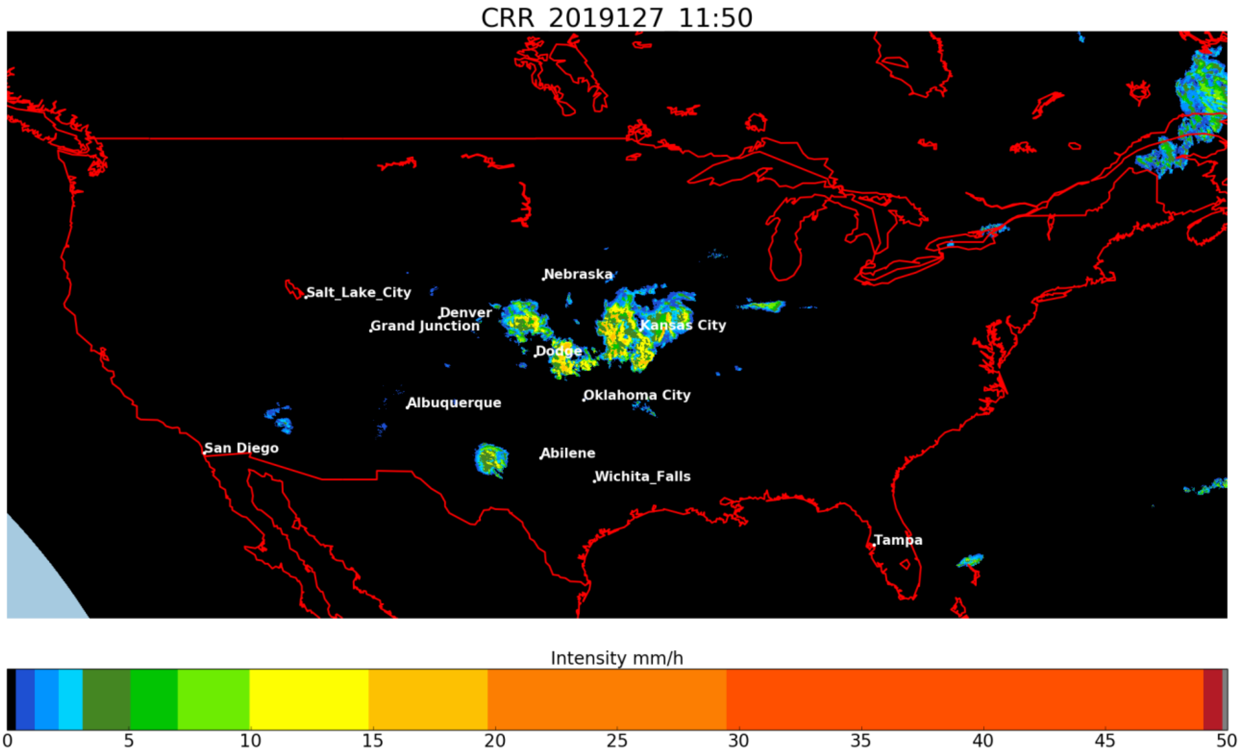

Figure 76. CRR product on 7th May 2019 at 11:50 UTC

7.3 8TH MAY 2019

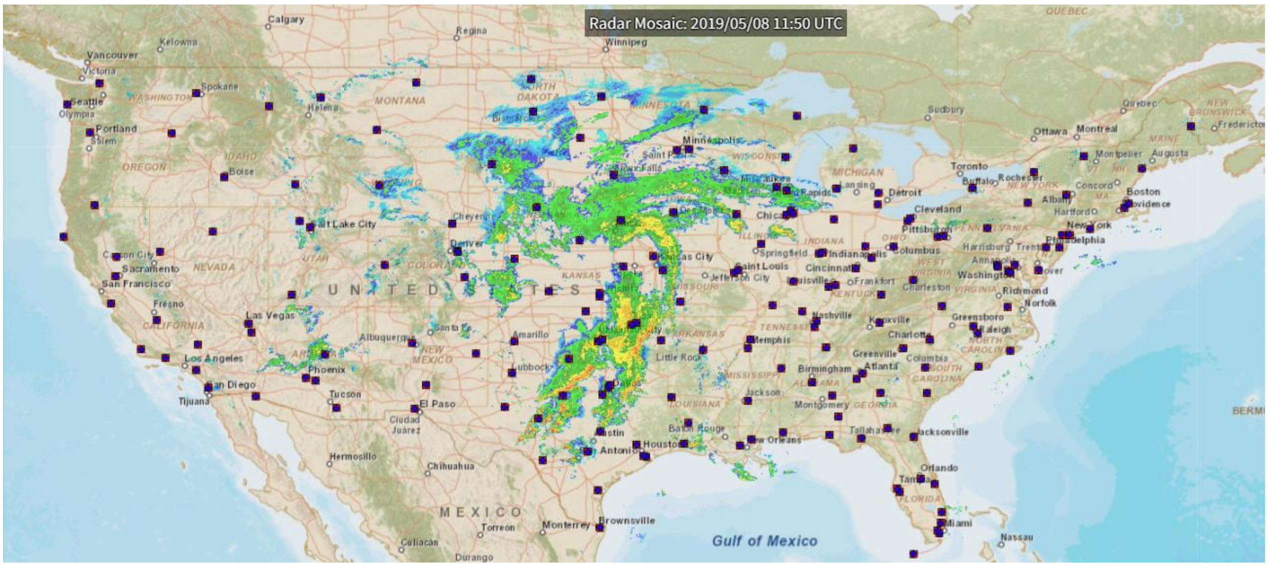

Figure 77. USA Radar mosaic (dBz) on 8th May 2019 at 11:50 UTC

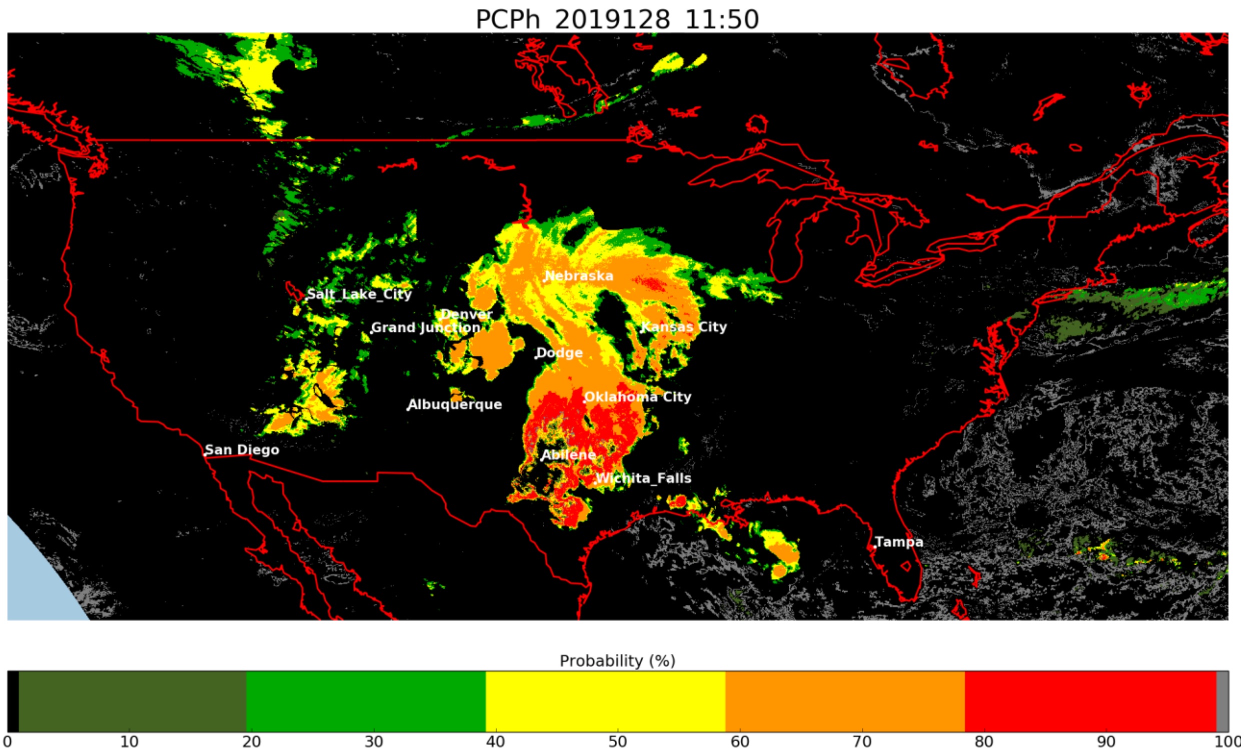

Figure 78. PCPh product on 8th May 2019 at 11:50 UTC

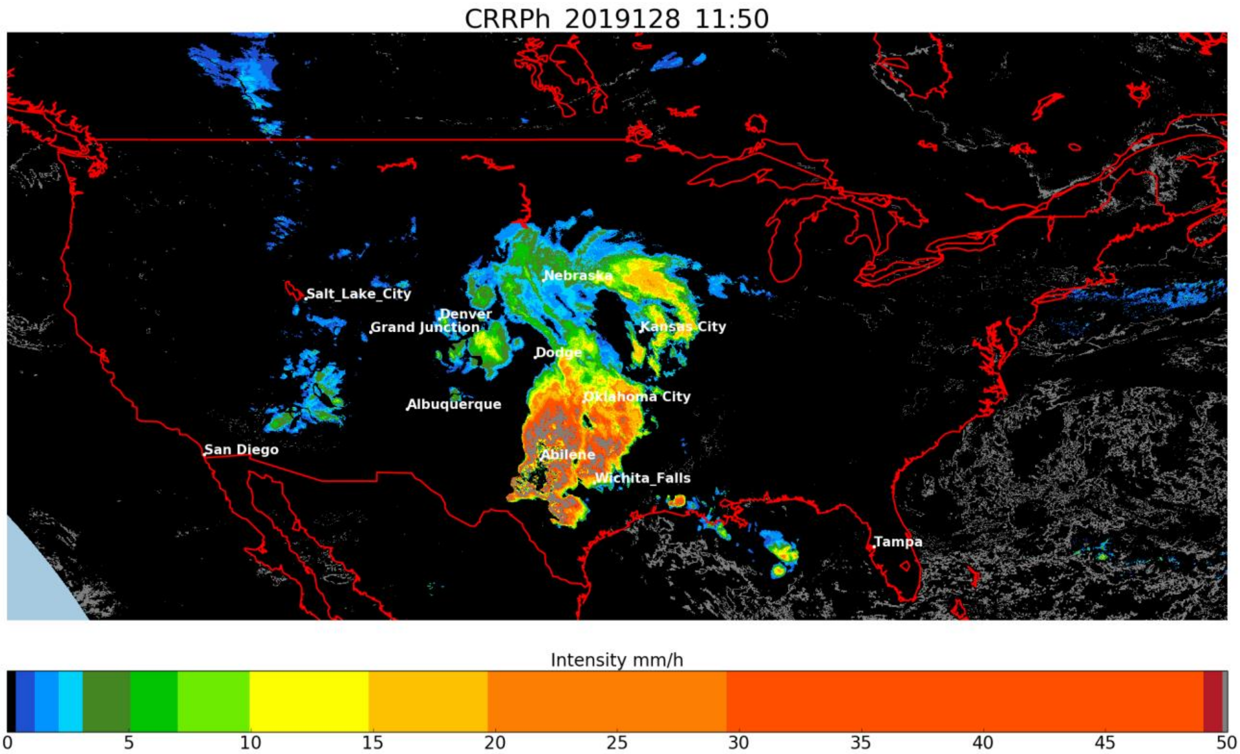

Figure 79. CRRPh product on 8th May 2019 at 11:50 UTC

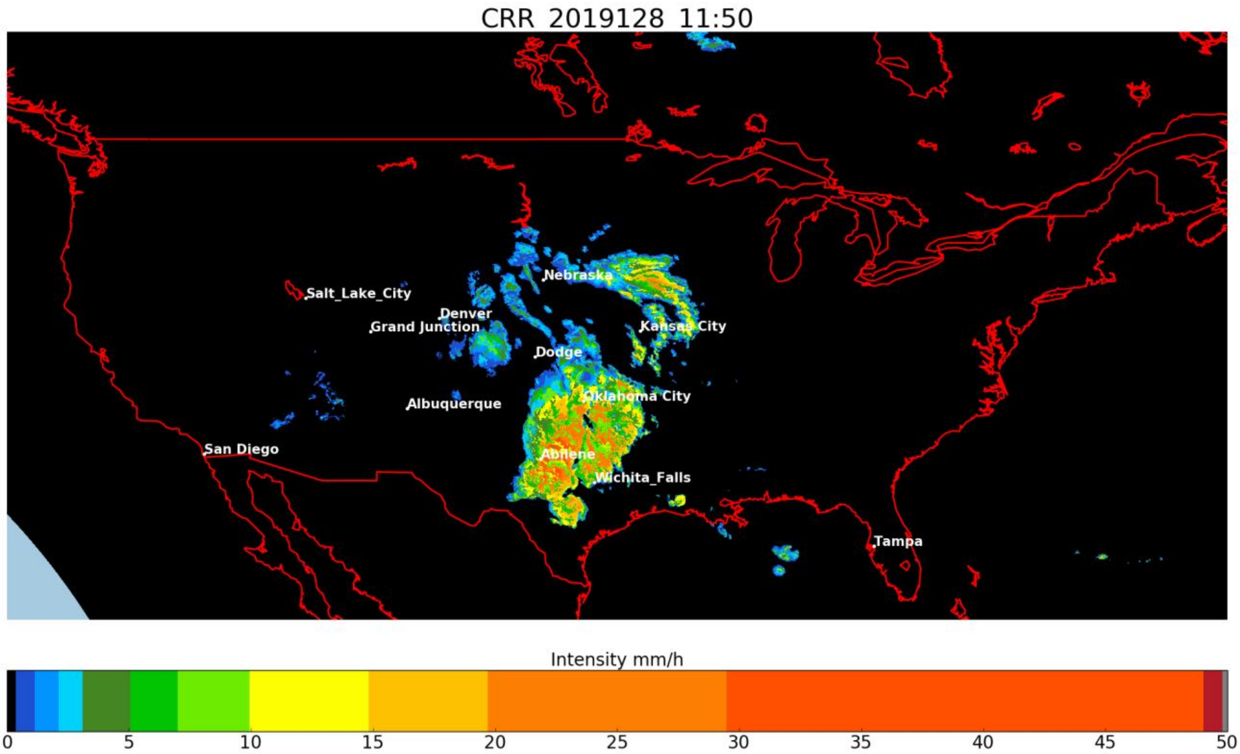

Figure 80. CRR product on 8th May 2019 at 11:50 UTC

During this last event, the same precipitating pattern is reproduced. A huge precipitating area in the centre of the image can be seen. The USA Radar mosaic (dBz) (Figure 77) shows heavy rain in the middle of the country. Both CRR and CRRPh detect it. CRRPh assigns more intensity of rain to the big convective nuclei placed at the centre and south of the image, and it also depicts a larger precipitating area at the north and east.

In general, the three precipitating products show a good behaviour, being more accurate the day algorithm. At night CRRPh detects more active convective nuclei and a larger precipitating area. The bigger convective cells are well reproduced by both of them: CRR and CRRPh. PCPh shows also a better performance at day time and a reasonable good behaviour at night time.

8. ANNEX 1: VERIFICATION METRIC

CATEGORICAL STATISTICS

The following scores derived from Table 34, have been calculated:

- False Alarm Ratio:

$$FAR = \frac{false\_alarms}{hits + false\_alarms}$$

Measures the fraction of estimated events that were actually not events.

- Probability of Detection:

$$POD = \frac{hits}{hits + misses}$$

Measures the fraction of observed events that were correctly estimated.

- Critical Success Index:

$$CSI = \frac{hits}{hits + misses + false\_alarms}$$

Measures the fraction of observed and/or estimated events that were correctly diagnosed.

- Percentage of Corrects:

$$PC = \frac{hits + correct\_negatives}{hits + misses + false\_alarms + correct\_negatives}$$

Is the percentage of correct estimations.

		Estimated (CRRPh, PCPh)	
		occurred[1]	no occurred
Observed (Radar)	occurred*	hits	misses
	no occurred	false alarms	correct negatives

Table 34. Contingency table convention

9. REFERENCES

Vicente, G.A., Scofield, R.A. and Menzel W.P. 1998: The Operational GOES Infrared Rainfall Estimation Technique, Bull. American Meteorological Society, Vol. 79, No. 9, pp. 1883-1898.

Steiner M., Houze J.A. Jr., Yuter S.E.: Climatological characterization of three-dimensional storm structure from operational radar and rain gauge data. J. Appl. Meteor., 34, 1978-2007, DOI: https://doi.org/10.1175/1520-0450(1995)034<1978:CCOTDS>2.0.CO;2

Poelman D., Delobbe L.: Daily convective precipitation maps. EUMETNET OPERA. Work Package OD19, 2018

[1] *Occurred means values higher than or equal to 0.2 mm/h for instantaneous rates and higher than or equal to 0.2 mm for hourly and daily accumulations.*